

**Exploring causes and impacts of disturbance  
of nutrient biogeochemistry along the river  
continuum from land to sea**

**Xiaochen Liu**

Utrecht Studies in Earth Sciences

No.251

ISBN: 978-90-6266-618-8

Cover design: The Rhine River as seen from Vierseenblick in Boppard, April 2017. Photo by Xiaochen Liu, design by Margot Stoete (Faculty of Geosciences, Utrecht University).

Copyright © 2022 Xiaochen Liu

All rights reserved. No part of this publication may be reproduced in any form without written permission by the authors.

# **Exploring causes and impacts of disturbance of nutrient biogeochemistry along the river continuum from land to sea**

**Op zoek naar de oorzaken en effect van verstoringen van de nutriënten biogeochemie in het continuüm van riviertransport van land naar zee**

(met een samenvatting in het Nederlands)

## **Proefschrift**

ter verkrijging van de graad van doctor aan de  
Universiteit Utrecht  
op gezag van de  
rector magnificus, prof.dr. H.R.B.M. Kummeling,  
ingevolge het besluit van het college voor promoties  
in het openbaar te verdedigen op

maandag 25 april 2022 des middags te 4.15 uur

door

**XIAOCHEN LIU**

geboren op 16 april 1986  
te Gaomi, Shandong, China

## **Promotoren:**

Prof. dr. A.F. Bouwman

Prof. dr. J.B.M. Middelburg

## **Copromotor:**

Dr. A.H.W. Beusen

Learning without thought is labour lost; thought without learning is perilous.

(Confucius)

Dedicated to my beloved Feifei & Yuhe.

**Members of the dissertation committee:**

Prof. Dr. M. Dai

State Key Laboratory of Marine Environmental Science, Xiamen University  
Xiamen, China

Prof. Dr. D.J. Conley

Department of Geology, Lund University  
Lund, Sweden

Prof. Dr. H. Tian

International Center for Climate and Global Change Research, Auburn University.  
Auburn, United States of America

Prof. Dr. M.F.P. Bierkens

Department of Physical Geography, Utrecht University  
Utrecht, Netherlands

Prof. Dr. Karline Soetaert

Department of Earth Sciences, Utrecht University  
Utrecht, Netherlands

# Contents

<b>1. Introduction.....</b>	<b>1</b>
1.1 <i>General background</i> .....	1
1.2 <i>Models of quantifying biogeochemical cycling</i> .....	3
1.3 <i>Thesis objective and outline</i> .....	8
<b>2. Nitrogen and phosphorus flows in urban and rural wastewater in China for the period 1970 to 2015 .....</b>	<b>11</b>
Abstract .....	11
2.1 <i>Introduction</i> .....	11
2.2 <i>Methods and Data</i> .....	13
2.3 <i>Results and Discussion</i> .....	18
Supplementary Information.....	27
SI2.1 <i>Comparison of WWTPs technologies among provinces in different regions</i> ..	27
SI2.2 <i>Rural household Sanitation systems in China</i> .....	28
SI2.3 <i>N and P removal rates in WWTPs in different regions</i> .....	29
SI2.4 <i>Comparison with other studies</i> .....	30
SI2.5 <i>Sanitation data for China</i> .....	32
SI2.6 <i>P content of detergents</i> .....	32
<b>3. Exploring long-term changes in silicon biogeochemistry along the river continuum of the Rhine and Yangtze (Changjiang).....</b>	<b>35</b>
Abstract .....	35
3.1 <i>Introduction</i> .....	35
3.2 <i>Methods</i> .....	38
3.3 <i>Results and Discussion</i> .....	46
Supporting Information .....	55
SI3.1 <i>Construction of weathering</i> .....	55
SI3.2 <i>Validation and sensitivity analysis method</i> .....	56
SI3.3 <i>The parameters and values used in DISC-SILICON</i> .....	58
SI3.4 <i>Sensitivity analysis results</i> .....	59

<b>4. Exploring spatiotemporal changes of the Yangtze River (Changjiang) nitrogen and phosphorus sources, retention and export to the East China Sea and Yellow Sea .....</b>	<b>67</b>
<i>Abstract .....</i>	<i>67</i>
4.1 <i>Introduction .....</i>	<i>67</i>
4.2 <i>Methods.....</i>	<i>69</i>
4.3 <i>Results and discussion .....</i>	<i>71</i>
4.4 <i>Conclusion.....</i>	<i>82</i>
<i>Supporting Information .....</i>	<i>83</i>
<i>SI4.1. Model description .....</i>	<i>83</i>
<i>SI4.2 Validation data .....</i>	<i>85</i>
<i>SI4.3. Data analysis.....</i>	<i>85</i>
<i>SI4.4. Modeled output data .....</i>	<i>87</i>
<i>SI4.5. Movies.....</i>	<i>88</i>
<i>SI4.6. Comparing with other studies.....</i>	<i>90</i>
<i>SI4.7. Tables N and P sources to streams for the whole Yangtze river basin.....</i>	<i>90</i>
<b>5. Nutrient legacies in the Rhine, Mississippi, Yangtze and Pearl River basins and consequences for future water quality .....</b>	<b>101</b>
<i>Abstract .....</i>	<i>101</i>
5.1 <i>Introduction .....</i>	<i>101</i>
5.2 <i>Methods and data used.....</i>	<i>104</i>
5.3 <i>Results.....</i>	<i>107</i>
5.4 <i>Discussion .....</i>	<i>114</i>
5.5 <i>Concluding remarks .....</i>	<i>118</i>
<b>References.....</b>	<b>121</b>
<b>Summary.....</b>	<b>141</b>
<b>Samenvatting in het Nederlands.....</b>	<b>145</b>
<b>Acknowledgement.....</b>	<b>151</b>
<b>Curriculum vitae.....</b>	<b>153</b>



# Chapter 1

## Introduction

### 1.1 General background

Over the past decades, the number of rivers with severe human perturbations of the plant nutrient cycles of nitrogen (N) and phosphorus (P) has increased dramatically (Billen et al. 2005, Mackenzie et al. 2005, Turner and Rabalais 1994). These perturbations have been triggered by increasing food and energy production, which lead to land-use changes due to expansion and intensification of agriculture, increasing fertilizer use and animal manure production, increasing gaseous N emissions from fossil fuel combustion, increasing atmospheric deposition, increasing nutrient discharge from sewage systems and aquaculture.

Rapidly increasing fertilizer use has enabled farmers to produce food for the rapidly growing human population (Galloway and Cowling 2002). A negative effect of increasing fertilizer use and animal manure production is that nutrients have been spreading over the globe's inland waters and are transported towards coastal waters (Beusen et al. 2016a). N and P export to global coastal waters has doubled during the 20<sup>th</sup> century (Alvarez-Cobelas et al. 2008, Beusen et al. 2016, Dumont et al. 2005, Seitzinger et al. 2005, Vitousek et al. 1997). At present, agriculture is the dominant source of N and P in global inland waters (Beusen et al. 2022).

China is an interesting case, with its rapid development since 1970. China experienced the impact of a rapidly growing population to a current 1.4 billion inhabitants, rapidly growing food demand driving the intensification of agricultural land use, and rapid urbanization to 57% during the last decades, and as a consequence, rapidly increasing nutrient discharge from urban point sources (FAO 2019). China's acceleration of nutrient cycles started decades after that in industrialized regions such as Western Europe.

Accelerated N and P cycles have been shown to disturb both inland water and coastal ecosystems, particularly in semi-enclosed seas, where there is no rapid dilution and flushing of riverine nutrients into the open ocean (Meybeck et al. 2006). Furthermore, increasing nutrient availability leads to eutrophication, i.e. enhanced phytoplankton production, which may lead to oxygen depletion during the decay of the algal biomass, ultimately to hypoxia or anoxia.

Although urban areas cover only a tiny fraction (0.2-2.4%) of the global land area (Potere and Schneider 2007), large amounts of N and P are discharged in urban centers

to inland and coastal waters (Morée et al. 2013) because currently, more than 55% of the global human population lives in cities (United Nations 2018). The N and P discharged from these point sources stem from human households (human excreta and P-based detergents) with or without a sewage connection, from industries that discharge wastewater containing nutrients, and from domestic animals (Billen et al. 2012, Li et al. 2012, Morée et al. 2013, Nyenje et al. 2010, Quynh et al. 2005, van Puijenbroek et al. 2019b).

Commonly, the construction of waste water treatment plants (WWTPs) lags the sewage construction by several decades in many countries (Van Drecht et al. 2009). For example, in Europe and North America, the P and N loads showed a significant increase in the 1960s and 1970s due to massive connection of households to sewage systems and declined in the late 20<sup>th</sup> century due to construction and increased efficiency of WWTPs and the use of P-free detergents (Morée et al. 2013).

However, the nutrient discharge from the 45% of the global population living in rural areas, where next to sewage systems also other forms of sanitation such as septic tanks and pit latrines are found, is poorly known and often ignored. Several studies have explored the N and P fluxes from urban areas both at local, national and global scales using models and data-based approaches (Chen et al. 2019, Morée et al. 2013, Tong et al. 2017b, Van Drecht et al. 2009, van Puijenbroek et al. 2019b, Zhang et al. 2020).

In China, available estimates of nutrient loading of inland waters by sewage discharge are either regional (Tong et al. 2017b) or based on national statistics (Chen et al. 2019), consider urban wastewater discharge only, and ignore changes in sewage connection rates. In addition, the number of inhabitants served by wastewater treatment plants and their removal efficiency is poorly quantified, and the fate of nutrients from households in rural areas is fraught with large uncertainties.

While many studies focus on N and P, much less attention has been paid to the fluxes of dissolved silicon (DSi). DSi is an essential nutrient for siliceous algae (diatoms) (Treguer et al. 1995a). Parallel to accelerated nutrient cycles, there is also enhanced nutrient trapping due to the construction of artificial dam reservoirs (Conley et al. 1993, Liu et al. 2018a, Liu et al. 2020a, Maavara et al. 2014, Seitzinger et al. 2005). Diatoms consume N, P, and Si according to the Redfield-Brzezinski ratio of 16:1:20 (Brzezinski 1985, Redfield et al. 1963). Enhanced diatom growth in reservoirs in response to the increasing N and P loading leads to enhanced trapping of nutrients (N, P and Si), and thus to a reduction of their downstream transport to coastal waters (Conley et al. 1993). Since rock weathering is the primary source of DSi in rivers, reduction of DSi supply due to deforestation (Struyf et al. 2010) and enhanced trapping of DSi in reservoirs (Liu

et al. 2020a, Maavara et al. 2014) leads to a deficiency of Si relative to N and P.

Thus, DSi retention in inland water bodies may have significant effects on the eutrophication in the coastal ecosystem due to distorted N:P:Si ratios deviating from the Redfield-Brzezinski ratio, which may induce harmful non-siliceous algal blooms (Billen and Garnier 2007b, Humborg et al. 1997), especially in coastal marine ecosystems.

Nowadays, many nations limit or at least control the amount of fertilizers entering the waterways. However, the excessive use of fertilizers, particularly since the 1970s and 1980s in developed countries, has left a nutrient legacy that has degraded the aquatic environment. European and U.S. rivers currently feel the effects of excessive nutrient mobilization in the 1970s and 1980s, i.e. the legacy of historical nutrient use. This is because in the depletion phase, i.e. after measures have been taken to reduce nutrient discharge to surface water, the landscape buffer or memory acts differently from the accumulation phase. With declining nutrient inputs, soils may be releasing nutrients by organic matter decomposition, and aquifers (particularly N) and sediments (particularly P) in lakes, reservoirs, and rivers continue to deliver nutrients. For example, the N concentration in the Mississippi has not decreased in recent decades, despite policies to reduce nutrient loading. The flow-normalized N export by the Mississippi has even increased since 1980, and the increased N concentration at low stream flows is a strong indication that nitrate delivery by groundwater has a strong effect on river concentrations (Sprague et al. 2011b). Latecomers to massive urbanization and with large and intensive agricultural production systems like India and China will probably face similar nutrient legacies if in future their fertilizer use will decrease.

## **1.2 Models of quantifying biogeochemical cycling**

### **General**

Monitoring nutrient concentrations and flows is necessary to identify historical changes and trends. However, these observations often do not help to understand the changes in nutrient loading and the nutrient biogeochemical processes that determine nutrient retention. Models are essential tools to support and interpret nutrient monitoring data by improving our knowledge of the interaction of multiple processes in different landscapes and predict the biogeochemistry processes of nutrients along the river continuum.

Models are simplified representations of complex systems and do not contain all the features of the actual system. However, models should include the essential components to describe the system at the scale considered and for the purpose of the study. Various models have been developed to quantitatively assess the transfer of nutrients from land to streams and their processing and transport along rivers to coastal waters. These

models can be classified in two categories (Bouwman et al. 2013b). One category is the lumped river-basin scale regression model (Figure 1.1a, b). The second category uses distributed approaches, where all components of land and waterscapes (soil, vegetation, land types, riparian zones, wetlands, streams, lakes, and reservoirs) are simulated considering the various hydrological transport pathways (surface runoff, leaching, groundwater transport, direct discharge from sewage and aquaculture, and atmospheric deposition) (Figure 1.1c).

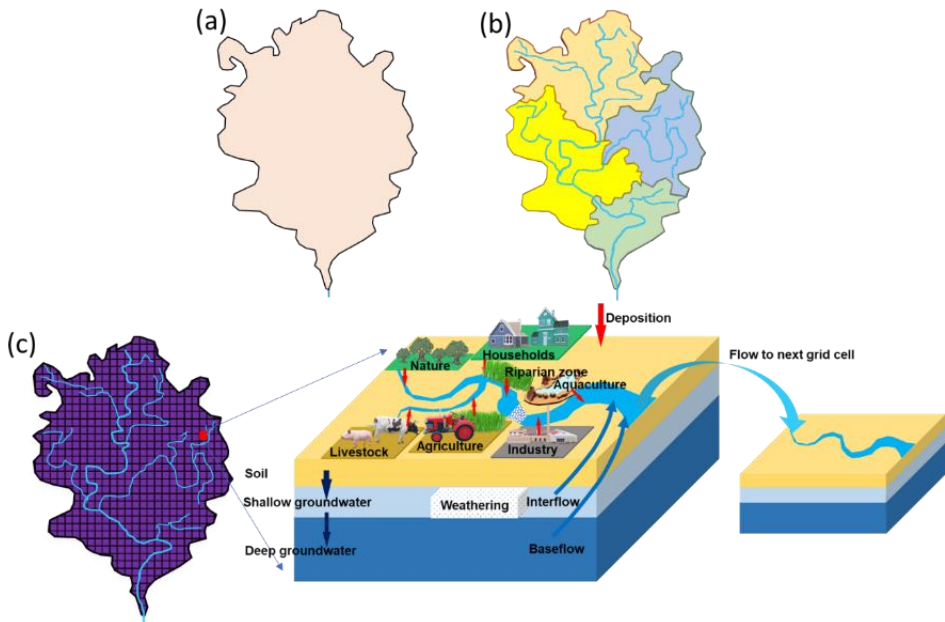


Figure 1.1. Different parameterization concepts, including (a) lumped regression model for a whole river basin, (b) lumped regression model for one sub-basin and (c) fully distributed model for different sources and pathways within each spatial unit (e.g. grid-cell).

## Lumped approaches

Lumped approaches (Figure 1.1a, b) generally use regression analysis to obtain model predictor variables or coefficients for the whole basin. The best model can be obtained from predictor variables selected by regression (Beusen et al. 2009a) or by finding the coefficients for a priori selected model parameters (Mayorga et al. 2010a) that best explain the observed nutrient load or yield (load per unit of area) at the river mouth. Examples include regressions of N export from large watersheds on human energy consumption (Meybeck 1982), population density (Peierls et al. 1991), or net

anthropogenic sources (Howarth et al. 1996a). Such models explain up to 80 percent of the variability of river N export and have the advantage of being simple, easy to use, and based on readily available statistical data.

Quasi-empirical models (Caraco and Cole 1999, Kroeze and Seitzinger 1998) of nitrate-N export from the world's largest rivers were developed using empirical regression methods and literature-based rate coefficients. These models serve to estimate continental N budgets and evaluate the effects of anthropogenic sources on N export in some of the world's largest river basins.

More recently, quasi-empirical models were developed to estimate the dissolved inorganic, organic, particulate N, P and carbon, and sediments (Mayorga et al. 2010, Seitzinger et al. 2010b). These models have helped to identify the major source regions of nutrient and carbon export to global coastal waters. However, these simple regression models are limited in some respects: (i) all these approaches work at the annual temporal scale and fail to provide insight into the seasonal variation of nutrient flows. (ii) lumped river export models represent sources and sinks as homogeneously distributed in space and do not separate terrestrial filters (e.g. denitrification in soils and groundwater) from in-stream loss processes. (iii) regression models do not account for nonlinear interactions between sources and loss processes, such as the dependence of denitrification on nitrate concentrations. Therefore, they are less useful for assessing the complex interactions induced by disturbance, for example, in scenario projections.

## **Distributed approaches**

The second class of distributed models (Figure 1.1c) describes how nutrients reach surface water via different pathways (atmospheric deposition, leaching from soils to groundwater, groundwater transport, surface runoff, and wastewater discharge from human activities). Most distributed models are also spatially explicit (within the river basin). Each transport pathway requires a specific modeling approach. We can distinguish semi-distributed and fully distributed models. (i) semi-distributed (hybrid) models use export coefficients to several aggregate processes between the surface and the point where nutrients enter surface water; and (ii) Fully distributed models simulate the water flow explicitly as a medium for transport and biogeochemical processing.

A recent case of a hybrid approach is the SPARROW model (SPATIally Referenced Regression On Watershed attributes) (Smith et al. 1997), which expands on conventional regression methods by using a mechanistic model structure in correlating measured N flux in streams with spatial data on N sources, landscape characteristics (e.g. soil permeability, temperature), and stream properties (e.g. streamflow, water travel time). By spatially referencing N sources and watershed attributes to surface water

flow paths, defined according to a digital drainage network, and imposing a mass-balance constraint, the model produces accurate predictions of stream export (Chen et al. 2009).

Fully distributed models include various landscape components, delivery processes and transfers throughout the landscape continuum from headwaters to the river mouth. Delivery processes include surface runoff, transport through aquifers, delivery to riparian zones, direct groundwater flow to water bodies, and in-stream biogeochemical processes. Ideally, models include all these processes and transfers, but often landscape compartments distinguished in models are lumped (e.g. aquifers and riparian zones). A range of available models commonly uses hydrology as the basis of calculations. Therefore, these models often have a time scale of one day or less.

In a recent review, Borah and Bera (2003) compared a range of fully distributed continuous and event-based models for watershed-scale hydrology and nonpoint-source pollution. A problem with all these models is that they require large amounts of data. Except for a limited number of intensively studied local systems, generally, data on the input of nutrients and transfer to the adjacent or downstream compartments in a river basin are scarce. This often means that the sediment and nutrient concentrations at one particular location in the system may be known, for example, in the stream, and that the processing and retention in those landscape elements delivering to the stream are poorly known. This problem of missing information is not easily solved and will require targeted and appropriate-scale data collection efforts coupled to model calibration or development.

A recent example of a fully distributed model is the Integrated Model to Assess the Global Environment-Global Nutrient Model (IMAGE-GNM), a global, spatially explicit model to describe nutrient loading and in-stream biogeochemistry (Beusen et al. 2015). Water is used as a transport medium in the model, as described by the global hydrology model PCRaster Global Water Balance (PCR-GLOBWB) (Sutanudjaja et al. 2018).

One advantage of IMAGE-GNM is the internal consistency by coupling of models and common use of data (e.g. soils, lithology, relief, climate, land use) and the ability to simulate long time periods, i.e. from the year 1900 onwards in order to compute accumulation and depletion of nutrients in landscape reservoirs such as groundwater and sediments. IMAGE-GNM calculates the soil N and P delivery for each grid cell from diffuse sources (agricultural systems, natural systems, vegetation in flooded areas, deposition) and point sources (aquaculture, wastewater from urban areas). For agricultural land, the basis for computing runoff, leaching and groundwater transport

are the N and P soil budgets which are calculated for each grid cell. N inputs include animal manure, atmospheric deposition, fertilizer and N fixation. P inputs include fertilizer and manure. The outputs are withdrawal by crops harvest, grazing, and ammonia volatilization. Floodplains are included where part of litter from vegetation ends in surface water and is transported by streams. The in-stream biogeochemistry in every water body in each grid cell is based on the spiraling approach (Stream Solute Workshop 1989), using physical properties of water bodies to compute the travel time, together with uptake velocity as a measure for the biological retention processes. After calculating retention in waterbodies (streams, rivers, floodplains, lakes, and reservoirs), each grid cell receives all the N and P output from all upstream cells and the N and P input from sources within the grid cell.

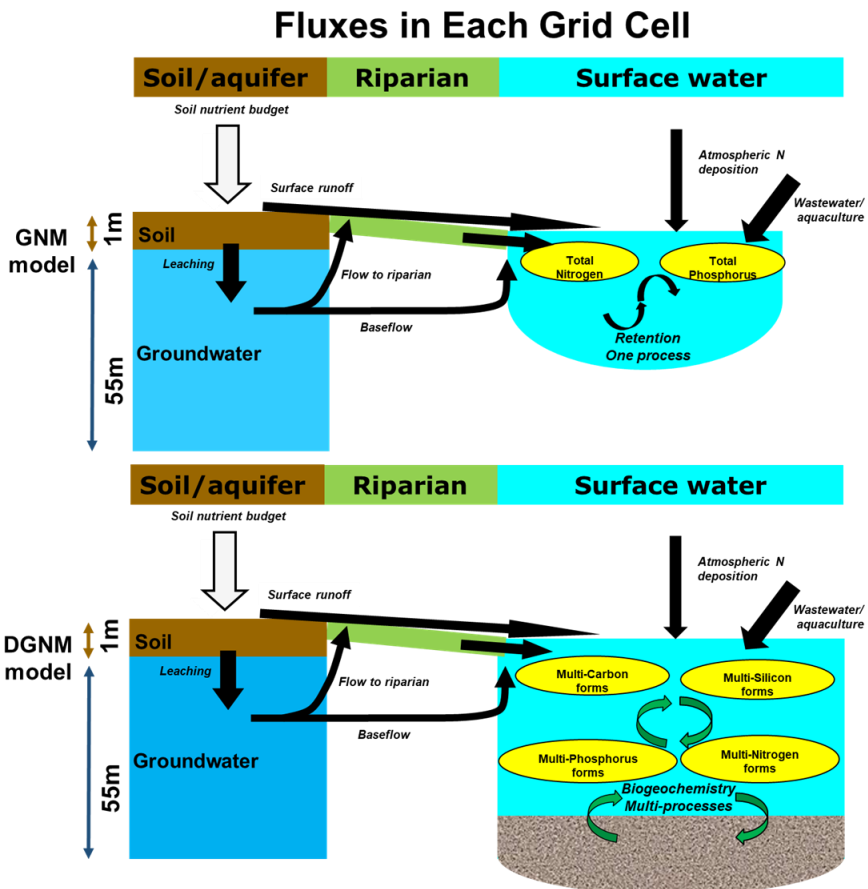


Figure 1.2. Scheme of water and nutrients flows within one 0.5 by 0.5 degree grid cell in IMAGE-GNM (up) and IMAGE-DGNM (down).

Recently, IMAGE-GNM was updated with a dynamic model by replacing the spiraling method (Figure 1.2) with IMAGE-DGNM (Vilmin et al. 2020b). This model version also requires temporal distributions of nutrient mobilization and the transition of total N and P into different nutrient forms and species (Vilmin et al. 2018). IMAGE-DGNM is inspired by the RIVERSTRAHLER model (Garnier et al. 2002, Sferratore 2006), which also couples hydrology and biogeochemistry. While in RIVERSTRAHLER, the inputs of all stream segments of the same Strahler order are lumped within a sub-basin, in DGNM, every grid cell has its specific environmental, hydrological, and land use conditions. All data used in IMAGE-GNM and DGNM have a 0.5 by 0.5 degree spatial resolution. The temporal resolution of calculations in GNM is annual, while in DGNM, it is variable, selected based on the process considered.

### **1.3 Thesis objective and outline**

The goal of my Ph.D. research was to improve the understanding of the long-term regional and global change processes affecting N, P and Si cycling by comparing the biogeochemistry of nutrients in different basins in different climate zones, on time scales ranging from years to decades to a century. This improved knowledge will allow for comparing river basins in industrialized countries, which experienced accelerated nutrient cycles in the 1950s to 1990s, with rivers in China, where intensification of nutrient cycles started decades later. This improved knowledge will allow for developing future research strategies and form a basis for formulating policy strategies for reducing the impact of eutrophication and nutrient distortions.

IMAGE-GNM was applied and further developed to reach these dual goals, covering N and P fluxes from wastewater, aquaculture, soil nutrient budget model, and dynamic instream chemistry processes. The specific effort of this thesis is to explore the long-term response to perturbation by the spatially explicit distributed process-based models IMAGE-GNM and DGNM. Since a model for Si delivery, retention and export was lacking in the IMAGE framework, I developed a new module DISC-SILICON, part of the dynamic IMAGE-DGNM version. Descriptions of wastewater treatment technologies in China were uncertain and nutrient flows in rural areas in China were lacking in the global version of IMAGE-GNM and DGNM. I therefore developed a new wastewater nutrient model at the scale of Chinese provinces.

The long-term nutrient dynamics, accumulation and depletion were calculated in Rhine and Mississippi and compared with two major Chinese rivers, i.e. Yangtze and Pearl. These four rivers differ considerably in terms of hydrology, land use and population. With the massive deforestation, economic growth and urban development in the Yangtze and Pearl in the past four decades, their massive river transport of nutrients to



the South China Sea, East China Sea and Yellow Sea led to excessively high N and P concentrations and an increasing frequency of HABs. The Mississippi River drains the largest area, while the Yangtze is the longest river with the largest discharge. The Mississippi has the largest reservoir volume, both in absolute terms and fraction of the annual discharge. The Mississippi has the largest agricultural coverage of the four basins in 2015. The number of inhabitants in the Yangtze is the largest of the four river basins, but the population density is highest in the Pearl and Rhine, while that in the Mississippi is lowest.

**Chapter 2** presents a new version of the wastewater model, which is part of IMAGE-GNM, applied to simulate nitrogen (N) and phosphorus (P) emissions from households and industries and their fates in rural and urban areas in China. The model is a spatially explicit and distributed model that describes the long-term spatial patterns of global N and P transport in the urban and rural continuum. This new wastewater model uses long-term changes in the drivers of the N and P emissions from point sources by coupling sanitation types, sewer connection rate, detergents use, and wastewater treatment plants (WWTPs) technologies and forms a major step forward compared with existing approaches that lack the capability to simulate long-term dynamic changes. This new approach generates province-scale inventories of N and P sources in wastewater using detailed information on the location and functioning of WWTPs covering China for the period 1970-2015.

While it is well known that Si export to China's coastal waters is declining, the causes are not well known. IMAGE-DGNM lacked a model for describing the Si delivery and in-stream biogeochemical processing. To investigate the processes causing declining Si export, **Chapter 3** presents the new DISC-SILICON module within DGNM for simulating Si transport and biogeochemical processing and its application to the Rhine and Yangtze, two major rivers with contrasting geohydrological conditions, history of land-use change and dam construction. The study covers the period 1900-2010. The model is, by using long-term changes in the drivers of the Si cycle, and coupling climate, land use, hydrology with in-stream processing, a major step forward compared with regression models, basin-scale box models and reservoir box models that all produce snap shots and lack the capability to simulate legacies. DISC-SILICON is the first dynamic, spatially explicit, and distributed model that allows to describe the long-term spatial patterns of global Si transport and biogeochemical processing in the river continuum from headwaters to the river mouth, taking into account the impact of climate, land-use changes and dam construction.

**Chapter 4** presents a study on N and P delivery to and retention in the Yangtze River Basin in China and the eventual export of these nutrients to the East China Sea and the

Yellow Sea. The study covers the period 1900-2010, which comprises a period of dramatic socioeconomic changes in this river basin, including massive population growth, food and energy production, and the construction of reservoirs including the Three Gorges Dam. The results demonstrate that the current nutrient load exported from the Yangtze River Basin toward the East China Sea and the Yellow Sea is much larger (almost twice) than previously estimated based on statistical models.

Finally, **Chapter 5** explores the differences in nutrient legacies due to past accumulation in groundwater and sediments between four major global rivers, i.e. the Rhine, Mississippi, Yangtze and Pearl. The four rivers went through a phase of nutrient accumulation, but there is a difference in the timing. The Rhine changed from accumulation to a depletion phase after the 1980s, while the Mississippi and the two Chinese rivers are still in the accumulation phase, with stable or increasing N and P loading from both agriculture and point sources. The groundwater system in the Rhine is currently releasing N that has accumulated in groundwater in previous decades. The Yangtze has many similarities with the Mississippi situation in the 1970s, with large amounts of N that are temporarily stored in groundwater; this accumulation will form a future legacy of current management, since the effects of any reduction achieved today will inevitably be retarded by continued N outflow from groundwater. P accumulation in sediments is particularly important in rivers with large lakes in their stream network or where dams and reservoirs have a major influence on the hydrology. Future scenarios were analyzed to investigate the importance of nutrient (N and P) legacies.

## Chapter 2

# Nitrogen and phosphorus flows in urban and rural wastewater in China for the period 1970 to 2015

---

Xiaochen Liu, Arthur H.W. Beusen, Peter J.T.M. van Puijenbroek, Xuedong Zhang, Junjie Wang, Wim Joost van Hoek, Alexander F. Bouwman

---

*Paper in revision (Environmental Science & Technology, 2022).*

### Abstract

China has experienced population growth and increasing human N and P discharge from point sources. This paper presents estimates of N and P discharge from urban and rural areas in China and their fates (surface water, agriculture, and other) during the past decades. Between 1970 and 2015, China's nutrient discharge to surface water increased 22 fold from 177 to 3909 Gg N yr<sup>-1</sup> and 29 fold from 20 to 577 Gg P yr<sup>-1</sup> in urban areas. The ten strongly urbanized and industrialized provinces along the Eastern coast contributed 43% of China's total N and P discharge to surface water in 2015. At present, the contribution of rural areas to total wastewater discharge (2082 Gg N yr<sup>-1</sup> and 434 Gg P yr<sup>-1</sup>) is 35% for N and 43% for P. This study indicates that policies aiming at improving water quality need to consider these regional differences, i.e. improvement of the wastewater treatment technology level in Eastern regions and increasing both the sewage connection and wastewater treatment in Central and Western regions. A nationwide ban of P-based detergents is urgently needed.

### 2.1 Introduction

Human-induced intensification of the global cycles of nitrogen (N) and phosphorus (P) has detrimental impacts on aquatic ecosystems through eutrophication; ultimate symptoms of eutrophication include increased frequency and areal expansion of hypoxia and harmful algal blooms (Billen et al. 2001, Cloern 1996, Dodds 2002, Gruber and Galloway 2008). Nutrients are discharged to surface water from diffuse and point sources. Diffuse sources include nutrient flows in surface runoff, erosion, groundwater flows from agricultural fields, natural ecosystems and atmospheric deposition, and direct flows from aquaculture and vegetation in riparian and flooded areas. Point sources of nutrients are urban sewage systems that discharge at a limited number of locations in urban centers.

The impact of nutrient loading depends not only on the amounts of nutrients and the composition in terms of nutrient forms and their proportions but also on discharge location (Kemp et al. 2009, Seitzinger et al. 2010a). Therefore, it is essential to know both the diffuse (agricultural and natural) and point (wastewater) sources of nutrients when studying water quality and impacts of nutrient distortions caused by human activities.

Although urban areas cover only a small fraction (0.2-2.4%) of the global land area (Potere and Schneider 2007), N and P discharge to freshwater and coastal areas from point sources are substantial (Bouwman et al. 2005a, Harrison et al. 2005, Liu et al. 2018b, Van Drecht et al. 2009) because currently more than 55% of the global human population lives in cities (United Nations 2018). The N and P discharged from point sources stem from human households (excreta and P-based detergents) with or without a sewage connection, from industries that discharge wastewater containing nutrients, and from domestic animals (Billen et al. 2012, Li et al. 2012, Morée et al. 2013, Nyenje et al. 2010, Quynh et al. 2005, van Puijenbroek et al. 2019b). Construction of waste water treatment plants (WWTPs) often lags the sewage construction by several decades in many countries (Van Drecht et al. 2009). For example, in Europe and North America, the N and P loads showed a major increase in the 1960s and 1970s due to the massive connection of households to sewage systems and declined in the late 20th century due to the construction of WWTPs and the use of P-free detergents (Morée et al. 2013).

However, the nutrient discharge from the 45% of the global population living in rural areas, where next to sewage systems also other forms of sanitation such as septic tanks and pit latrines are found, is poorly known and often ignored. Several studies have explored the N and P fluxes from urban areas both at local, national and global scales based on models and data-based approaches (Chen et al. 2019, Morée et al. 2013, Tong et al. 2017b, Van Drecht et al. 2009, van Puijenbroek et al. 2019b, Zhang et al. 2020).

China has experienced a rapidly growing population to a current 1.4 billion and rapid urbanization to 57% during the last decades which caused rapidly increasing nutrient discharge from urban point sources (FAO 2019). However, available estimates are either regional (Tong et al. 2017b) or discontinued (Chen et al. 2019), consider urban wastewater discharge only and ignore changes in the number of inhabitants with a sewage connection. In addition, the number of inhabitants served by WWTPs and the removal efficiency of these WWTPs is poorly quantified and the fate of nutrients from households in rural areas is fraught with large uncertainty. Therefore, the long-term nutrient fluxes from China's point sources need to be systematically studied.

The aim of our study is to assess the actual functioning of wastewater treatment

throughout China and improve our knowledge on the rural wastewater flows. This paper presents a new spatial and temporal model-based, province-scale inventory of N and P in wastewater using detailed information on the location and functioning of WWTPs covering China for the period 1970-2015. Together with long-term estimates of nutrients from aquaculture (Wang et al. 2020) and agriculture (Bouwman et al. 2017), the results of the present work contribute to an up-to-date quantification of the nutrient loading to Chinese inland waters. This is an essential basis for analyzing the nutrient retention and accumulation in landscapes and waterscapes and nutrient export to coastal waters.

## 2.2 Methods and Data

This study is based on the spatially explicit wastewater nutrient model (Morée et al. 2013, Van Drecht et al. 2009, van Puijenbroek et al. 2019), which is part of the Integrated Model to Assess the Global Environment-Dynamic Global Nutrient Model (IMAGE-DGNM) (Liu et al. 2020, Vilmin et al. 2020). Here, we present a brief description and updates of input data and model.

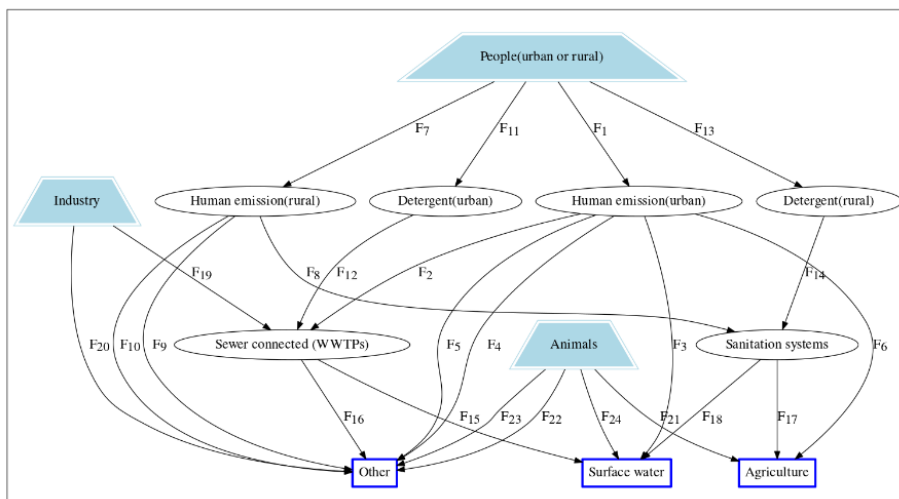


Figure 2.1. Scheme of the wastewater nutrient model in the IMAGE-DGNM framework, modified from Morée et al. (2013). Arrows indicate the fluxes  $F$  of N and P (see Table 2.1 for details) in human excreta, animal excreta, P-based detergents and industries to the agriculture system, surface water (i.e. discharge) and other compartments (including non-agricultural soils, atmosphere and groundwater). Light blue trapezoids represent the original sources of N and P. Blue rectangles represent the sinks of N and P.

The model calculates N and P fluxes in the human system, i.e. emissions from human

Table 2.1. List of nutrient fluxes in the human system.

Flux <sup>a</sup>	Description
$F_1$ and $F_7$	Human excreta from people in urban and rural areas, respectively
$F_2$	Human excreta to WWTPs through sewer connection in urban areas
$F_3$	Human excreta to surface water from urban population lacking sewer connection
$F_4$ and $F_9$	Retail and household waste
$F_5$ and $F_{10}$	Loss of skin and hair
$F_6$	Human excreta collection and use as fertilizer in agriculture
$F_8$	Human excreta to sanitation systems in rural areas
$F_{11}$ and $F_{13}$	P-detergent use in urban and rural areas
$F_{12}$	Detergent-P to WWTPs through sewer connection in urban
$F_{14}$	Detergent-P to sanitation systems in rural areas
$F_{15}$	Effluent from WWTPs to surface water
$F_{16}$	Sludge from WWTPs to other
$F_{17}$	Rural human excreta collection and use as fertilizer in agriculture
$F_{18}$	Effluent from rural sanitation systems to surface water
$F_{19}$	Industrial wastewater to WWTPs through sewer systems in urban areas
$F_{20}$	Industrial waste to ‘other’
$F_{21}$	Animal excreta collection and use as fertilizer in agriculture
$F_{22}$ and $F_{23}$	Volatilization and seepage of animal excreta
$F_{24}$	Animal excreta to surface water

<sup>a</sup> The fluxes numbers correspond to those routes in Figure 2.1.

excretion, urban industry, urban animal excretion and P emission from the use of detergents (dishwasher and laundry), and the fate of the nutrients (e.g. use in agriculture, direct discharge or wastewater treatment, direct defecation in surface water, and emission to the atmosphere) (Figure 2.1 and Table 2.1). In contrast to earlier applications at the national scale, we simulate the wastewater nutrient flows at the scale of 31 Chinese

provincial-level administrative regions (Figure 2.2) and include both urban and rural populations.

Rural and urban populations per province (Dataset S1) were obtained for the period 1970-2015 from the National Bureau of Statistics of China (National Bureau of Statistics of China 2015). Human N excretion was assumed to be equal to protein-N consumption minus N in retail and household losses and N stored in human bodies (hair, nails, skin, etc.) based on various sources (Neset et al. 2006, Oddoye and Margen 1979, Takahashi 1985). The model uses equal protein intake rates for rural and urban populations because there are no significant differences (Ju et al. 2018) in China. Data on protein consumption were obtained from FAO (FAOSTAT 2017). P excretion was assumed to be a fixed fraction of N ( $P=0.1 N$ ).



Figure 2.2. Chinese provincial-level administrative regions and geographical breakdown of the four economic regions in China. (Note: the relevant data of Hongkong, Taiwan and Macao are not included due to the lack of data).

Provincial data for sewage connection rate in urban areas was obtained from the Ministry of Housing and Urban-Rural Development of the People's Republic of China (Ministry of Housing and Urban-Rural Development of the People's Republic of China, 2016), assuming that households connected to a system of drinking water pipes also have a connection to a sewer. Sewage connection in rural areas exists (Table SI2.1), but

is not accounted for specifically (regarding nutrient removal) in the calculations.

Detailed data on 4436 WWTPs were obtained from the Ministry of Ecology and Environment of the People's Republic of China (Ministry of Ecology and Environment of the People's Republic of China, 2014). The dataset includes the location, treatment capacity, average load and technology for each WWTP in each province. These data were used to calculate the treatment capacity and actual operation loading for each WWTP and the aggregated results at the provincial scale for every year during the period 1970-2015.

The 42 treatment technologies distinguished (SI2.1) were grouped into four classes: primary, secondary, tertiary and quaternary treatment (Figure 2.3). Primary treatment includes the physical separation of large objects, plastic, wood, sand, et al. Secondary treatment is primary treatment plus aeration with active sludge (various organisms from archaea and bacteria to insects). Tertiary treatment is secondary treatment with additional (i) N removal by nitrification (aerobic) and subsequent denitrification (anaerobic), (ii) biological P removal by P accumulating bacteria with alternating starvation (low oxygen and nitrate) and banquet conditions (plenty oxygen and nutrients) and (iii) chemical P precipitation with Fe and Al coagulants; in recent years

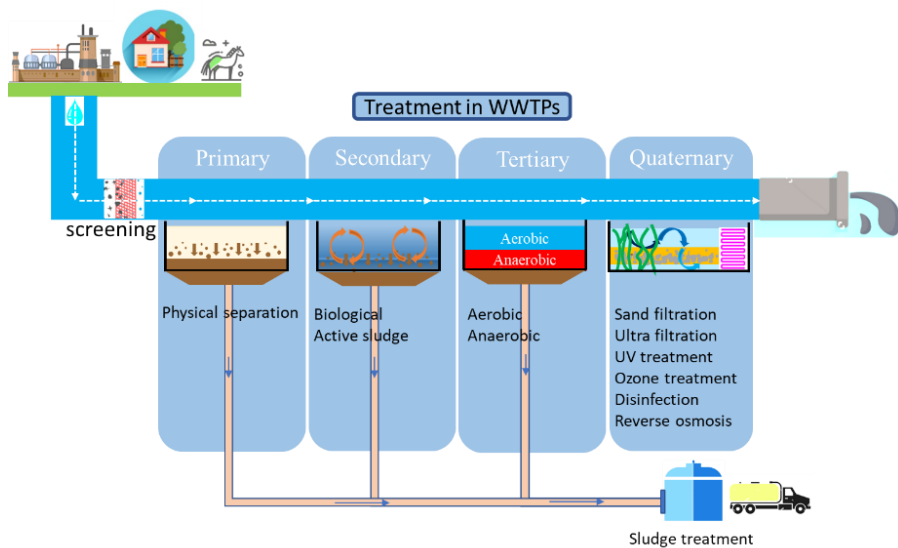


Figure 2.3. Scheme of wastewater treatment stages in the four sewage treatment classes. Every wastewater treatment class adds one or more treatment stages to those of the previous class(es)



also with Mg oxide or hydroxide to produce struvite. Quaternary treatment is tertiary treatment with additional steps such as sand filtration, ultra-filtration, ozone treatment, UV treatment, nano-filtration (NF), reverse osmosis (RO) and disinfection.

These treatment classes have typical removal rates, i.e. for primary, 10% for both N and P; for secondary, 35% for N and 45% for P; for tertiary, 80% for N and 90% for P; and for quaternary, 95% for both N and P. We recognize that these efficiencies are uncertain as they vary between installations depending on differences in design, operational and management conditions and skills of the operators (Barat et al. 2013, Hu et al. 2012, Oleszkiewicz and Barnard 2006a). Particularly efficient N removal requires a careful and tuned management of the various treatment steps.

The model is extended to calculate the contribution from rural human emissions discharged via sanitation systems (Figure 2.1,  $F_7$ ) (Table SI2.1). The most common systems in China are the septic tank, followed by the double-container composting system and biogas system (Ministry of Housing and Urban-Rural Development of the People's Republic of China, 2016). The national rural sanitation access rate for the period 1996-2014 (Figure SI2.2) is used for all provinces due to a lack of provincial data. For the year 1970, the sanitation access rate is assumed to be equal to that in urban areas. For the period 1971-1996, the sanitation access rate is interpolated by the model. For rural areas, we calculated the N and P fluxes with access to sanitation systems ( $F_8$ ), and the rest ( $F_9$ ,  $F_{10}$ ) is added to the sink “other” (Figure 2.1). The outflow from the sanitation systems is separated into fluxes to surface water ( $F_{18}$ ) and agriculture ( $F_{17}$ ). The difference between sanitation systems in rural area is not accounted for specifically in the calculations. Although there are large differences in the N and P removal rates from sanitation systems in rural areas (through biological processes, soil seepage and volatilization) depending on the prevailing sanitation system (SI2.1) (Li et al. 2009, Wang et al. 2008b), here a nutrient removal rate of 15% is used for rural inhabitants with access to sanitation systems (76% of rural population in 2014, Figure SI2.2) for both N and P. This also includes sewage systems in rural areas, where the 15% removal is in between those for primary and secondary wastewater treatment discussed above.

For urban areas, N and P waste from inhabitants lacking a sewage connection together with retail household waste and sewerage leakage ends in the “other” pool ( $F_4$ ,  $F_5$ ) and partially ends in surface water ( $F_3$ ) (Figure 2.1). The wastewater from sewage systems can be discharged to surface water directly ( $F_3$ ) or treated in the WWTPs ( $F_2$ ) (where the removal fraction depends on the type of wastewater treatment technologies (Figure 2.3). The model specifically accounts for urban draught animals, their excreta and the fate of these excreta. Animals in livestock production systems are not part of the wastewater model, and are part of the calculations of diffuse sources of nutrients

(Beusen et al. 2015).

The calculation method of detergent use ( $F_{11}$ ,  $F_{13}$ ) is a function of GDP as described in Van Puijenbroek et al. (2019b). For P content in laundry and dishwasher detergents, we used 6.25% and 11.7% (see SI2.6). For all the provinces in China, P detergents were linearly interpolated for the period 1970–2015. The use of dishwashers and laundry detergents in rural areas was assumed to be 50% of that in urban areas. P concentrations of detergents are described in SI2.6,

The sensitivity of model results to variation of 46 model parameters was calculated using Latin hypercube sampling (LHS) (Saltelli et al. 2000), using default ranges for each parameter (Morée et al. 2013). We performed 1000 runs for the year 2010. Expressing this sensitivity as standard regression coefficient (SRC) allows for ranking model parameters based on their effects on the N and P discharge to surface waters for the year 2010.

## 2.3 Results and Discussion

### 2.3.1 Emissions from urban areas

For China as a whole, the total N emission (prior to treatment) in urban areas increased from 0.5 to 5.4 Tg N yr<sup>-1</sup>, and that of P from 0.05 to 0.8 Tg P yr<sup>-1</sup> (Figure 2.4) between 1970 and 2015. The increase in total N emission was largely due to the increase of N from human emissions with an increasing contribution from 70 to 87% (Figure 2.4b, 2.4c). The increase in total P emission was mainly due to increases of P from human emissions (with a decreasing contribution from 68 to 56%) and detergent use (with an

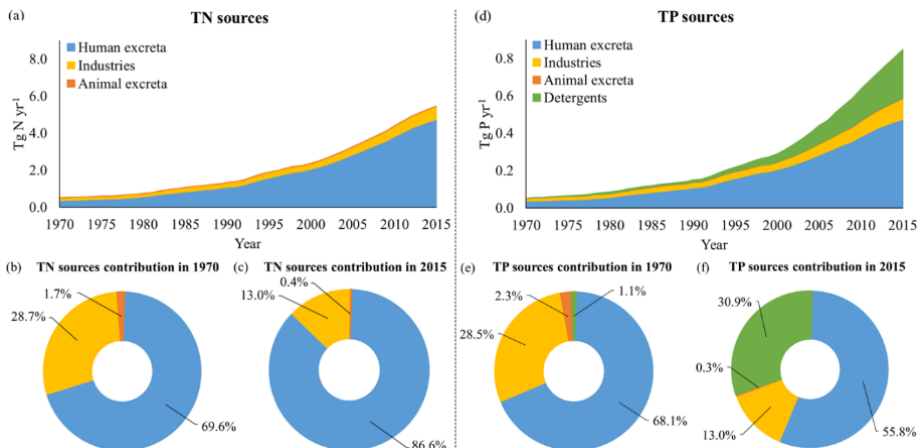


Figure 2.4. (a) National N emissions prior to treatment from different sources for the

period 1970–2015, and N sources in (b) 1970 and (c) 2015; (d) National P emissions prior to treatment from different sources for the period 1970–2015, and P sources in (e) 1970 and (f) 2015.

increasing contribution from 1 to 31%) (Figure 2.4e, 2.4f). Between 1970 and 2015, N emissions from industries (5 fold) and human waste (13 fold) increased less rapidly than the corresponding P emissions (7 fold for industries, 13 fold for human excretion, and 473 fold for detergents). The contribution of animal waste in urban areas declined from 2% to 0.4% for N and from 1% to 0.3 % for P during the same period.

### 2.3.2 Provincial and regional discharge to surface water from urban areas

N and P discharge to surface waters increased throughout the period 1970–2015 in all the provinces and economic regions (Figure 2.5, 2.6a, 2.6c). Urban N and P fluxes to surface water varied widely among the 31 provinces (Figure 2.5) and 4 economic regions (Figure 2.5 and 2.6a, 2.6c, Movie “P load to rivers.mp4”). N and P discharge to surface water increased by a factor of 21 and 27 (depending on the province between 1970 and 2015, primarily since 2000). The discharge in coastal provinces in Eastern China (Figure 2.5, 2.6a, 2.6c) is the largest of all regions for both N and P (Figure 2.6a, 2.6c) and the provinces of Guangdong, Shandong and Jiangsu are the three dominant provinces in Eastern China in 2015 (Figure 2.5b, 2.5d). In Central and Western China, Hunan and Sichuan account for the largest increases for both urban N and P discharge (Figure 2.5b, 2.5d).

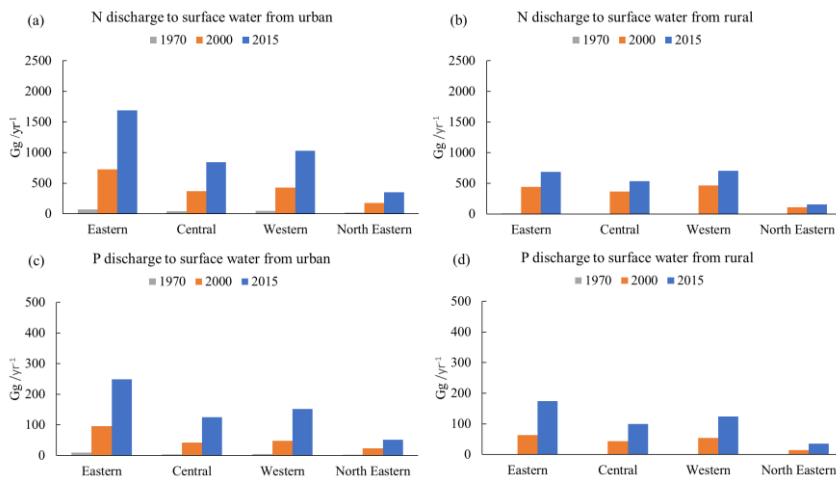
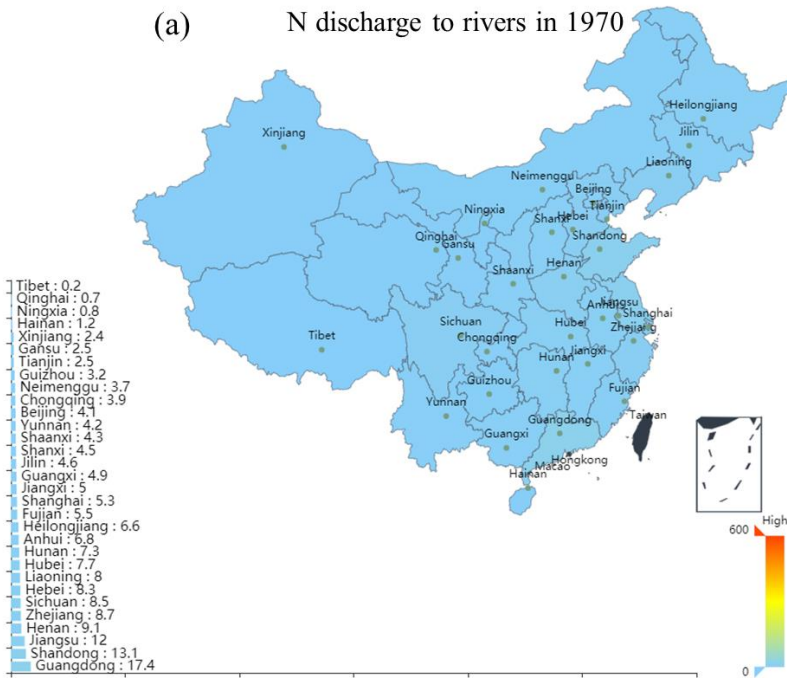
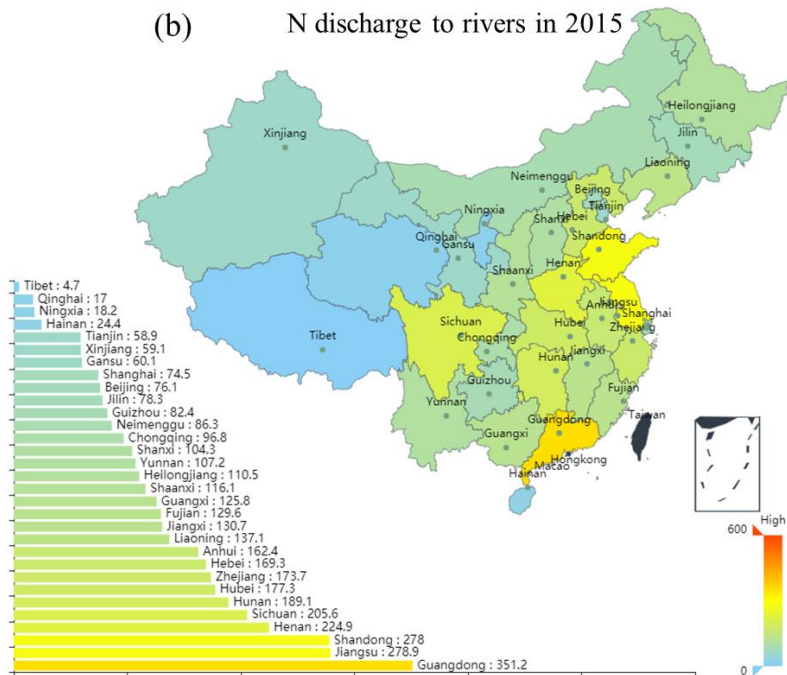


Figure 2.6. N (a,b) and P (c, d) discharge to surface water from the urban (left) and rural (right) areas for the period 1970–2015.

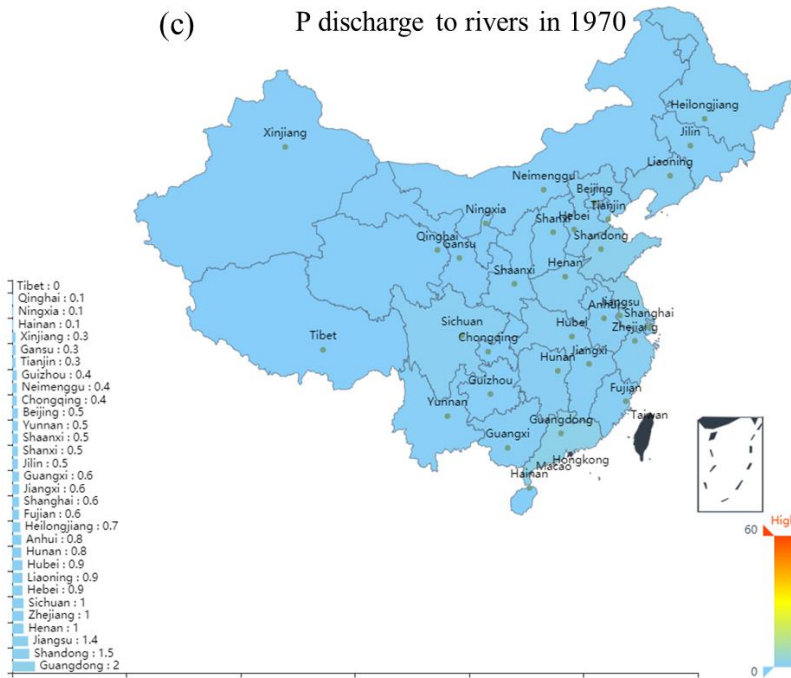
(a) N discharge to rivers in 1970



(b) N discharge to rivers in 2015



(c) P discharge to rivers in 1970



(d) P discharge to rivers in 2015

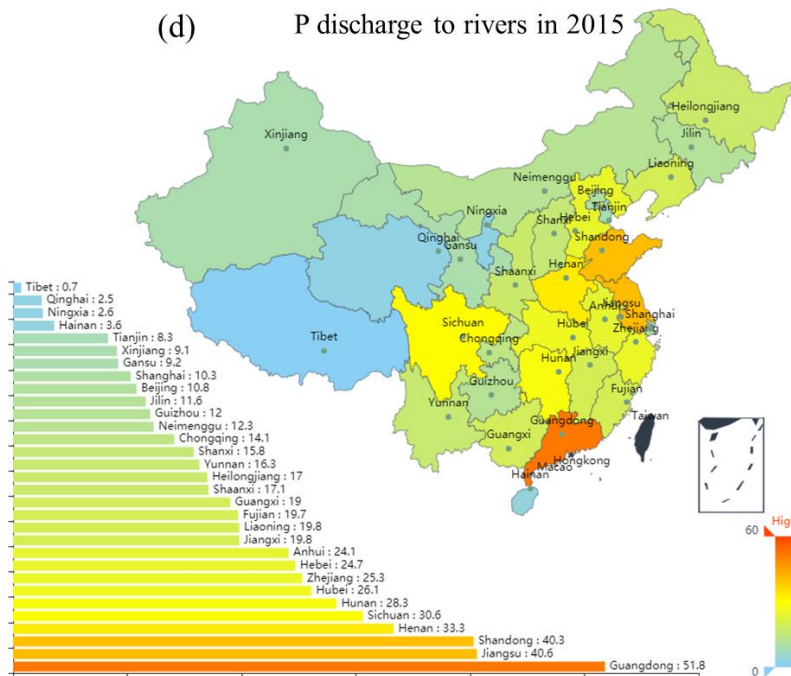


Figure 2.5. Spatial distribution of nutrient discharge from urban areas to surface water for N in a) 1970 and b) 2015; and for P in c) 1970 and d) 2015. Unit is  $Gg\ yr^{-1}$  of N or P.

### 2.3.3 Sewer connection and treatment removal from urban areas

The sewer connection rates in the two largest municipalities in China, Beijing and Shanghai, both increased from 5% in 1970 to 100% in 2015 (Figure 2.7c). During the same period, the N and P treatment removal in individual provinces showed different patterns (Figure 2.7a, 2.7b) due to differences in treatment technologies and the average provincial capacities of all WWTPs. For example, the nutrient removal in Beijing and Shanghai (red circles in Figure 2.7a, 2.7b) is much more efficient than those in other provinces.

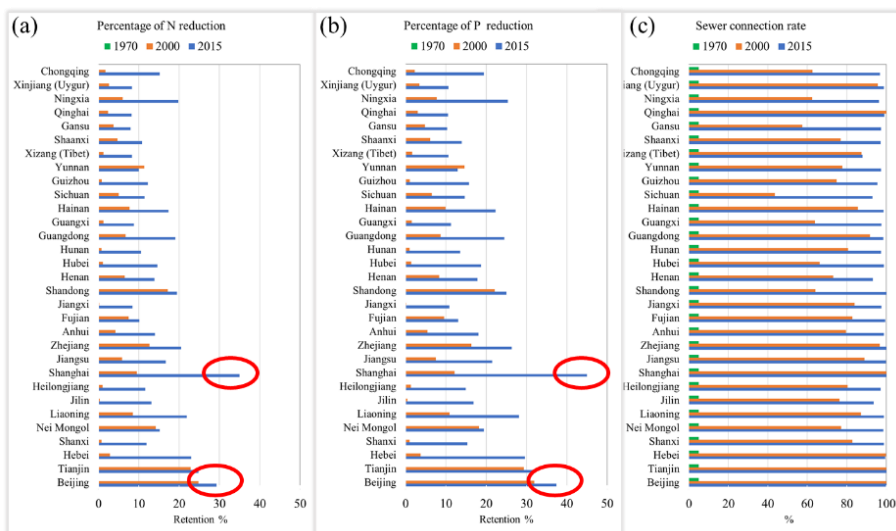


Figure 2.7. Removal percentage of (a) N and (b) P for all the treatment in WWTPs and (c) sewage connection for the 31 Chinese provinces for the years 1970, 2000 and 2015. Red circles represent removal efficiency in Beijing and Shanghai, China's most developed provincial-level administrative regions.

P is removed more efficiently than N in all the provinces (Figure 2.6b). By aggregating all actual operational loading and technologies of the WWTPs present in the cities in three coastal provinces (Shanghai, Jiangsu and Zhejiang) in 2014, the removal rates of P are 45%, 21% and 25% for Shanghai, Jiangsu and Zhejiang, respectively.

Even in the most developed city of Shanghai with a 100% sewage connection rate, most wastewater treatment plants have secondary technology. Therefore, the P and N treatment removal rates calculated in this study are lower than the 82% for P and 63% for N estimated in recent studies (Qi et al. 2020, Zhang et al. 2020), which ignored the considerable contribution of detergents and the actual capacity and loads of WWTPs. Another recent estimate (Chen et al. 2019) did not capture the spatiotemporal differences presented here because it used an overall sewer connection rate of 73% in all urban areas and 1.8% in rural areas and ignored the differential changes over time in the various provinces. More details of the comparison with other studies are summarized in Table SI2.2.

### 2.3.4 Total urban discharge to surface water and N:P ratio change

The urban N discharge to surface water increased 22-fold from 177 Gg N yr<sup>-1</sup> to 3909 Gg N yr<sup>-1</sup> (For P, 29-fold from 20 Gg P yr<sup>-1</sup> to 577 Gg P yr<sup>-1</sup>) between 1970 and 2015 (Figure 2.8a). For 2000, our estimated nutrient discharge of 1670 Gg N and 206 Gg P (Figure 2.8a) can be compared with a recently estimated discharge of 1327 Gg N and 165 Gg P (van Puijenbroek et al. 2019). The difference is small, but this is a result of two counteracting features: a higher sewer connection rate based on provincial data in the present study versus national data (van Puijenbroek et al. 2019), combined with higher removal rates (mostly secondary treatment in this study versus mostly primary treatment in van Puijenbroek et al. (2019)).

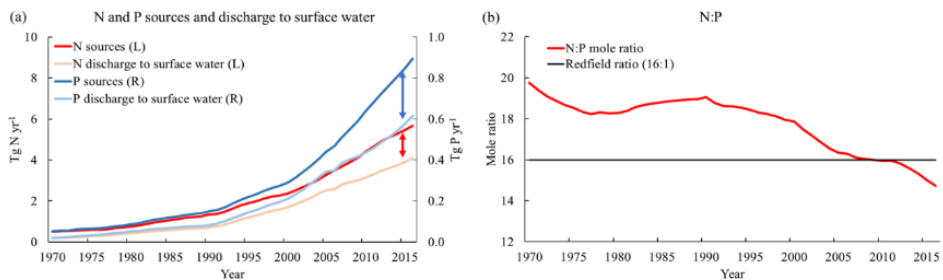


Figure 2.8. (a) N (L, left) and P (R, right) urban sources (inputs from human excreta, P detergents, animal excreta and industries), and N and P discharge to surface water via WWTPs, and (b) N to P molar ratio.

The substantial increase in the discharge of P relative N is due to the rapid increase in the use of dishwasher and laundry detergents, which primarily occurred between 2000-2015 (Figure 2.4d, 2.4f). The increase in WWTPs and upgrade of treatment technologies were not sufficient to balance the increase of the P discharge from detergents.

In China, a local ban on the sale of P-detergents started from 1999 in the Lake Tai basin, due to severe eutrophication problems (even disrupting the drinking water supply). Other regions like Lake Dianchi and Lake Chao and megacities like Shenzhen and Shanghai followed with similar regulations. However, there is no national-wide ban on the use of P-containing detergents, and the existing national detergents criteria still allow for the production and sale of P-containing laundry and dishwasher detergents (Standardization Administration of China).

As a consequence of the increasing P discharge induced by boosting detergent use, the N:P molar ratio in urban wastewater discharge decreased from 20 to 15 during the period 1970-2015 (Figure 2.7b), even though the removal efficiency of P is much higher than N in WWTPs (Figure SI2.3 and Figure 2.7a).

The WWTPs with tertiary and quaternary technologies account for 3% of total WWTPs (file *Dataset S1.xlsx*). Even in the wealthiest cities like Beijing and Shanghai, with a 100% sewage connection rate, most wastewater treatment technologies are secondary. In the developed western EU countries where tertiary WWTPs prevail, the P removal fractions in WWTPs range between 68%-90% (for N 49%-85%) (Hendriks and Langeveld 2017, Longo et al. 2019, Oleszkiewicz and Barnard 2006b, van Puijenbroek et al. 2019b). Therefore, our results suggest that the P and N treatment removal fractions in WWTPs of 82% for P and 63% for N estimated were overestimated in recent studies (Qi et al. 2020, Zhang et al. 2020).

### 2.3.5 Discharge from rural areas

At the national scale, China's N discharge to surface water in rural areas increased from 16 Gg to 2082 Gg from 1970 to 2015, mainly stemming from human waste. For P, the discharge to surface water increased from 3 Gg to 434 Gg from 1970 to 2015. The contribution of rural areas to total wastewater discharge is 35% for N and 43% for P in 2015.

Although massive and rapid urbanization has taken place in recent decades, rural inhabitants still accounted for 43% of the total population in 2015. The rural migrants working and living in urban areas increased from 30 million in 1989 to 277 million in 2015 (National Bureau of Statistics of China, 2015), while part of them are still counted as rural population due to Hukou (household) system of residency permit (Keung Wong et al. 2007), which may lead to overestimation of the contribution from rural areas and underestimation of the contribution from urban areas. Assuming the rural migrants live in urban areas for half of the year, implies an additional ~18% nutrient emission (Figure 2.1,  $F_1$ ) from urban populations in 2015.



The N discharge from rural areas (Figure 2.6b) is increasing much more slowly than that from urban areas since 2000 (Figure 2.8a). This slight increase in rural areas is the combined effect of the increase in protein consumption resulting from income growth and the decrease of the absolute number of rural inhabitants. Nevertheless, despite this declining rural population, the P discharge to surface water showed a rapid increase, which is mainly due to the increasing use of dishwashers and laundry detergents. At present, the contribution of rural areas to total wastewater discharge is 35% for N and 43% for P.

### **2.3.6 Policy implications**

On the basis of the mass fluxes of N and P from humans, animals and industries to surface water using the data on the capacity and removal efficiency for 4436 WWTPs, our results indicate that to bend the increase of N and P discharge to surface water, the stagnant treatment technologies in WWTPs need to be incrementally improved from secondary to tertiary treatment over time, especially in the 10 provinces of Eastern China.

A major finding from this study is that the P discharge to surface water showed a rapid increase both in rural and urban areas, which is mainly due to the lack of nation-wide ban of P-based detergents and manifold increasing use of P-containing dishwasher and laundry detergents. Therefore, eliminating the production and sale of P-containing detergents via national legislation is urgently needed.

Finally, the N and P contributions of the rural population have been neglected in quantitative studies until now. Our results suggest a considerable contribution of the rural population to N and P pollution of freshwater environments in China, although the fate of the nutrients discharged through septic systems, double-container composting systems, biogas systems and sewage systems is poorly known. As a strategy for controlling wastewater pollution, the “Toilet Revolution” has become a buzzword in China in recent years (Cheng et al. 2018). However, relevant estimates are uncertain due to a lack of data on the removal rates in the different sanitation technologies used in rural areas, such as different septic systems and the unknown role of direct discharge of human waste to surface water.

Construction of wastewater treatment installations and sewage systems in urban areas may technically be the most common way to dispose of human waste. However, future developments should consider that the traditional sewage connection itself may not be the best option to mitigate eutrophication with the risk of wasting large quantities of economically accessible high-quality N and P (Cordell et al. 2013, Cordell and White 2014, Van Vuuren et al. 2010). Sophisticated sewage systems with separate urine

collection from households may be an efficient option in future urban planning to recycle nutrients, such as fertilizer in agriculture.

A number of biological, physical and chemical process separation systems have been developed for nutrient removal from urine (Maurer et al. 2006, Pronk and Kone 2009, Wilsenach et al. 2007), (Zhang et al. 2014). This can substitute considerable amounts of N and P fertilizers and largely mitigate water pollution. Another option, especially for rural areas, is ecological sanitation, which combines improved sanitation with the recycling of nutrients (Langergraber and Muelleggera 2005, Simha and Ganesapillai 2017).

## Supplementary Information

### SI2.1 Comparison of WWTPs technologies among provinces in different regions

For the complete list of all the 4436 WWTPs, the total 42 technologies in China, the cumulative capacity and average loading in every province, see the separate file *Dataset SI.xlsx*.

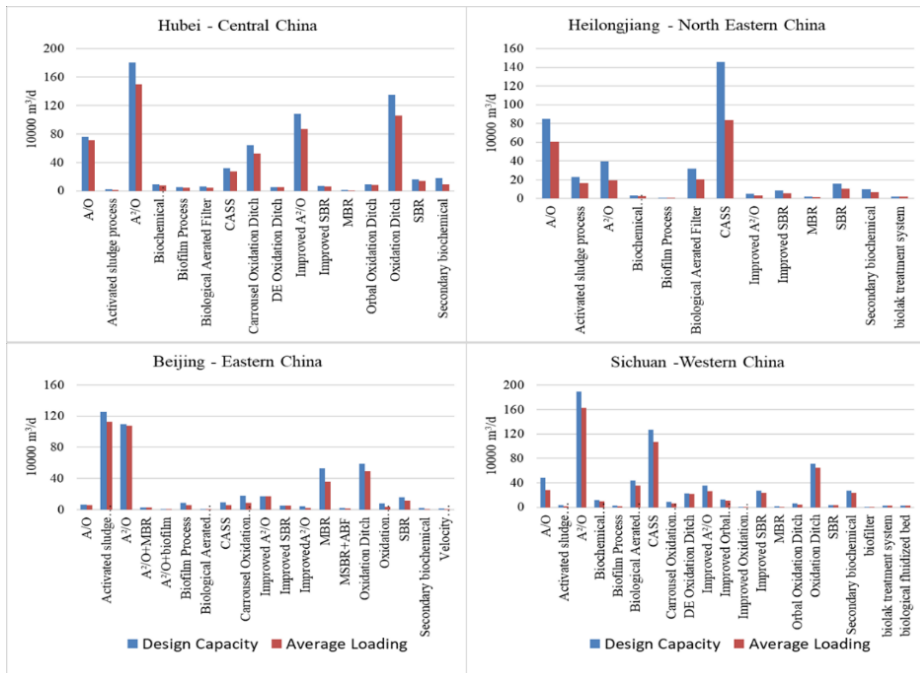


Figure SI2.1 Comparison of WWTPs technologies in the representative provinces in different regions

## SI2.2 Rural household Sanitation systems in China

Table SI2.1 Rural household sanitation systems in China in 2002

No.	Description	Coverage (% of the rural population)
1	Three-Compartment Septic Tank	13
2	Double container composting system	5
3	Biogas system	4
4	Toilets with separation of excrement and urine	27
5	Toilets connected to sewerage systems	
6	Latrines with deep pits / double pits / improved ventilation	
	Total	49

Source: National Patriotic Health Campaign Committee of China (NPHCC) Annual Report 2002.

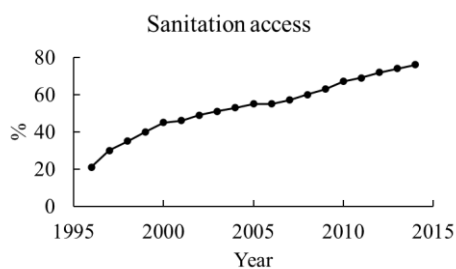


Figure SI2.2 China's national sanitation access in rural areas during 1996-2014. Source: China Urban-Rural Construction Statistical Yearbook 2015.

### SI2.3 N and P removal rates in WWTPs in different regions

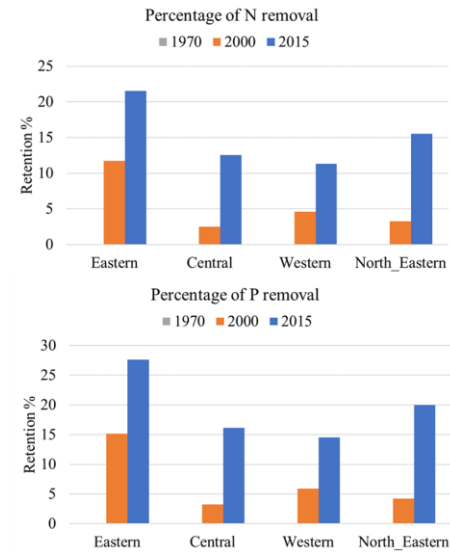


Figure SI2.3 N and P removal in WWTPs in different regions.

## SI2.4 Comparison with other studies

Table SI2.2 Comparison of the differences between this study and other studies

Description	Morée et al. (2013)	Puijenbroek et al. (2019)(van Puijenbroek et al. 2019)	Tong et al. (2017)(Qi et al. 2020, Tong et al. 2020, Tong et al. 2017b, Zhang et al. 2020)	Chen et al. (2019)(Chen et al. 2019)	This study
Spatial resolution	Nation	Nation	Province	County	Province/region
Temporal resolution	Year	Decade	Year	Year	Year
Covering period	1900-2000	1970-2050	2006-2014	2012	1970-2015
Detergents	Included	Included	Not included	detergents not included in equations	Included
Sewage connection rate	Dynamic sewage connection rate for every country in every year	Dynamic sewage connection rate for every country in every decade	Not considered; most of the flux in provinces with low connection rates was ignored	Constant sewage connection rate for all the urban/rural area	Dynamic sewage connection rate for every province in every year
Capacity and loading of WWTPs	Not included	Not included	Not included; based on designed effluent standards	Not included	Included; the cumulative loading and capacity are dynamically calculated

N and P removal rates for different technologies in WWTPs	primary/ secondary/ tertiary/ quaternary	primary/ secondary/ tertiary/ quaternary	Removal rate based on designed effluent standards ignoring types of WWTPs	Removal rate for different technologies based on 1822 WWTPs	Based on 4436 WWTPs; all the technologies covering the mainland China are sorted; all technologies are aggregated to primary/  secondary/ tertiary/  quaternary
Urban/rural sanitation	Urban sewage	Urban sewage	Urban sewage	Urban and rural sewage	Urban and rural sanitation types
Calibration	No calibration	No calibration	No calibration	With calibration	No calibration

## SI2.5 Sanitation data for China

The Joint Monitoring Programme for Water Supply, Sanitation and Hygiene (JMP) data from WHO-UNICEF are used to compare service levels in different countries. It has been updated and expanded to facilitate enhanced global monitoring of sanitation and hygiene. The newly established classification of sanitation types covers urban and rural areas. Data are listed in the file Dataset S1.xlsx. It can be used to extend our model further.

## SI2.6 P content of detergents

- 1) What is P-free laundry detergent in China?

The national standard “*Laundry powders (P-free) (GB/T 13171.2-2009)*” was initially issued in 1997 and updated in 2004 and 2009. In China, P-free detergent has a P content of less than 1.1%, but this national standard has not been enforced at the national scale. The first local ban on the sale of P-detergents started in 1999 in the Lake Tai basin due to severe problems (disruption of drinking water supply) arising from the severe eutrophication. Even recent years, some local authorities ban P-containing detergents, but a national policy is still lacking.

- 2) What is P-containing laundry detergent in China?

According to the national standard “*Laundry powders (P-contained) (GB/T 13171.1-2009)*” issued in 2004 and updated in 2009, P-based laundry detergents have a P content of  $\geq 8\%$ . This national standard still exists today.

- 3) What is P-containing dishwashing detergent in China?

There is no P limitation in the national standard “*Detergents of hand dishwashing (GB/T 9985-2000)*”.

- 4) What is the use of sodium tripolyphosphate (STPP) in China?

Global sodium tripolyphosphate consumption was more than 3 million tons in 2015, China accounting for more than 40%.

- 5) What is the P concentration in our model?



With the use of STPP and the total volume of laundry and dishwasher detergents, and lacking national legislation for the use of P-free detergents, we employ the following estimates for the P content in detergents:

P content of laundry detergents (kg P /kg detergents) = 6.25%.

Regarding the P-content of dishwasher detergents, P content of dishwasher detergents (kg P /kg detergents) = 11.7%.

Regarding the P-free of detergents, P content of laundry detergents is 0%.



## Chapter 3

# Exploring long-term changes in silicon biogeochemistry along the river continuum of the Rhine and Yangtze (Changjiang)

---

Xiaochen Liu, Wim Joost van Hoek, Lauriane Vilmin, Arthur H.W. Beusen, José M. Mogollón, Jack J. Middelburg, Alexander F. Bouwman

---

*Environmental Science & Technology*, 2020, 54, 19, 11940–11950.

### Abstract

This paper presents the spatially explicit (0.5 degree spatial resolution) DISC-SILICON module, which is part of the IMAGE-DGNM global nutrient cycling framework. This new model for the first time enables to integrate the combined impact of long-term changes in land use, climate and hydrology on Si sources (weathering, sewage and soil loss) and sinks (uptake by diatoms, sedimentation and burial) along the river continuum. Comparison of discharge and dissolved silica results with observations shows a good agreement both in the Rhine and Yangtze. The simulated total Si export for the Rhine is stable during the period 1900-2000. The total Si export for the Yangtze decreased (155 to 51 Gmol yr<sup>-1</sup>) due to damming and transformation of 40% of the natural vegetation to cropland. As a result of dam construction in the Yangtze, diatom primary production (from 14 to 26 Gmol yr<sup>-1</sup>) and burial (11 to 24 Gmol yr<sup>-1</sup>) increased and the DSi export decreased (145 to 56 Gmol yr<sup>-1</sup>) from 1950s to 1990s. The Three Gorges Reservoir has a large contribution to diatom primary production (11%) and burial (12%) in the Yangtze River basin. DISC-SILICON reproduces a flooding-induced increase in Si inputs and burial and the legacy of this temporary storage in subsequent dry years.

### 3.1 Introduction

Silicon (Si) occurs in the Earth's crust primarily as silicate minerals in igneous, sedimentary and metamorphic rocks. Weathering of silicate minerals is the ultimate source of dissolved silicate (DSi) in rivers and the global ocean (Berner and Berner 1996, Treguer et al. 1995b, Tréguer and De La Rocha 2013). Terrestrial vegetation incorporates Si in phytoliths, forming biogenic silica (BSi). BSi stored in plants and soils can be transported to streams and rivers by surface runoff and erosion and can dissolve to form DSi (Conley 1999, 2002, Derry et al. 2005). DSi is required for the growth of siliceous algae (diatoms), an important phytoplankton group that uses Si to build their external skeleton (frustule). A change in DSi availability thus directly

influences phytoplankton composition and overall primary production in both inland and coastal marine waters (Garnier et al. 2010, Tavernini et al. 2011).

Anthropogenic perturbations impact DSi delivery to rivers and transport through the river continuum, including land use change, dam construction and nutrient loading to rivers. BSi and DSi are connected via precipitation, dissolution, and uptake by plants and diatoms (Struyf et al. 2010). Land use has a major impact on the mobilization of Si in river basins through its impact on all these processes (Phillips and Cowling 2019, Struyf et al. 2010). Silicate weathering rates are higher in forests compared to cropland (Humborg et al. 2002, Kelly et al. 1998), leading to high uptake rates and transformation to BSi in phytoliths (in plant biomass, and via litter in soil organic matter). DSi stemming from rock weathering is thus cycled in the soil-plant system. A small part of the Si stored in soils can be lost via surface runoff and erosion and delivered to surface water (Derry et al. 2005).

Human perturbation has major consequences for the riverine Si cycle in several ways: (i) By transforming natural vegetation to cropland or grassland, the soil-plant Si cycle is perturbed by harvesting the crop or grass biomass and thus removing BSi. Enhanced soil erosion from agricultural fields will further deplete the soil BSi pool (Struyf et al. 2010), which eventually leads to reduced Si delivery to surface water. (ii) By constructing reservoirs, the water travel time increases, which causes an increase in DSi retention due to burial of BSi in dead diatoms (Beusen et al. 2009b, Garnier et al. 1999, Harrison et al. 2012, Humborg et al. 2006, Maavara et al. 2014, Ran et al. 2013). Sediments in lakes and reservoirs are thus (temporary) BSi stores which by dissolution can be a source of DSi (Ran et al. 2019). (iii) By enhanced nutrient loading from agriculture and wastewater, which causes eutrophication. Eutrophication enhances DSi retention in reservoirs, as increasing nitrogen (N) and phosphorus (P) inputs stimulate diatom growth (Ran et al. 2019). As a result, the molar N:Si and P:Si ratios in the water transported to the coastal ocean in dammed rivers are often higher than in the pre-dam situation (Conley 1997). The overall result of all these processes is an excess of N and P over the requirements of diatoms. This causes proliferation of non-diatom phytoplankton and may eventually lead to harmful algal blooms (HABs) (Anderson et al. 2002, Billen et al. 2007, Conley 1999, Humborg et al. 2008, Wollheim et al. 2008, Xiao et al. 2019, Yu et al. 2018, Zhou et al. 2020) in coastal ecosystems.

Since the first observations of DSi concentrations in rivers (Clarke 1920), a series of studies focused on the global Si budget and retention in lakes and reservoirs (Dürr et al. 2011, Laruelle et al. 2009, Treguer et al. 1995, Van Bennekom and Salomons 1981). There is an increasing interest in understanding the changing DSi loads of the world's rivers, lakes and reservoirs and their relation to anthropogenic changes (Beusen et al.

2009, Harrison et al. 2012, Humborg et al. 2000, Humborg et al. 1997, Maavara et al. 2014, Moon et al. 2014). Future plans for the construction of a series of dams in the Yangtze river and other rivers worldwide (Lehner et al. 2011), changing climate and continued land-use changes are a major cause of concern. Models are often used to study the impact of anthropogenic activities on riverine Si biogeochemistry. Beusen et al. (2009) developed a river-basin scale multiple regression model to describe global river export of dissolved DSi. Laruelle et al. (2009) and Dürr et al. (2011) presented a global Si box model to estimate Si retention and export. Maavara et al. (2014) developed a process-based model of Si retention in global reservoirs. All above global approaches generate snap-shot estimates for a single year and lack long-term variation. Furthermore, these studies are based on poorly constrained hydrology, and lack the spatial distributions of the controls of Si supply from weathering, the impact of land-use change, the temporary storage of Si in sediment, and the in-stream biogeochemistry in streams, rivers, lakes, and reservoirs.

We therefore need a spatially explicit, process-based biogeochemistry model that can describe diatom production and DSi uptake, decay of diatoms, BSi dissolution and Si transformations under decades-long human interferences to include the impact of large-scale accumulation or depletion of Si stores in soils of the watershed or in sediment. We developed the biogeochemistry module Dynamic In-Stream Chemistry (DISC)-SILICON, which is part of the Integrated Model to Assess the Global Environment (IMAGE)-Dynamic Global Nutrient Model (IMAGE-DGNM) (Vilmin et al. 2020d). Within IMAGE-DGNM, DISC-SILICON describes the supply and processing of Si, considering long-term (20th century) changes in land use, climate, and hydrology to link Si sources (weathering, sewage and soil erosion) and sinks (uptake by diatoms, sedimentation and burial) for every global 0.5 by 0.5 degree grid cell.

We tested whether our model reproduces the observed long-term changes in the riverine Si cycle as influenced by human activities for two major rivers with contrasting geohydrological conditions, history of land-use change, and dam construction, i.e. the Rhine and Yangtze (Changjiang) (see Table SI3.4). The Yangtze River is the largest river in the Eurasian continent, with an average annual discharge of  $892 \text{ km}^3 \text{ yr}^{-1}$  (1950-2000), covering an area of  $1.8 \times 10^6 \text{ km}^2$  and with a length of 6400 km (Changjiang River Water Resource Committee 1955-1985). It hosts 35% of China's population and receives 32% of the total Chinese fertilizer inputs (Xing and Zhu 2002). Expansion of agricultural land in the Yangtze basin has been dramatic during the 20th century (Yan et al. 2003), and the construction of a series of major and minor dams has drastically changed the hydrology (Ran et al. 2019). The most recent dam is the Three Gorges Dam, that led to formation of the Three Gorges Reservoir (TGR) in the Yangtze valley with a length of 550 km. The water level reached 175 m after filling between 2003 and 2009

and with the TGR capacity of 39 km<sup>3</sup>, the total reservoir capacity in the Yangtze River basin reached 142 km<sup>3</sup> (Ran et al. 2013). The Rhine River is the second-longest river in Western and Central Europe, with an average annual discharge of 75 km<sup>3</sup>, a length of 1350 km and an area coverage of 185,620 km<sup>2</sup> (Van der Weijden and Middelburg 1989). The Rhine drains intensive agricultural land and strongly urbanized areas and hosts 58 million inhabitants (Tockner et al. 2009). In contrast to the Yangtze, the river Rhine has not experienced important forest clearing to expand agricultural land during the 20th century, has a series of small dams (Admiraal et al. 1990) and it has no major dams (Admiraal et al. 1990).

## **3.2 Methods**

### **3.2.1 Model description**

#### **3.2.1.1 General aspects**

IMAGE-DGNM (Vilmin et al. 2020) is a global, spatially explicit coupled nutrient cycling - hydrology model, which calculates nutrient delivery, in-stream retention and export to the coastal ocean. This model is inspired by the Riverstrahler model (Garnier et al. 2002, Sferratore et al. 2006) which also couples hydrology and biogeochemistry. In Riverstrahler, the inputs of all stream segments of the same Strahler order are lumped within a sub-basin. Instead, in DGNM every grid cell has its specific environmental, hydrological, and land use conditions. In IMAGE-DGNM (Figure SI3.1), the spiraling method for calculating in-stream retention is replaced by the process-based biogeochemical module Dynamic In-Stream Chemistry (DISC) (Vilmin et al. 2020). All data used in the model have a 0.5 by 0.5 spatial degree resolution. The temporal resolution is variable, selected on the basis of the process considered, and here we use an output time step of one year.

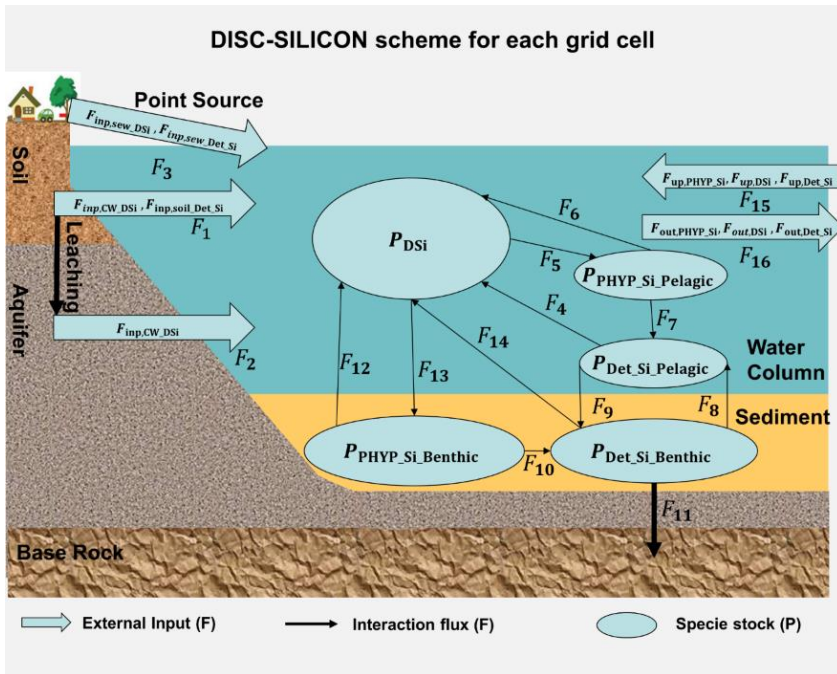


Figure 3.1 Scheme of the DISC-SILICON module showing the external input fluxes ( $F_1$ ,  $F_2$ ,  $F_3$ ), the transformation fluxes  $F_4$ - $F_{16}$  between the pools  $P_{DSi}$ ,  $P_{PHYP\_Si\_Pelagic}$ , and  $P_{Det\_Si}$  in the water column and  $P_{PHYP\_Si\_Benthic}$  and  $P_{Det\_Si\_Benthic}$  in the sediment within each grid cell and the transfers with neighboring grid cells. The numbers correspond to the fluxes listed in Table 3.2.

In the framework, IMAGE-DGNM provides data to DISC on (i) spatial land cover, climate and water use, (ii) spatial distributions of population density as a source of Si in wastewater, (iii) Si flows via soil loss to surface water, and (iv) soil types and lithology as a source of DSi weathering (Figure SI3.1). The hydrology model PCR-GLOBWB (Sutanudjaja et al. 2018, Van Beek et al. 2011) provides runoff, waterbody area and volume, discharge, and flow direction for the Strahler stream orders  $\geq 6$ , while simulation of hydrology for the smaller stream orders ( $< 6$ ) hydrology is parameterized following Wollheim et al. (2008) as described in detail by Beusen et al. (2015). An important feature is that the history of dam construction is captured using data on date of construction and filling, reservoir area, depth and volume (in the Yangtze basin, this includes Danjiangkou reservoir (1960s), Gezhouba (1980s) and TGR (2003) (Table 3.1)).

Table 3.1 Source of input and validation data.

Parameter/data type	Data Source
<b>Hydrology</b>	
Runoff, water area and volume, discharge, flow direction for 1900-2010	PCR-GLOBWB (Sutanudjaja et al. 2018, Van Beek et al. 2011)
Reservoirs	Date of construction, area, depth and volume for 6862 dams in the world <sup>36</sup>
Lakes	Global Lakes and Wetlands Database (GLWD)(Lehner and Döll 2004)
<b>Meteorology</b>	
Temperature	Global climate database (New et al. 2000)
Solar radiation	Model describing irradiation as a function of latitude and turbidity (van Hoek et al. 2021)
<b>Diffuse Sources</b>	
Soil loss, soil type	IMAGE-GNM (Beusen et al. 2015)
Lithology	Global lithology map at 5 by 5 minute resolution (Dürr et al. 2005)
Det_Si content in soil	Data from Riverstrahler model (Sferratore et al. 2006)
<b>Point Source</b>	
Population	IMAGE-GNM (Beusen et al. 2015)
DSi and Det_Si wastewater effluent	Data from Riverstrahler model (Sferratore et al. 2006)
<b>Water quality</b>	
Validation data in Rhine	GLORICH database ( <a href="https://www.geo.uni-hamburg.de/en/geologie/forschung/geochemie/glorich.html">https://www.geo.uni-hamburg.de/en/geologie/forschung/geochemie/glorich.html</a> ) (Hartmann et al. 2014a)
Validation data in Yangtze	Changjiang Water Resources Commission (Changjiang River Water Resource Committee 1955-1985) from 1960 to 1984 and literature (Li et al. 2007, Wang et al. 2018) for the period after 1984



Table 3.2 List of processes and equations in each grid cell. All parameters and values including units are presented in SI3.3.

Flux #	Description
$F_1$	Det_Si input from soil particles into the water (erosion) DSi input from weathering via surface runoff
$F_2$	DSi input from weathering via ground water
$F_3$	DSi input from point source Det_Si input from point source
$F_4$	Det_Si_Pelagic dissolution which is dependent on water temperature, the dissolution rate and size of the pool of the Det_Si_Pelagic. $f(T_W) * k_{\max\_Det\_Si\_Pelagic\_dissolution} * P_{Det\_Si\_Pelagic}$ where $T_W(^{\circ}C)$ is the water temperature and $f(T_W) = e^{-\frac{(T_{opt\_growth}-T)^2}{(T_{sigma\_growth})^2}}$
$F_5$ and $F_{13}$	Primary production (diatom growth) $k_{\max\_growth} * Lim_{light} * f(T_W) * DSi_{conc} / (K_{DSi,PP} + DSi_{conc})$ Where $k_{\max\_growth}$ , is the maximum diatom growth rate which differs between pelagic and benthic diatoms. $DSi_{conc}$ is the DSi concentration in water column, $K_{DSi,PP}$ is the half saturation concentration in the Michaelis-Menten function. The light intensity limitation is calculated both for pelagic and benthic diatoms, by using the spatial distribution of solar radiation and light attenuation with depth using turbidity of the water column. $Lim_{light}$ is the light limitation which is calculated using solar radiation and water turbidity. $Lim_{light} = \frac{I_z(lat)}{(I_z(lat) + k_{l,PHYP\_Si\_Benthic})}$ , for benthic diatoms $Lim_{light} = \frac{\int_0^z I_0(lat)}{(\int_0^z (I_0(lat) + k_{l,PHYP\_Si\_Pelagic}) dz)}$ , for pelagic diatoms Where $I_z$ and $z$ are light intensity and depth, $k_l$ is the half saturation for light limitation with Michaelis-Menten equation, here we use the Beer-Lambert equation. $I_z = I_0(lat) * e^{-\eta_{tot} * z}$

	<p>Where <math>I_{0(lat)}</math> is the solar radiation at water surface at latitude <math>lat</math>,</p> $I_0(lat) = \theta_s(lat) * I_{solar\_constant}$ <p><math>\theta_s</math> is the solar zenith angle, <math>I_{solar\_constant}</math> is the solar constant <math>1367 \text{ Wm}^{-2}</math>.</p> <p><math>\eta_{tot}</math> is the water turbidity which is calculated with all the particulate matter that affect the light attenuation:</p> $\eta_{tot} = \eta_{water} + \eta_{Det\_Si} * [P_{Det\_Si\_Pelagic}] + \eta_{PHYP\_Si\_Pelagic} * [P_{PHYP\_Si\_Pelagic}] + \eta_{PIM} * [P_{PIM}]$ <p>Where <math>P_{PIM}</math> is the total particulate inorganic matter, mostly is sediment.</p>
$F_6$ and $F_{12}$	<p>Sum of DSi from diatom respiration and diatom excretion.</p> <p>Diatom respiration:</p> $f(T_W) * k_{resp} * P_{PHYP\_Si\_Pelagic/Benthic}$ <p>Diatom excretion:</p> $f(T_W) * k_{excr} * P_{PHYP\_Si\_Pelagic/Benthic}$
$F_7$ and $F_{10}$	<p>Det_Si_Pelagic/Benthic from diatom mortality</p> $f(T_W) * k_{lysis} * (1 + \alpha * (1 + V_f)) P_{PHYP\_Si\_Pelagic/Benthic}$ <p>Where <math>\alpha</math> is 1 (if <math>P_{PHYP\_Si\_Pelagic/Benthic} &gt; PHYP\_Si_{lim\_pelagic/benthic}</math> or <math>T &gt; 15^\circ\text{C}</math>), otherwise <math>\alpha</math> is 0</p>
$F_8$	<p>The erosion of Det_Si_Benthic is a fraction of the total erosion <math>\Phi ERO_{tot}</math> [<math>\text{ton yr}^{-1}</math>].</p> $ERO_{Det\_Si\_Benthic} = \frac{P_{Det\_Si\_Benthic}}{P_{tot\_sed}} * ERO_{tot}$ <p>Where <math>P_{Det\_Si\_Benthic}</math> is the benthic Det_Si pool. Total erosion is calculated according to:</p> $ERO_{tot} = k_{ero} * (P_{tot\_sed} / Area) / (k_{sed} + P_{tot\_sed} / Area) * S * Area * v$ <p>Where <math>k_{ero}</math> is the erosion coefficient, <math>k_{sed}</math> is the half-saturation constant, <math>P_{tot\_sed}</math> is the total mass of sediment in the water body, <math>S</math> is the slope, <math>Area</math> is the bedarea, <math>v</math> is the flow velocity. The total sedimentation is the sum of benthic PIM and benthic Det_Si:</p> $P_{tot\_sed} = P_{PIM\_Benthic} + P_{Det\_Si\_Benthic}$
$F_9$	<p>Sedimentation of detritus silicon from the pelagic to the benthic pool.</p> $V_{sed,Det\_Si\_Pelagic} / Depth * P_{Det\_Si\_Pelagic}$
$F_{11}$	<p>Burial of Det_Si_Benthic</p>

	$burial = MIN (0 \text{ if } SED < SED_{lim}, k_{burial\_max} * \frac{SED - SED_{lim}}{SED})$ <p>Where <math>k_{burial\_max}</math> is the maximum burial rate, <math>SED</math> is the deposited PIM and <math>P_{Det\_Si\_Pelagic}</math>, <math>SED_{lim}</math> is the threshold sediment stock. Burial occurs when <math>SED &gt; SED_{lim}</math>.</p>
$F_{14}$	<p>Dissolved silica flux from the Det_Si_Benthic pool in the upper sediment layer to the <math>P_{DSi}</math> pool. We assume no DSi production from buried Det_Si.</p> $F_{Det\_Si\_Benthic\_dissolution} = -f_{Si} * P_{Det\_Si\_Benthic} * k_{max\_Det\_Si\_Benthic\_dissolution}$ <p>Where Det_Si_Benthic is the detritus Si in the upper sediment layer.</p> $f_{Si} = [1 - Det\_Si\_Benthic / (Det\_Si\_Benthic + \exp(0.08 * T_W))] - (0.3 + 0.02 * T_W) * DSi_{conc} / 28$ <p>Where <math>DSi_{conc}</math> is the DSi concentration, <math>T_W</math> is the water temperature.</p>
$F_{15}$	Input flux from upstream grid cell
$F_{16}$	Output flux to downstream grid cell

The DISC-SILICON module simulates the pelagic (PHYP\_Si\_Pelagic) and benthic diatoms (PHYP\_Si\_Benthic), and pelagic (Det\_Si\_Pelagic) and benthic detritus silicon (Det\_Si\_Benthic) by coupling hydrological parameters, temperature, and solar radiation (Figure 3.1). DSi inputs to the model occur via rock weathering and sewage wastewater discharge. Det\_Si includes allochthonous (phytoliths from soil erosion) and autochthonous (mortality of PHYP\_Si\_Pelagic) material. BSi is the sum of pelagic and benthic PHYP\_Si and Det\_Si. Physical dynamics of Det\_Si are controlled by sedimentation and erosion equations which are linked to particulate inorganic matter (PIM), mostly sediment.

In general terms, DISC-SILICON dynamically computes various Si pools (denoted with capital  $P$ ) and flows (capital  $F$ ) for each stream, river, lake and reservoir from headwaters to the coast along the river continuum (Figure 3.1). For every time step, the change of a Si pool for species  $i$  in the grid cell  $c$  considered is calculated as follows:

$$\frac{dP_{i,c}}{dt} = F_{up,i,c} + F_{inp,i,c} - F_{out,i,c} + \sum_n^{Num} F_{n,c} \quad (1)$$

Where  $F_{up,i,c}$  is the input flux [ $Mmol \text{ yr}^{-1}$ ] of Si species  $i$  from upstream grid cells to grid cell  $c$ .  $F_{inp,i,c}$  is the input flux [ $Mmol \text{ yr}^{-1}$ ] from within grid cell  $c$ ,  $F_{out,i,c}$  is the output flux [ $Mmol \text{ yr}^{-1}$ ] from grid cell  $c$  to a neighboring grid cell downstream.  $F_{n,c}$  ( $Mmol \text{ yr}^{-1}$ ) is the transformation flux from one Si species to another one within grid cell  $c$  as a result of in-stream biogeochemical processing (see Figure 3.1 and Table 3.2),  $Num$  is the total number of fluxes (see Figure 3.1 and Table 3.2).  $F_{n,c}$  is positive, when

it enters pool  $P_{i,c}$ ; it is negative, when it leaves pool  $P_{i,c}$ . The benthic species are not transported to downstream (i.e.  $F_{up,i,c} = 0$  and  $F_{out,i,c} = 0$ ).

Section 2.2 discusses the inputs ( $F_{inp,i,c}$ ) of DSi and Det\_Si to surface water and the in-stream biogeochemical Si fluxes ( $F_{n,c}$ ) are presented in section 2.1.3. The data used to drive DISC-SILICON are listed in Table 3.1.

### 3.2.1.2 Si delivery to water bodies

The DSi weathering fluxes  $F_1$  and  $F_2$  (Figure 3.1) are based on the model presented by Hartmann et al. (2014b). We added the impact of land use on silicon biogeochemistry, represented by a factor based on Struyf et al. (2010) for 52 Scheldt sub-basins (see details in SI3.1).

The detritus Si input flux ( $F_{inp,soil\_Det\_Si}$ ) representing soil erosion loss (Figure 3.1) is based on the approach of Cerdan et al. (2010), considering soil texture, land cover, and slope (Beusen et al. 2015). The land-use specific soil loss rates for the fractions of natural ecosystems, grassland and arable land areas were applied to every grid cell. Soil loss input to the river is in the form of particulate inorganic matter (PIM), and Si is a fraction of PIM based on the observed Si content in arable soil samples in the Seine River basin (4.9 mg Det\_Si Si/g soil, with a range of 2.5 to 7.3 (Sferratore et al. 2006)). Here, the average fraction of 4.9 mg Si/g is multiplied with PIM to calculate Det\_Si input from soil loss.

The Si input flux  $F_3$  (Figure 3.1) from sewage water effluent ( $F_{inp,sew\_Det\_Si} + F_{inp,sew\_DSi}$ ) is assumed to be 1.0 g Si per capita per day (Sferratore et al. 2006), and total input per grid cell is obtained by multiplying with the number of inhabitants within the grid cell ( $N_{population}$ ) (Table 3.1). The Det\_Si fraction of total Si in wastewater is assumed to be 25%, the complement (75%) being in the form of DSi.

$$F_{inp,sew\_Det\_Si} = r_{sew\_Det\_Si} * N_{population} \quad (2)$$

$$F_{inp,sew\_DSi,c} = r_{sew\_DSi} * N_{population,c} \quad (3)$$

Where  $r_{sew\_Det\_Si}$  and  $r_{sew\_DSi}$  are the specific Si load per inhabitant which equal 0.75 g and 0.25 g Si per capita per day, respectively.

### 3.2.1.3 In-stream Si cycling

In the water column, DISC-SILICON includes five Si pools and 16 process fluxes (Figure 3.1, Table 3.2). As the model describes processes generically for different water bodies, DISC-SILICON allows to assess the impact of external drivers (land-use change,

sewage source, weathering, climate, and hydrology) on the Si biogeochemistry along the river continuum. We initialize the model with a spinup period of 50 years to obtain the equilibrium state for the benthic pools.

The change in the DSi pool  $P_{\text{DSi},c}$  in the water column in grid cell  $c$  is computed for each time step. DSi in the water column can be taken up by diatom growth (PHYP\_Si\_Pelagic growth and PHYP\_Si\_Benthic growth) (Figure 3.1, Table 3.2,  $F_5$  and  $F_{13}$ ). DSi is released by decomposition and dissolution from the pelagic and benthic detritus (Det\_Si\_Pelagic and Det\_Si\_Benthic). The degradation rate for pelagic detritus is temperature dependent. Det\_Si\_Benthic is transferred to pelagic DSi across the sediment-water interface according to the empirical relationship presented by Billen et al. (2015) (Figure 3.1, Table 3.2,  $F_{14}$ ).

The pools  $P_{\text{PHYP\_Si\_Pelagic},c}$  and  $P_{\text{PHYP\_Si\_Benthic},c}$  are the Si pools in pelagic and benthic diatoms, respectively, in grid cell  $c$ . Benthic diatoms are the primary consumers of DSi in shallow water bodies (Bowes et al. 2005, House et al. 2001, Leira and Sabater 2005). With the variation of temperature, turbidity, depth and light attenuation, DISC-SILICON simulates the growth of diatoms in every water body and grid cell (Figure 3.1, Table 3.2,  $F_5$  and  $F_{13}$ ). Pelagic and benthic diatoms are transformed into Det\_Si\_Pelagic and Det\_Si\_Benthic using diatom mortality (Figure 3.1, Table 3.2,  $F_7$  and  $F_{10}$ ). The Det\_Si\_Pelagic and Det\_Si\_Benthic are linked by in-stream sedimentation and resuspension (Figure 3.1, Table 3.2,  $F_9$  and  $F_8$ ). Det\_Si\_Benthic can be removed by burial in the sediment, which occurs when the accumulated bed sediments (total mass) exceed  $500 \text{ g/m}^2$  (Figure 3.1, Table 3.2,  $F_{11}$ ).

### 3.2.2 Sensitivity analysis

We have deliberately not calibrated our model. Instead, to investigate model performance and model defects, we analyzed the sensitivity of the export of all forms of Si to the ocean and the diatom production in the water column (pelagic diatom primary production  $\text{PP\_PHYP\_Si\_Pelagic} = F_5$  in Figure 3.1) to changes in 53 model parameters using Latin Hypercube Sampling (Saltelli et al. 2000). We executed 750 runs to calculate the sensitivity for the period 1996-2000 for both the rivers Rhine and Yangtze. The Standardized Regression Coefficient (SRC, more details are provided in SI3.2) is used as an indicator of the relative influence of a model parameter on model results (export of Si to the ocean and diatom production). Parameters are considered to be important if their influence on the model result exceeds 4% (i.e.  $\text{SRC} < -0.2$  or  $\text{SRC} > 0.2$ ; see SI3.4).

### 3.3 Results and Discussion

#### 3.3.1 Comparison with measurement data and sensitivity analysis

The model results show a good agreement with the observed data both for Datong station in the Yangtze (Figure 3.2a, 3.2b) and Lobith in the Rhine (Figure 3.2c, 3.2d) for the period 1960 to 2000. The Root Mean Squared Error (RMSE, more details in SI3.2) for the discharge and DSi concentration are 10% and 16%, respectively, for the Datong station in the Yangtze. The model reproduces the trend of DSi during the period 1960s-1980s (Figure 3.2b). The RMSE for the discharge and DSi concentration are 14% and 20%, respectively, for the Lobith station in the Rhine. Considering that DISC-SILICON is a global model based on global data and parameter settings, the agreement with the available observations is satisfactory based on general model performance criteria (Moriassi et al. 2015).

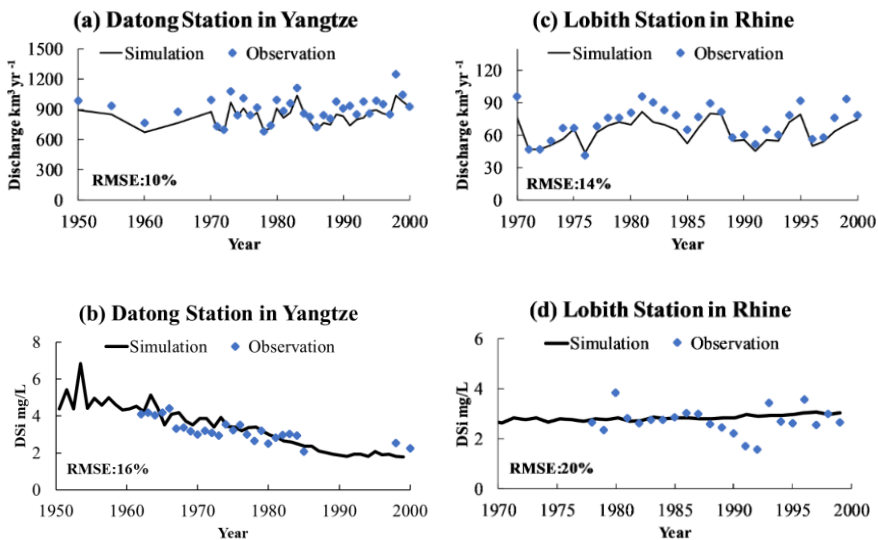


Figure 3.2 Comparison of measured and modeled discharge and DSi (Si) concentrations at the stations of Datong in Yangtze (a,b) and Lobith in Rhine (c,d). The sources of the measurement data are listed in Table 3.1.

The full list of input parameters that have a significant effect on the model output is provided in SI3.4. Here, the focus is on DSi and BSi export to the river mouth and pelagic diatom primary production (Table 3.3). Both in Rhine and Yangtze, the DSi\_Export is strongly controlled by DSi\_Input from weathering. The SRC for DSi\_Export in the Yangtze (0.76) and Rhine (0.97) are both much higher than values for

other model parameters. For the Yangtze the optimal temperature for the benthic dissolution process influences the DSi\_Export, in contrast to the Rhine. This is because in-stream processes are playing a much more important role in the Yangtze than in the Rhine due to the much longer average travel time: 0.19 and 0.04 yr in 2000 for the Yangtze and Rhine, respectively.

The BSi\_Export from the Yangtze River basin is negatively influenced by the detritus settling velocity for waterbodies. In contrast, there is a positive effect of solar radiation, discharge, optimal temperature for dissolution, the maximum growth rate for pelagic diatoms and the threshold concentration for mortality of diatoms. Compared with the Yangtze, the BSi\_Export in the Rhine basin is sensitive to the slope and particulate inorganic matter. The difference between the Rhine basin and Yangtze basins is caused by the absence of major reservoirs in the Rhine basin, causing the average travel time of water to be much shorter than that in the Yangtze. For pelagic diatom primary production, the results of the sensitivity analysis show that solar radiation, half saturation of light limitation, maximum growth rate, threshold concentration for mortality and the mortality rate are important parameters.

Table 3.3 Standardized regression coefficient (SRC) representing the relative sensitivity of the model performance for 3 output parameters (dissolved Si export to mouth (DSi\_Export), phytoplankton Si and detritus Si export to mouth (BSi\_Export), pelagic diatom primary production (PP\_PHYYP\_Si\_pelagic, F5 in Figure 1) for the Rhine and Yangtze Rivers to the variations of 53 model input parameters<sup>a</sup>.

Parameters	Rhine			Yangtze		
	DSi_Export	BSi_Export	PP_PHYYP_Si_Pelagic	DSi_Export	BSi_Export	PP_PHYYP_Si_Pelagic
Solar_radiation	-0.10	0.14	0.18	-0.14	0.27	0.22
Temperature	0.03	-0.08	0.55	0.17	-0.19	0.19
Slope	0.02	0.23	-0.01			
Discharge	0.02	0.66	-0.05		0.50	-0.07
$T_{opt\_Det\_Si\_Benthic\_dis}$ solution			-0.02	-0.20	0.31	-0.02
$k_{I,PHYYP\_Si\_Pelagic}$	0.02	-0.03		0.10	-0.18	-0.24
$T_{opt\_Det\_Si\_Benthic\_dis}$ solution	-0.12	0.22				
$V_{sed,Det\_Si\_Pelagic}$		-0.34		-0.08	-0.26	-0.01
$T_{opt\_growth}$	0.08	-0.10	-0.50			
$T_{sigma\_Det\_Si\_Pelagic\_menera}$	-0.04	0.05	0.23			
$k_{max\_growth\_pelagic}$	-0.06	0.09	0.32	-0.20	0.35	0.47
PHYYP_Si <sub>im</sub> _pelagic	-0.05	0.10	0.28	-0.15	0.33	0.45
PIMload2river	-0.02	-0.22				
$F_{inp,CW\_DSi}$	0.97	0.03	0.02	0.76	0.06	0.08

<sup>a</sup>The complete results of the sensitivity analysis are presented in SI3.4. Values without color indicate  $-0.2 < SRC < 0.2$ ; values with green and salmon colors indicate values  $< -0.2$  and  $> 0.2$  respectively. Positive values indicate that a higher input parameter value generates a higher model output variable, and negative values indicate that a higher input parameter value generates a lower model output variable.

The sensitivity analysis indicated that the modeled Si export and diatom primary production are sensitive to DSi input from weathering, growth factors (growth rate and mortality rate of diatoms, temperature, and solar radiation) and factors related to the



travel time of water (discharge, slope, water body width and depth). These factors and the growth and mortality rates of diatoms require further attention, for example, by involving mechanistic knowledge from other disciplines (hydrology and biology) in model development.

### 3.3.2 Si input, export and retention

To compare the two rivers, we aggregated the total Si input fluxes to the Rhine and Yangtze networks. The total Si delivery and export for the Rhine shows interannual variation but lacks a trend for the period 1900 to 2000 (Figure 3.3a); the retention (calculated as the difference between Si inputs and exports divided by Si inputs) varied between -4% and 19% (average 8%) (Figure 3.3a). For the Yangtze River basin we see a different pattern, with total annual Si delivery varying between 128 and 205 Gmol yr<sup>-1</sup> between 1900 and 1950, followed by a sharp decrease from 161 to 85 Gmol yr<sup>-1</sup> during 1950-2000 (Figure 3.3d). This decline is mainly due to land-use changes. Since 1950, around 40% of the area covered by natural ecosystems has been transformed to cropland, and thus Si inputs from terrestrial sources have declined significantly. In the first half of the 20<sup>th</sup> century, the retention in the Yangtze varied between -0.7% and 13% (average 6%) (Figure 3.3d). After 1950, the retention rapidly increased to 29% in 2000 (Figure 3.3d) due to the construction of reservoirs and Si input decrease.

The DISC-SILICON model properly reproduces the impact of extremely wet years, such as 1995 in the Rhine, and 1954 and 1998 in the Yangtze. In such wet years the model simulates a significant increase of total Si and Det\_Si inputs; part of the enhanced DSi is transformed into diatom biomass and accumulates in the benthos. The model results point to a legacy (red circle in Figure 3.3a, 3.3d), especially when a wet year is followed by a dry year (for instance, 1996 in the Rhine, 1955 in the Yangtze), and the Si retention then even becomes negative as a result of DSi release from Det\_Si\_Benthic.

The average DSi and BSi budgets for the 1950s and 1990s for the Rhine River show no obvious trend. However, for the Yangtze the DSi input showed a dramatic decrease from the 1950s to 1990s of 145 to 61 Gmol yr<sup>-1</sup>, while the BSi input increased from 19 to 23 Gmol yr<sup>-1</sup> (Figure 3.3e, 3.3f). Due to the construction of dams, the pelagic diatom primary production increased from 14 to 26 Gmol yr<sup>-1</sup>, burial of detritus increased from 11 to 24 Gmol yr<sup>-1</sup> and DSi\_Export decreased from 145 to 56 Gmol yr<sup>-1</sup> from the 1950s to the 1990s.

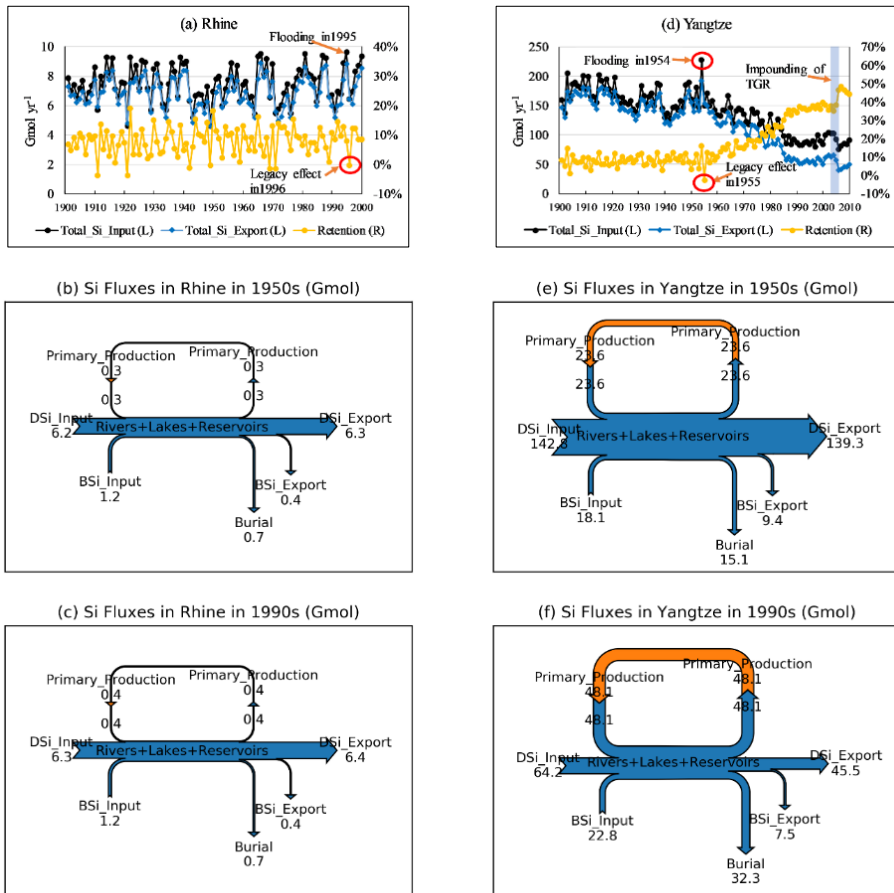


Figure 3.3 Total Si input into the river and export to the river mouth (left y-axis) and retention in percentage (right y-axis) in the Rhine (a) and Yangtze (d). Annual average DSi, and BSi (Det\_Si\_Pelagic + PHYP\_Si\_Pelagic) budget for the Rhine (b, c) and Yangtze (e, f) in the 1950s and 1990s. All fluxes are expressed in Gmol yr<sup>-1</sup>.

While the Rhine River shows no trend for the export flux of Si, the Si export to the East China and Yellow Seas from the Yangtze has been rapidly declining since the second half of the 20<sup>th</sup> century as a result of dramatic changes in land use affecting the Si supply from weathering and erosion, and dam construction affecting the burial of BSi. This has been shown to lead to changes in the ecology of the reservoirs (Figure 3.4) and together with nutrient loading and changing stoichiometry has dramatic impacts in Chinese coastal marine ecosystems including causing harmful algal blooms (Glibert et al. 2018, Ran et al. 2019, Xiao et al. 2019, Yu et al. 2018, Zhou et al. 2020).

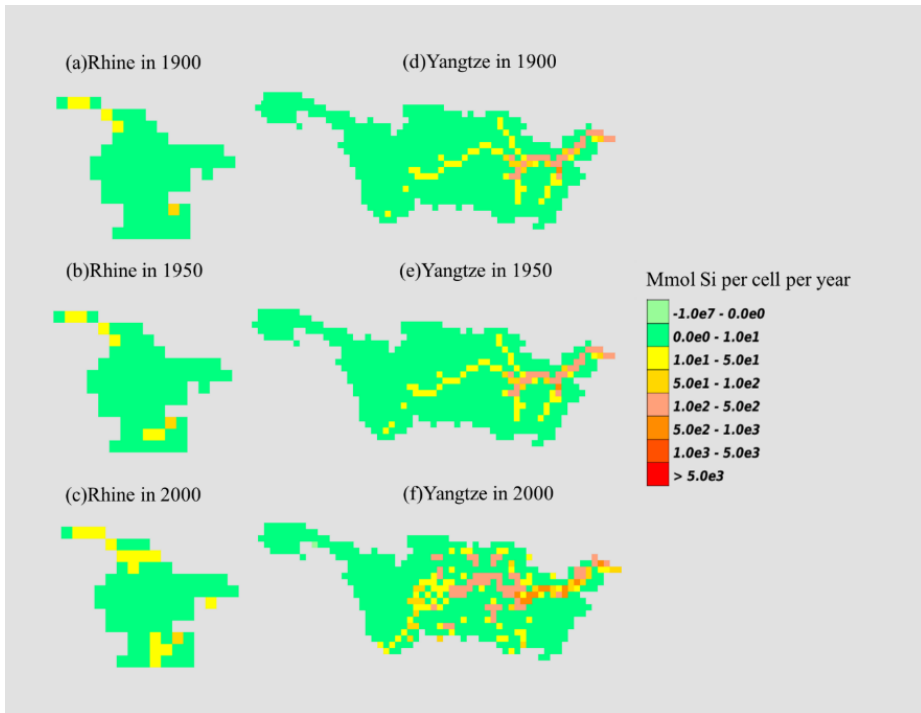


Figure 3.4 Spatial distribution of diatom primary production in the Rhine (a,b,c) and the Yangtze (d,e,f) in 1900, 1950 and 2000. Movies SI3.4 shows the yearly diatom primary production during the period 1900-2010 (for Rhine 1900-2000).

### 3.3.3 Spatial and temporal distribution of primary production by diatoms

Our results indicate that there is important spatial variations in diatom production and, hence, Si uptake. Furthermore, significant changes in the production have taken place during the course of the 20th century. DISC-SILICON simulates an almost two-fold increase of diatom primary production during the period 1900-2000 in the Rhine basin (Figure 3.3b, 3.3c, Figure SI3.3), with hotspots in the lower reach and Lake Constance (Figure 3.4a, 3.4b, 3.4c). In contrast, the Yangtze basin has been increasingly perturbed by reservoirs (Figure S3). The pelagic diatom primary production in the Yangtze basin varied between 18 and 22  $\text{Gmol yr}^{-1}$  (average 21  $\text{Gmol yr}^{-1}$ ) during the 1st half of the 20th century, but increased rapidly to 52  $\text{Gmol yr}^{-1}$  (Figure 3.3e, 3.3f) in 2000 due to the dam construction and increasing reservoir volume, which favored diatom growth (Figure 3.5a, 3.5b, 3.5c) and settling of BSi in the sediments of reservoirs. In both basins,

diatoms' increase of diatom primary production occurs especially in the middle and lower reaches (Figure 3.4d, 3.4e, 3.4f).

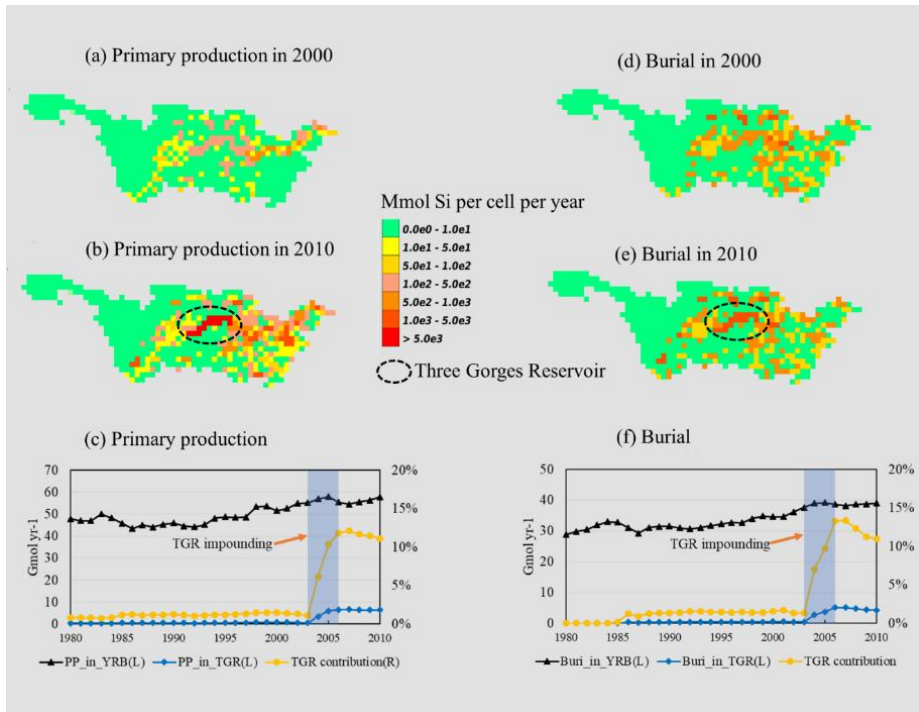


Figure 3.5 Spatial distribution of diatom primary production before (a) and after (b) the Three Gorges Reservoir (TGR) impounding in the Yangtze, and (c) diatom primary production in TGR and Yangtze River Basin (YRB) and TGR contribution to YRB. Spatial distribution of burial in the Yangtze before (d) and after (e) the TGR impounding, and (e) burial in TGR and YRB and TGR contribution to YRB. Blue bar (c, f) indicates the TGR impounding years.

### 3.3.4 Impact of the Three Gorges Reservoir

Our simulations show that total Si retention (Figure 3.3d) in the Yangtze River Basin (YRB) increased from 38% (average for 1999-2002) to 46% (average for 2007-2010). This retention increase is mainly due to the impounding of the Three Gorges Reservoir (TGR) between 2003 and 2006. The contribution of TGR to the whole-basin diatom primary production (PP) increased from 1% (average for 1999-2002) to 12% (average for 2007-2010) (Figure 3.5a, 3.5b, 3.5c), which also caused an increase of the Det\_Si\_Plegic and Det\_Si\_Benthic pools. The contribution of TGR to the whole-basin burial increased from 2% (average for 1999-2002) to 12% (average for 2007-2010)

(Figure 3.5d, 3.5e, 3.5f). In addition to the land-use impact on the weathering supply of Si, the enhanced retention in the TGR further reduces the Si export to the mouth, with two major consequences. Enhanced retention within the reservoir may have severe consequences for downstream ecosystems: e.g. a shift from diatoms to green algae in the lower river reach or the proliferation of harmful algae in the coastal ocean (Garnier et al. 2010, Middelburg 2020). DISC-SILICON estimates for retention in the TGR are in agreement with the estimated 6% retention of reactive dissolved and particulate Si (Maavara et al. 2014).

### **3.3.5 Model limitations and future improvements.**

Construction of a large number of dams is planned in the Yangtze River and many other rivers (Lehner et al. 2011). IMAGE-DGNM will be a helpful tool to project future changes in Si cycling and river Si export to the global coastal ocean under scenarios of climate change and human disturbances. IMAGE-DGNM, including DISC-SILICON is the first model that allows describing the long-term spatial patterns of global Si transport and biogeochemical processing in the river continuum (from bed rock weathering, soil to streams, from upstream to downstream, lakes and reservoirs). The model reproduces observed Si concentrations, the effect of dam construction and enhanced retention in reservoirs, the effect of land-use changes on the delivery of Si, and the effect of climate variability. The spatial variation of diatom production and uptake, decay of diatom biomass, dissolution of BSi as well as the changes in the course of the 20<sup>th</sup> century highlight the need for a spatially explicit model. However, the model has limitations that need attention in future model improvements.

The DSi input from weathering clearly depends on the Si biogeochemical cycling in soils. Since our approach for describing the impact of land-use on the weathering supply of Si is non-spatial (lumped for the whole river basin), future model improvements should focus on the improvement of the description of the Si transformation in the soil-plant system (crop harvest) at grid cell scale, and the subsequent transport via shallow and deep groundwater. A further limitation of the model is a lack of coupling of the Si to carbon and the other nutrients. Such a coupling will lead to a better description of the Si cycle in rivers accounting for N and P biogeochemistry changes.



## Supporting Information

### SI3.1 Construction of weathering

The original model proposed by Hartmann et al. (2014b) used the following formula:

$$F_{\text{inp,CW}_{\text{DSi},c}} = \sum_{l=1}^M CW_{l,c} * S_{l,c} * T_{l,c} * A_{l,c} \quad (\text{S1})$$

This model was validated on 382 basins in the Japanese archipelago (Hartmann 2009, Kobayashi 1961). The validation showed that this model without land use and in-stream processes showed a poor agreement with observed DSi delivery in basins with relatively high fractions of natural landcover. For bigger basins, the difference between the simulated and observed DSi is bigger (see Figure SI3.2). The integration of this factor in the Hartmann formula was not needed for the Japanese archipelago because most basins only had pristine land use. Therefore, we propose to add an additional factor “land use” to this formula. The land-use factor was already described by Struyf et al. (2010). The formula is made by nonlinear regression based on the original 52 sub-basins.

In this study, the new formula of chemical weathering rate  $F_{\text{inp,CW}_{\text{DSi},c}}$  (ton DSi yr<sup>-1</sup>) for each grid cell  $c$  is calculated as follows:

$$F_{\text{inp,CW}_{\text{DSi},c}} = L_r * \sum_{l=1}^M CW_{l,c} * S_{l,c} * T_{l,c} * A_{l,c} \quad (\text{S2})$$

Where  $CW_{l,c}$  is the chemical weathering rate for lithology type  $l$  (ton DSi km<sup>-2</sup> yr<sup>-1</sup>),  $S_{l,c}$  is the soil shielding reduction term for specific soil types causing a reduction in the chemical weathering of the underlying lithological class  $l$ , estimated on the basis of field data (no dimension;  $S_{l,c} = 0.1$  for Ferralsols, Gleysols, Acrisols, Lixisols, Nitisols and Histosols (organic soils); for all other soils  $S_{l,c} = 1$ );  $A_{l,c}$  is the land area covered by each lithology class (km<sup>2</sup>),  $M$  is the number of lithology classes.  $L_r$  is the factor that describes the impact of land use on the mobilization of Si in landscapes for each river basin  $r$ .

The chemical weathering rate is obtained from:

$$CW_{l,c} = b_{l,c} * q_{\text{tot},c} \quad (\text{S3})$$

Where  $b_l$  is a factor for each lithological class  $l$  (ton DSi km<sup>-2</sup> mm<sup>-1</sup> yr<sup>-1</sup>), and  $q_{\text{tot},c}$  is the total runoff (mm yr<sup>-1</sup>) in cell  $c$ . The effect of temperature ( $F_{T,l}$ , no dimension) is obtained from the Arrhenius equation:

$$T_{l,c} = \exp((-E_{a,l}/R^*)((1/T_{A,c}) - (1/T_0))) \quad (\text{S4})$$

Where  $E_{a,l}$  is the activation energy of lithology class  $l$  (J mol<sup>-1</sup>) (Table S1);  $R^*$  is the gas constant (8.3144 J mol<sup>-1</sup> K<sup>-1</sup>),  $T_A$  is the mean air annual temperature (K) for the grid cell,

and  $T_0$  (284.15 K) is the reference temperature. By introducing the impact of land use, the agreement of the model with observations is improved. The land use impact  $L_r$  on the DSi delivery based on 52 basins from Struyf et al. (Struyf et al. 2010) is calculated as follows:

$$L_r = 1 - ((105.35 - 11.57 * \exp(2.21 * AF_r))/105.35) \quad (S5)$$

Where  $AF_r$  is the natural area fraction for the whole river basin  $r$ .

### SI3.2 Validation and sensitivity analysis method

The modeled DSi concentration and discharge are validated with measurements at station Lobith in the Rhine and Datong in the Yangtze River. To express the model performance we use a statistical indicator RMSE (Root Mean Squared Error) (Chai and Draxler 2014), It is used for comparing observations and modeled results.

$$RMSE = \frac{100}{\bar{o}} \sqrt{\frac{\sum_1^n (O_i - M_i)^2}{n}} \quad (S6)$$

Where  $M_i$  is the simulated result  $i$ ,  $o_i$  is observed value  $i$ ,  $\bar{o}$  is mean of the observations and  $n$  is the number of observations. We consider RMSE values smaller than 50% acceptable (Beusen et al. 2015).

We analysed the sensitivity of 53 parameters on the instream fluxes and exports (Table SI3.3, SI3.4) to the coastal areas. As sample method, we used Latin Hypercube Sampling (LHS) (Saltelli et al. 2000). We used for all parameters a uniform distribution around the default values with a range of 5%. We executed 750 runs to analyze the standardized regression coefficient (SRC) for the burial and the BSi and DSi export to the coastal seas for the period 1996-2000 for the Rhine and Yangtze. The input parameters are all described in the supplementary information section SI3.3 We only highlight those input parameters which have an SRC value within the range  $SRC > 0.2$  and  $SRC < -0.2$  in Table SI3.3

The uncertainty contribution of each parameter ( $X_i$ ) to model outcome  $Y$  is assessed with linear regression (Beusen et al. 2015, House et al. 2001):

$$Y = \beta_0 + \beta_1 X_1 + \beta_2 X_2 \dots + \beta_n X_n + e \quad (S7)$$

where  $\beta_i$  is the coefficient for regression of parameter and  $e$  is the error of the approximation of  $Y$ . The linear regression model can be assessed for parameter contribution analysis by the coefficient of determination  $R^2$ , which means the  $Y$  variation can be explained by  $Y - e$ .



The Standardized Regression Coefficient ( $SRC_i$ ) is calculated to scale  $\beta_i$  to the relative contribution of variation of  $Y$ , the standard deviations of  $X_i$  and  $Y$  as follows:

$$SRC_i = \beta_i \frac{\sigma_{X_i}}{\sigma_Y} \quad (S8)$$

$SRC_i$  is independent of units and scale of parameters. The  $SRC_i$  take a value between -1 and 1 and is independent of unit scale and size. The positive  $SRC_i$  value indicates that an increasing parameter value leads to output  $Y$  increase. The negative  $SRC_i$  indicates a decreasing output  $Y$  with a parameter value increase.

### SI3.3 The parameters and values used in DISC-SILICON

Table SI3.1. List of parameters and their values as used in DISC-SILICON

Parameters	Description	Default values	Unit	Sources
$k_{\max\_growth\_pelagic}$	Max growth rate for pelagic diatoms	0.085	$h^{-1}$	Sferratore. (2006)
$k_{\max\_growth\_benthic}$	Max growth rate for benthic diatoms	0.04	-	Sferratore (2006)
$T_{opt\_growth}$	Optimal water temperature for primary production	18	$^{\circ}C$	Sferratore (2006)
$T_{\sigma\_growth}$	Standard deviation of temperature for primary production	13	$^{\circ}C$	Garnier et al. (2000)
$K_{DSi,PP}$	DSi half saturation concentration	7	$\mu mol Si/L$	Sferratore (2006)
$k_{lysis}$	Lysis rate of diatoms	0.004	$h^{-1}$	Garnier et al. (2000)
$V_f$	Lysis amplification factor at high temperature/algal biomass	20	-	Garnier et al. (2000)
$PHYP\_Si_{lim\_pelagic/benthic}$	Threshold diatom concentration for mortality (mortality occurs if concentration $i > Phy\_Si_{lim}$ )	26.83	$\mu mol Si/L$	Garnier et al. (2000)*
$k_{burial\_max}$	Maximum burial rate for deposited diatom biomass	0.0005	$h^{-1}$	Billen et al. (2015)
$SED_{lim}$	Threshold sediment stock;	500.00	$g / m^2$	Billen et al. (2015)
$k_{morta}$	Mortality rate of diatoms	0.004	$h^{-1}$	Garnier et al. (2000)
$k_{resp}$	Respiration rate of diatoms	0.003	$h^{-1}$	Garnier et al. (2000)
$k_{excr}$	Excretion rate of diatoms	0.002	$h^{-1}$	Garnier et al. (2000)
$V_{sed,PIM}$	Settling velocity of PIM	0.05	$h^{-1}$	Garnier et al. (2000)
$k_{ero}$	Erosion coefficient	20000	$ton/km^2$	Vilmin et al. (2015)
$k_{sed}$	Half-saturation constant	$1 * 10^{-6}$	km	Vilmin et

				al. (2015)
$V_{\text{sed,Det\_Si\_Pelagic}}$	Settling velocity of Det_Si_Pelagic	0.05	$\text{h}^{-1}$	Garnier et al. (2000)
$k_{\text{max\_Det\_Si\_Pelagic\_dissolution}}$	Maximum dissolution rate of pelagic Det_Si	0.002	$\text{h}^{-1}$	Garnier et al. (2000)
$T_{\text{opt\_Det\_Si\_Pelagic\_dissolution}}$	Optimal temperature for dissolution of pelagic Det_Si	25	$^{\circ}\text{C}$	Garnier et al. (2000)
$T_{\text{sigma\_Det\_Si\_Pelagic\_dissolution}}$	Standard deviation of temperature for dissolution of pelagic Det_Si	15	$^{\circ}\text{C}$	Garnier et al. (2000)
$k_{\text{max\_Det\_Si\_Benthic\_dissolution}}$	Maximum dissolution rate of benthic Det_Si	0.002	$\text{h}^{-1}$	Garnier et al. (2000)
$\eta_{\text{water}}$	The effect of water on light extinction in the water column	0.8	$\text{m}^{-1} \text{mg}^{-1} \text{L}$	Scheffer (2004)
$\eta_{\text{Det\_Si\_Pelagic}}$	The effect of Det_Si_Pelagic on light extinction in the water column	0.05	$\text{m}^{-1} \text{mg}^{-1} \text{L}$	Scheffer (2004)
$\eta_{\text{PHYP\_Si\_Pelagic}}$	The effect of PHYP_Si on light extinction in the water column	0.05	$\text{m}^{-1} \text{mg}^{-1} \text{L}$	Scheffer (2004)
$\eta_{\text{PIM}}$	The effect of PIM on light extinction in the water column	0.03	$\text{m}^{-1} \text{mg}^{-1} \text{L}$	Scheffer (2004)
$k_{I,\text{PHYP\_Si\_Benthic}}$	Half saturation of light limitation with Michaelis-Menten for PHYP_Si_Benthic	12.5	$\text{W m}^{-2}$	Garnier et al. (2000)
$k_{I,\text{PHYP\_Si\_Pelagic}}$	Half saturation of light limitation with Michaelis-Menten for PHYP_Si_Pelagic	25	$\text{W m}^{-2}$	Garnier et al. (2000)

\* C: Chlorophyll ratio of 0.035 mg C.  $\mu\text{g Chl yr}^{-1}$  and the Redfield molar ratio C:Si 106:15.

### SI3.4 Sensitivity analysis results

The sensitivity analysis results are in Table SI3.2 for Rhine and Table SI3.3 for Yangtze. The following model output was analyzed: total Si export (sum of DSi and BSi) to mouth ( $\text{TSi}_{\text{export}}$ ), dissolved Si export to mouth ( $\text{DSi}_{\text{export}}$ ), Phytoplankton Si and Detritus Si export to mouth ( $\text{BSi}_{\text{export}}$ ), Phytoplankton Si and Detritus Si burial ( $\text{BSi}_{\text{burial}}$ ), pelagic phytoplankton primary production ( $\text{PP}_{\text{pelagic}}$ ), benthic phytoplankton primary production ( $\text{PP}_{\text{benthic}}$ ).

Table SI3.2. Standardized regression coefficient (SRC) represents the relative sensitivity of the model performance for the Rhine River to the variations of 53 model parameters. Parameters which have no significant SRC values for none of the outputs are not shown. The description, default value and unit of the input parameters is provided in Table SI3.1

Parameters	TSi_exp ort	DSi_expo rt	BSi_expo rt	BSi_burial	PP_pelagic	PP_benthic
Solar_radiation	-0.06	-0.10	0.14	0.20	0.18	0.32
Temperature	0.01	0.03	-0.08	-0.03	0.55	0.11
Slope	0.08	0.02	0.23	-0.25	-0.01	-0.03
Discharge	0.19	0.02	0.66	-0.60	-0.05	-0.06
$k_{I,PHYP\_Si\_Pelagic}$	0.01	0.02	-0.03	-0.04	-0.02	-0.08
$T_{opt\_Det\_Si\_Benthic\_dissolutio}$ n	-0.06	-0.12	0.22	0.20		
$V_{sed,Det\_Si\_Pelagic}$	-0.09		-0.34	0.29		
$T_{opt\_growth}$	0.05	0.08	-0.10	-0.17	-0.50	
$T_{sigma\_Det\_Si\_Pelagic\_dissolutio}$ ion	-0.03	-0.04	0.05	0.09	0.23	
$k_{max\_growth\_pelagic}$	-0.04	-0.06	0.09	0.13	0.32	
$PHYP\_Si_{lim\_pelagic}$	-0.03	-0.05	0.10	0.09	0.28	0.03
$k_{I,PHYP\_Si\_Benthic}$	0.04	0.07	-0.09	-0.14		-0.34
$k_{max\_growth\_benthic}$	-0.08	-0.12	0.17	0.25		0.63
$k_{morta}$	0.04	0.07	-0.09	-0.13		-0.35
PIM load2river	-0.07	-0.02	-0.22	0.23		
DSi weathing input	0.96	0.97	0.03	0.06	0.02	0.05

Values without color indicate  $-0.2 < SRC < 0.2$ ; values with green and pink colors indicate values  $< -0.2$  and  $> 0.2$  respectively. Positive values indicate that a higher input parameter value generates a higher model output variable, and negative values indicate that a higher input parameter value generates a lower model output variable.

Table SI3.3 Standardized regression coefficient (SRC) representing the relative sensitivity of the model performance for the Yangtze River to the variations of 53 model parameters. Parameters which have no significant values for none of the outputs are not shown<sup>a</sup>. The description, unit and the default value of the input parameters are provided in Table SI3.1.

Parameters	TSi_Export	DSi_Export	BSi_Export	BSi_Burial	PP_PHYPSi_Pelagic	PP_PHYPSi_Benthic
Solar_radiation	-0.09	-0.14	0.27	0.30	0.22	0.29
Temperature	0.14	0.17	-0.19	-0.34	0.19	0.13
Discharge	0.09		0.50	-0.33	-0.07	-0.06
T <sub>opt,Det_Si_Benthic_dissolution</sub>	-0.15	-0.20	0.31	0.39	-0.02	-0.03
V <sub>sed,Det_Si_Pelagic</sub>	-0.12	-0.08	-0.26	0.27	-0.01	
k <sub>I,PHYPSi_Pelagic</sub>	0.07	0.10	-0.18	-0.17	-0.24	0.05
k <sub>max_growth_pelagic</sub>	-0.14	-0.20	0.35	0.32	0.47	-0.08
PHYPSi <sub>lim_pelagic</sub>	-0.09	-0.15	0.33	0.23	0.45	-0.05
k <sub>I,PHYPSi_Benthic</sub>	0.05	0.06	-0.07	-0.13	0.02	-0.33
k <sub>max_growth_benthic</sub>	-0.14	-0.16	0.15	0.27	-0.03	0.65
k <sub>morta</sub>		0.03	-0.02	-0.08	0.02	-0.24
PHYPSi <sub>lim_benthic</sub>		-0.05	0.10	0.11	-0.01	0.33
DSi_weathering_input	0.78	0.76	0.06	0.16	0.08	0.10

<sup>a</sup>Values without color indicate  $-0.2 < \text{SRC} < 0.2$ ; values with green and pink colors indicate values  $< -0.2$  and  $> 0.2$  respectively. Positive values indicate that a higher input parameter value generates a higher model output variable, and negative values indicate that a higher input parameter value generates a lower model output variable.

For both rivers, Rhine and Yangtze, the TSi\_Export and DSi\_Export are strongly controlled by DSi\_Input from weathering. This also shows that DSi is the main source of the total Si\_Export. The SRC in the Yangtze (0.78) and Rhine (0.96) are both much higher than values for other model parameters.

The BSi\_Export in the Yangtze is negatively influenced by the detritus sedimentation velocity of waterbodies. In contrast, there is a positive effect of solar radiation, discharge, the optimal temperature for dissolution of Det\_Si\_Pelagic, the max growth rate for

pelagic diatoms and the diatoms threshold over which mortality is triggered. Compared with the Yangtze, the BSi\_Export in the Rhine is sensitive to the width of waterbodies, slope and PIM. This difference is because the Rhine has no major reservoirs, causing the average water travel time to be much shorter than that in the Yangtze.

The BSi\_Burial in both river basins is negatively influenced by temperature (higher temperature causing higher dissolution of Det\_Si and therefore lowering BSi burial) and discharge (higher discharge causing higher flow velocity, more resuspension, and less BSi\_Burial), and positively controlled by solar radiation, settling velocity of Det\_Si\_Pelagic, and the max growth rate for benthic/pelagic diatoms.

For both pelagic and benthic primary production, the results of the sensitivity analysis show that solar radiation, the length of waterbodies, half saturation of light limitation, max growth rate, threshold over which mortality is triggered and the mortality rate are important parameters.

Table SI3.4. Basin reservoir volume, natural area fraction, dominant lithology for the Rhine and Yangtze Rivers.

Property	Rhine	Yangtze	References <sup>a</sup>
Reservoir volume (km <sup>3</sup> )	0.6 in 1950 1.5 in 2000	0 in 1950 103.3 in 2000	This study
Natural area fraction	42% in 1950 47% in 2000	73% in 1950 33% in 2000	This study
Dominant Lithology	Mixed consolidated sedimentary and Alluvial deposits	Silici-clastic Sedimentary Rocks and Carbonated consolidated sedimentary	(Dürr et al. 2005)

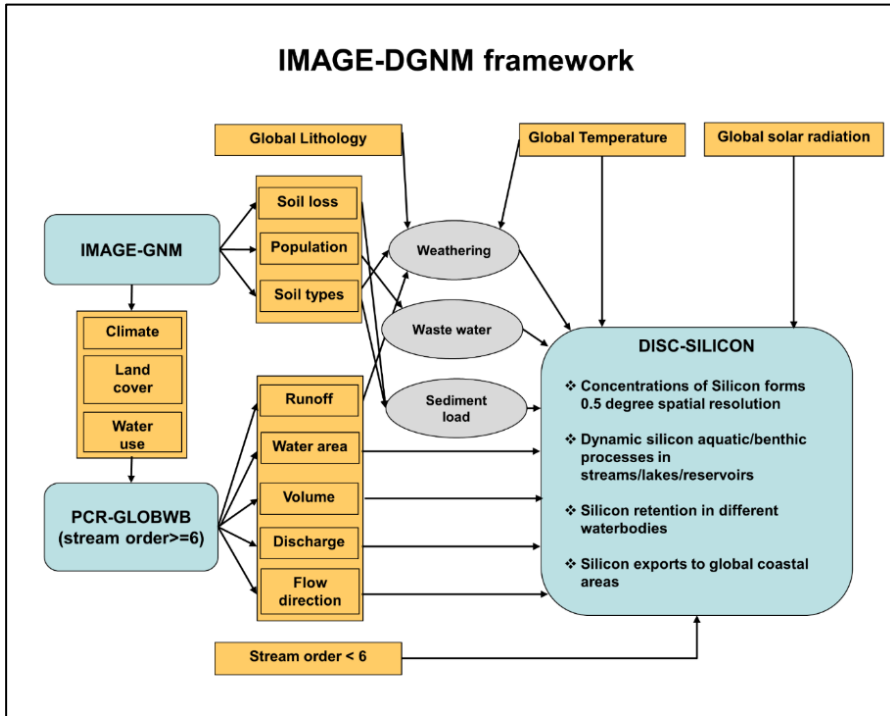


Figure SI3.1. Scheme of the IMAGE-DGNM framework

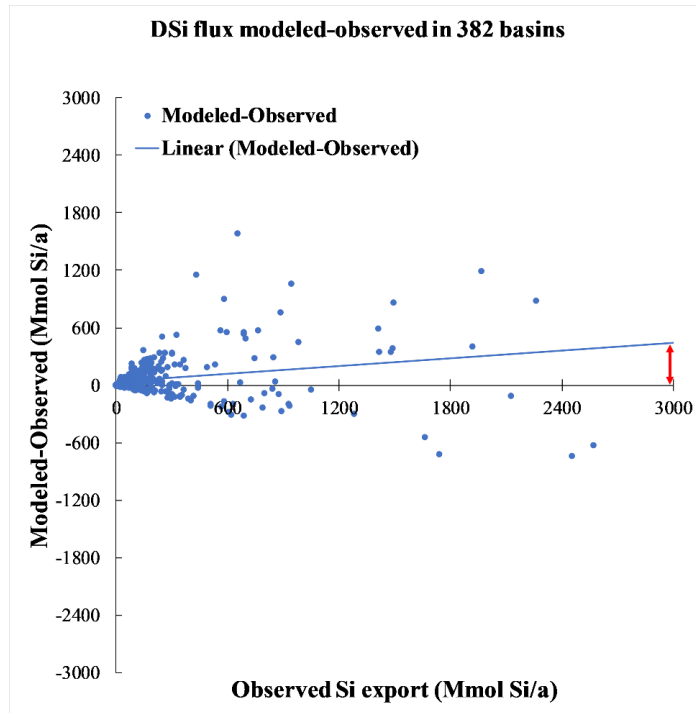


Figure SI3.2. Modeled based Hartmann et al (2014) minus Observed values for all the 382 basins. Red arrow indicates that the differences between simulations and observations are increasing.



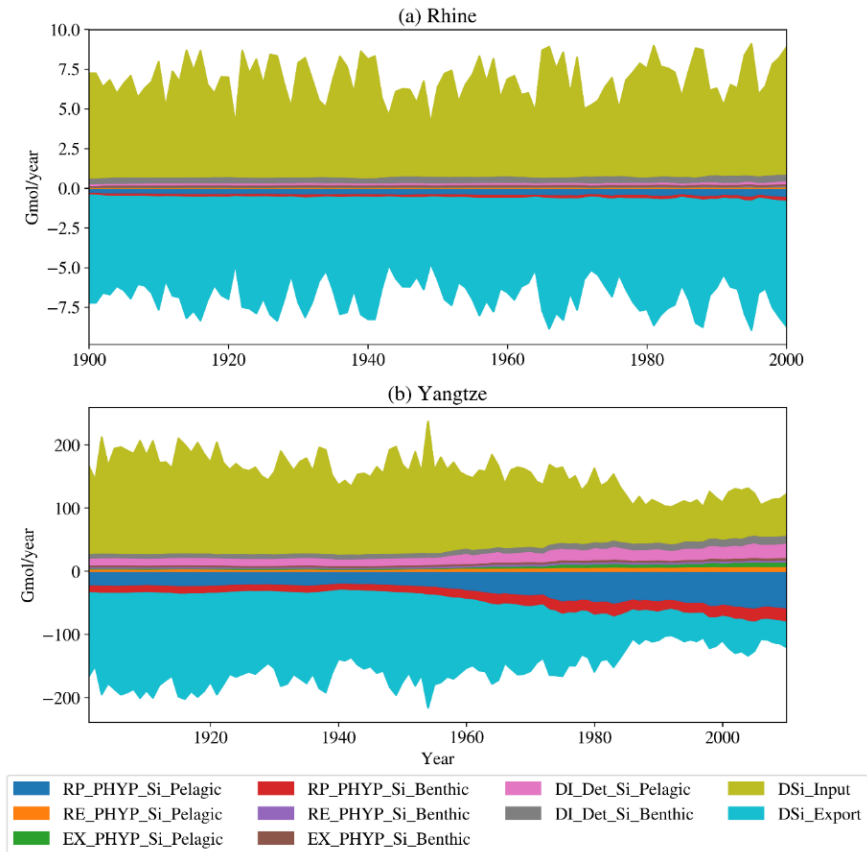


Figure SI3.3. Comparison of fluxes to and from the DSi pool in the Rhine (a) and Yangtze (b) for the period 1900-2000. PP = Primary production =  $F_5/F_{13}$ , RE = Respiration =  $F_6/F_{12}$ , EX = Excretion =  $F_6/F_{12}$ , DI = Dissolution =  $F_4/F_{14}$ , Input = Input to streams, Export = Export to mouth.



## Chapter 4

# Exploring spatiotemporal changes of the Yangtze River (Changjiang) nitrogen and phosphorus sources, retention and export to the East China Sea and Yellow Sea

---

Xiaochen Liu, Arthur H.W. Beusen, Ludovicus P.H. Van Beek, José M. Mogollón, Xiangbin Ran, Alexander F. Bouwman

---

*Water Research, 142 (2018) 246-255.*

## Abstract

Nitrogen (N) and phosphorus (P) flows from land to sea in the Yangtze River basin were simulated for the period 1900-2010, by combining models for hydrology, nutrient input to surface water, and an in-stream retention. This study reveals that the basin-wide nutrient budget, delivery to surface water, and in-stream retention increased during this period. Since 2004, the Three Gorges Reservoir has contributed 5% and 7% of N and P basin-wide retention, respectively. With the dramatic rise in nutrient delivery, even this additional retention was insufficient to prevent an increase of riverine export from 337 Gg N yr<sup>-1</sup> and 58 Gg P yr<sup>-1</sup> (N:P molar ratio = 13) to 5896 Gg N yr<sup>-1</sup> and 381 Gg P yr<sup>-1</sup> (N:P molar ratio = 35) to the East China Sea and Yellow Sea (ECSYS). The midstream and upstream subbasins dominate the N and P exports to the ECSYS, respectively, due to various human activities along the river. Our spatially explicit nutrient source allocation can aid in the strategic targeting of nutrient reduction policies. We posit that these should focus on improving the agricultural fertilizer and manure use efficiency in the upstream and midstream and better urban wastewater management in the downstream subbasin.

## 4.1 Introduction

Nitrogen (N) and phosphorus (P) are essential nutrients required for living organisms and often limit primary production in terrestrial and aquatic ecosystems (Elser et al. 2007, LeBauer and Treseder 2008). Modern human activities demand higher food and energy production, which helps accelerate N and P mobilization throughout the hydrosphere (Bouwman et al. 2009). Activities including fertilizer and manure use, fossil fuel consumption, the cultivation of leguminous crops, and wastewater discharge have more than doubled the rate at which biologically available nitrogen enters the terrestrial biosphere with respect to preindustrial levels (Galloway et al. 2008). This

anthropogenic nutrient mobilization has led to eutrophication and oxygen-depletion of freshwater and coastal marine ecosystems (Diaz and Rosenberg 2008), whose manifestations include changes in the structure of the food webs, loss of biodiversity, the eventual formation of toxic algae blooms, and a decline in fish production (Rousseau et al. 2000, Turner et al. 1998).

This change has been especially dramatic in China, where net N production increased from 9 Tg N yr<sup>-1</sup> to 56 Tg N yr<sup>-1</sup> from 1910 to 2010 (Cui et al. 2013, Gao and Wang 2008, Howarth et al. 1996b, Yan et al. 2010). In the Yangtze River basin (YRB), demographic growth and socioeconomic activities have risen drastically during the past century, especially since 1978. The total population dwelling by the mainstream of the Yangtze River increased by 134% from 213 million in 1949 to 498 million in 2010 (Committee 2014b). In the East China Sea, the frequency of harmful algal blooms (HABs) has increased by a factor of 3 every decade since the 1970s (Tang et al. 2006). In 2003, 119 HABs events were reported in all Chinese coastal areas, of which 89% were in the East China Sea (China 2009, Tang et al. 2006). Reported red tide occurrences in the Yangtze estuary region increased from 29 in the 1980s to 195 in the 2000s (China 2009).

Existing studies of nutrient transport within the Yangtze River have primarily focused on the nutrient load at the river mouth (Dai et al. 2010, Li et al. 2007, Qu and Kroeze 2012, Xu et al. 2013) or specific upstream monitoring stations or reaches (Cui et al. 2013, Duan et al. 2008, Tong et al. 2017a, Yan et al. 2003, Zhiliang et al. 2003). Furthermore, these studies of YRB nutrient loading, retention, and export are either based on the measurements at Datong station or on subbasin-scale regression models that only simulate one or two specific years.

Available studies lack spatiotemporal scales to analyze inter-annual patterns of river biogeochemistry and nutrient sources/exports under changing human pressures. This paper focuses on the Yangtze River, the main water body draining into the East China Sea and Yellow Sea (ECSYS). This study uses the Integrated Model to Assess the Global Environment - Global Nutrient Model (IMAGE-GNM) (Beusen et al. 2015), which couples models for hydrology and nutrient delivery to surface water with in-stream biogeochemistry and retention in a spatially explicit manner. We evaluate the changes in the various N and P sources and export to the coast for the period 1900-2010, with special attention to the impact of the Three Gorges Reservoir (TGR) (completed in 2004). Simulation results are compared to nutrient measurements from both upstream stations and the mouth. This study consists of two parts: (i) applying the model to identify the spatial distribution of nutrient sources and nutrient delivery for the upstream, midstream and downstream subbasins for the period 1900-2010, and (ii)

analyzing the nutrient retention in waterbodies and export to ECSYS, including the effects of Three Gorges Dam (TGD).

## 4.2. Methods

### 4.2.1 Study area

The Yangtze River is the largest river in the Eurasian continent, covering an area of  $1.8 \times 10^6$  km<sup>2</sup>, with an average annual discharge of 892 km<sup>3</sup> for the period 1950–2010 (Committee 2015) and a length of the main stream of 6400 km (Figure 4.1). The YRB covers 20% of the Chinese land area, hosts 35% of the nation's population and receives 32% of the Chinese fertilizer inputs (Xing and Zhu 2002). For our analysis, the YRB was divided based on watershed boundaries into three parts (Figure 4.1), the upstream (upstream of Yichang), midstream (between Yichang and Hukou) and downstream (downstream of Hukou) subbasins (Wang et al. 2008a).

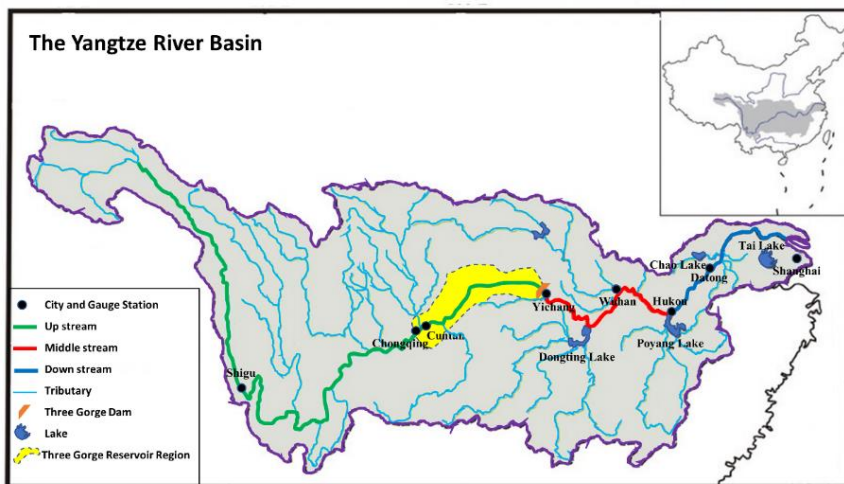


Figure 4.1. Location of the monitoring stations in the Yangtze River basin.

### 4.2.2 IMAGE-GNM model

IMAGE-GNM is a spatially distributed model with an explicit 0.5-degree resolution. This grid cell-based model simulates the N and P delivery to surface water via surface runoff, shallow groundwater and deep groundwater. The IMAGE-GNM model couples the IMAGE integrated assessment model (Stehfest et al. 2014) with the global hydrological model PCR-GLOBWB (Van Beek et al. 2011). PCR-GLOBWB provides the water flux direction, discharge, surface water area, flooding area, lakes and

reservoirs information, depth of water bodies and residence time of water bodies. IMAGE simulates the land-use change and provides the climate data, and IMAGE-GNM calculates the soil N/P budget arising from diffuse sources (agricultural systems, natural systems, vegetation in flooded areas, deposition) and point sources (aquaculture, wastewater urban areas). After calculating retention in waterbodies (streams, rivers, floodplains, lakes, and reservoirs), each grid cell receives all the N and P output from all upstream cells and the N and P input from sources within the grid cell. For each grid cell, the nutrient and water flow pathway is given (Figure SI4.1). Figure SI4.2 indicates the data flows between PCR-GLOBWB and IMAGE. Additional details on the model are given in SI4.1.

IMAGE-GNM includes (i) N and P delivery from agricultural and natural land systems, via runoff to surface water and via leaching through shallow groundwater and deep groundwater, riparian zones and finally to surface water, (ii) N and P delivery from wastewater discharge and aquaculture, (iii) nutrient input from allochthonous organic material from vegetation in floodplains, (iv) N inputs from atmospheric deposition to terrestrial surfaces and water bodies, and (v) the nutrient spiraling method (Newbold et al. 1981, Wollheim et al. 2008a) to calculate the in-stream N and P retention. For details on input and ancillary data we refer to Beusen et al. (2015). Land use and climate data are obtained from the IMAGE model (Stehfest et al. 2014).

Observations of annual discharge, concentrations of dissolved inorganic N (DIN, consisting of nitrate, ammonium and nitrite) and dissolved inorganic P (DIP) were collected from the Yangtze Water Resources Commission (CWRC) and published literatures (See SI4.2). Total N (TN) and total P (TP) concentrations were obtained by using TN:DIN and TP:DIP ratios from the literatures (see SI4.2). Nutrient input and output data were obtained from provincial-scale Chinese statistics (China 2014a, China 2014b, Committee 2014a). The start year depends on the data availability. When possible, we use 1961, otherwise the earliest available year. Missing years are interpolated. For years preceding the first available year, we combine the distribution of subnational data for the first available year together with FAO data for the whole country for the specific preceding year. If data for similar categories is available (e.g. livestock data for estimating feed use), the trend for that item is used to compute preceding years for the item with missing data. The provincial data are scaled so that the national total for China matches the FAOSTAT data (Bouwman et al. 2005b). Data for the period 1900-1961 is from a recent study (Bouwman et al. 2013c). We validated our model by calculating the root mean square error (RMSE) with respect to measured nutrient loads (see SI4.3.1).

The model sensitivity for the years 1900, 1950 and 2000 was investigated using the

Latin Hypercube Sampling method, with uncertainty ranges for 48 input parameters for N and 34 for P (SI4.3.2). The standardized regression coefficient (SRC) was calculated to represent the relative sensitivity of output to the variations of model input parameters.

## **4.3 Results and discussion**

### **4.3.1 Comparison with measurements**

For the 1960-2010 period, the model predictions generally agree with the observed data at the monitoring stations (Figure 4.2). The RMSE for the discharge is 20%, 24%, 10%, and 11% for the Cuntan, Yichang, Wuhan, and Datong stations, respectively. The modelled discharge matches better with the observations (Committee 2014c) at downstream stations than at upstream stations. The annual trend is well represented, although the model slightly underestimates the discharge at Cuntan and Yichang stations.

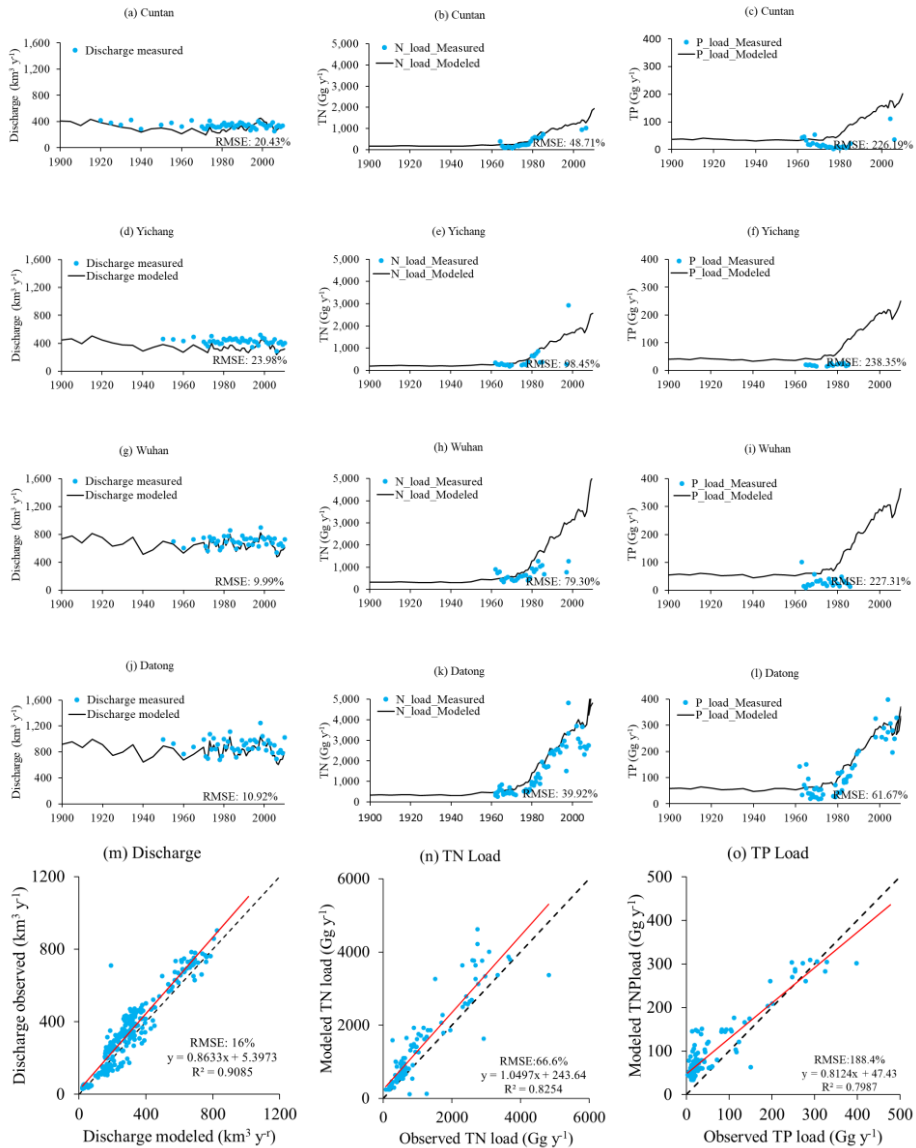


Figure 4.2. Comparison of measurements (blue dots) and modeled (black line) discharge, TN load and TP load in the stations of Cuntan (a-c), Yichang (d-f), Wuhan (g-i) and Datong (j-l) for the period 1900-2010; and relationships between observed and modeled discharge, TN and TP loads (m-o) for all data for all the stations shown in (m-o). The black dashed line is the 1:1 line.



The simulated TN load also agrees fairly well with observations (Figure 4.2b, 4.2f, 4.2h, 4.2k). The RMSE for TN are 49%, 98%, 79% and 40% for the Cuntan, Yichang, Wuhan, and Datong stations, respectively. The uncertainty in the measurement data is shown by comparing different annual TN load estimates (Figure 4.2n) obtained from different literature sources (SI4.2). The simulated TP load does not unreasonably deviate from the observed data at Datong (Figure 4.2). The RMSE for TP are 226%, 238%, 227% and 62% for the Cuntan, Yichang, Wuhan and Datong stations, respectively. For the simulated period 1900-2010, there is a rapid increase of both the TN and TP loads after 1978 at all the stations, as is well reproduced by the model. However, we calculate on an annual basis, which may not appropriately capture short-term observations (due to, for example, flooding or dry months). Furthermore, the subbasins with a higher mismatch cover a smaller number of grid cells, which entails more uncertainty.

The discrepancy between simulations and observations for TP in upstream stations can also be partly attributed to the fixed TP/DIP ratio (Yang et al. 2008) used to estimate TP, which may be different for the various hydrogeological settings (e.g. sediment loads). However, these have not been measured for the different river segments or subbasins. Furthermore, the overestimation of the TP load may result from downscaling during the soil TP budget calculation and scarcity of measurements. This scaling problem arises as the provincial-wide fertilizer, livestock, and crop production data are allocated to grid cells with agricultural land use according to the IMAGE model. This may lead to overestimations for regions upstream of Cuntan where the actual dominant landscape is a natural forest in mountainous areas (Su et al. 2017) (SI4.5, Movie SI4.3). The discrepancies between model and observations, however, do not affect our main conclusion that the agricultural fertilizer and manure use dominate in the upstream and midstream and point sources in the lower subbasin (see below).

### 4.3.2 Spatial-temporal variations of the nutrient sources

The whole-basin soil N budget increased almost 10 folds from 1.5 Tg N yr<sup>-1</sup> in 1900 to 14.2 Tg N yr<sup>-1</sup> in 2010 (Figure 4.3a), particularly after 1970. With expanding agricultural activity and massive amounts of chemical fertilizer use, the soil N budget increased dramatically after 1980 in many parts of the YRB (SI4.5, Movie SI4.2). The soil P budget for the YRB went from slightly negative to 1.7 Tg P yr<sup>-1</sup> for the period 1900-2010 (Figure 4.3b). Prior to 1970, the P soil budget was negative in most grid cells due to no fertilizer input and leading to soil P mining (SI4.5, Movie SI4.3). However, nutrient inputs may be underestimated as we did not include the use of human excreta in agriculture (FAO 1977).

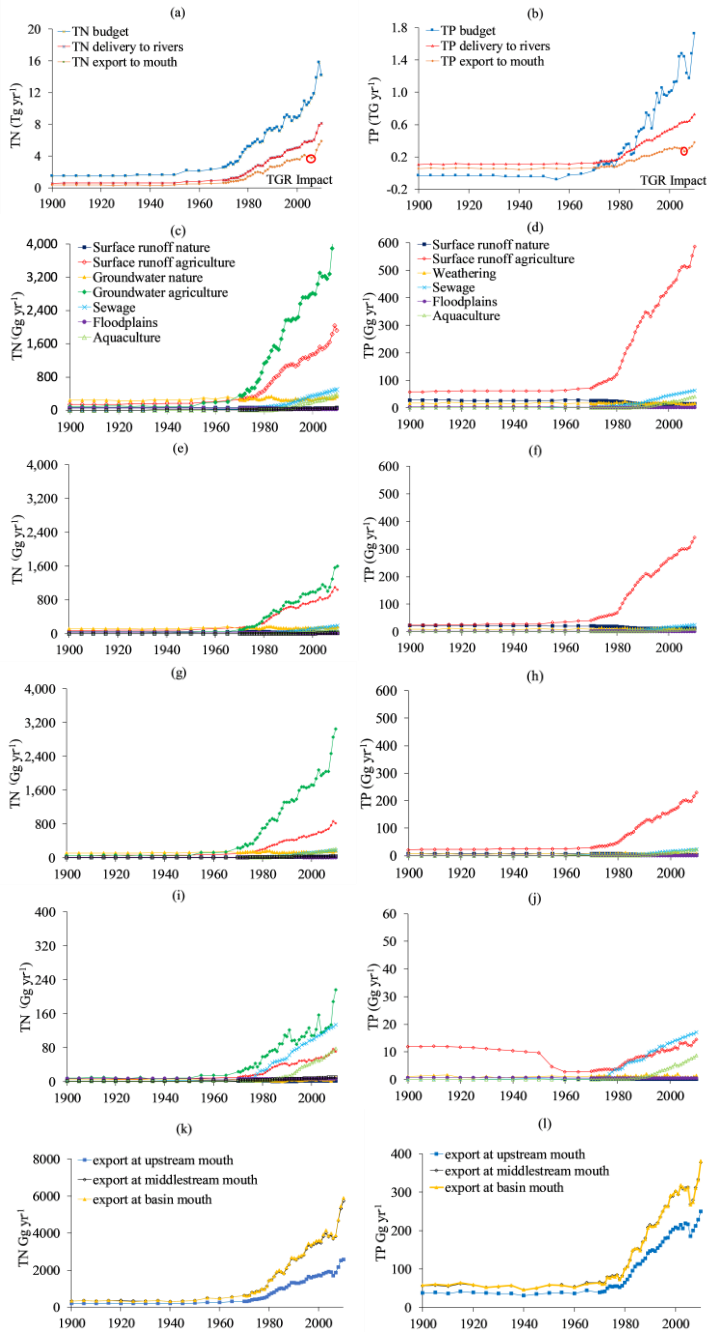


Figure 4.3. (a) N and (b) P soil budget, loads to rivers and exports to mouth for the Yangtze River basin for the period 1900-2010; river TN and TP delivery to surface water

from different sources for the period 1900-2010 for the whole basin (c, d), the upstream subbasin (e, f), the midstream subbasin (g, h), and the downstream subbasin (i, j); N and P export from the upstream, midstream and the whole Yangtze River basin during the period 1900-2010 (k, l).

The nutrient soil budget, delivery, and river export (Figure 4.3a, b) rapidly diverge after 1980, which results from N and P accumulation in soils and groundwater systems and the inability of the river biogeochemistry to retain the increasing nutrient delivery. Parallel to the nutrient budgets, the modeled N and P delivery to surface water in YRB was stable for the period 1900-1970 and started to accelerate after the 1970s in most places (SI4.5, Movie SI4.4, SI4.5). Along with the increasing delivery since the 1970s, agricultural activities were the dominant source for N and P to the surface water in most parts of the YRB (SI4.5, Movie SI4.6, SI4.7). Groundwater discharge from agricultural areas became the dominant N source in most grid cells and runoff from agricultural land became the dominant P source after 1970 (Figure 4.3c). The sum of surface runoff and groundwater from land under natural vegetation was stable at about 325 Gg N yr<sup>-1</sup> and 18 Gg P yr<sup>-1</sup> during 1900-2010 (Figure 4.3c). However, the share of these natural sources to total surface water delivery decreased sharply during this period from 52% to 5% for N and 16% to 2% for P. In contrast, agricultural sources increased 31 folds from 221 Gg N yr<sup>-1</sup> to 6791 Gg N yr<sup>-1</sup> and 10 fold from 58 Gg P yr<sup>-1</sup> to 587 Gg P yr<sup>-1</sup> (Figure 4.3d). The agricultural share of total delivery to rivers increased continuously from 38% to 83% for N and from 55% to 81% for P. These trends follow the Chinese agricultural development during the 20<sup>th</sup> century, which not only was the main economic driver during this period, but also saw a rapid technological increase after 1970s (Zhao et al. 2008).

The contribution of natural vegetation in floodplains decreased from 48 Gg N yr<sup>-1</sup> to 28 Gg N yr<sup>-1</sup> and from 4 Gg P yr<sup>-1</sup> to 2 Gg P yr<sup>-1</sup> (Figure 4.3c). Its share decreased from 8% to almost 0% for N and from 4% to almost 0% for P, mainly due to the increasing contribution from agricultural land and the construction of dams, which led to a regulation of river discharge and thus decreasing flooding areas.

The contribution of point sources (sewage) for the 1900-2010 period increased three orders of magnitude from 2 Gg N yr<sup>-1</sup> to 505 Gg N yr<sup>-1</sup> and 0 to 64 Gg P yr<sup>-1</sup>. With lagging wastewater treatment, rapid urbanization led to increasing amounts of untreated human waste which was discharged to surface water directly. The share of sewage increased from 1% to 9% for N and from 0% to 11% for P. The contribution of direct atmospheric deposition on waterbodies increased from 5 Gg N yr<sup>-1</sup> to 57 Gg N yr<sup>-1</sup>, but its share was stable due to the proportional increase of the total N sources.

Nutrients from aquaculture showed a dramatic increase from 1950 to 2010 of 1 Gg N yr<sup>-1</sup> to 415 Gg N yr<sup>-1</sup> and from 0 to 47 Gg P yr<sup>-1</sup>. For this period, aquaculture's contribution to total delivery increased from 0% to 7% for N from 0% to 9% for P. This is also reflected in recent statistical trends for Chinese agriculture, with the contribution of fisheries steadily increasing its share within total agricultural production (Zhao et al. 2008).

The contribution of the various nutrient sources to the Yangtze River varied in different subbasins (Figure 4.3; SI4.8; SI4.5). The shares of upstream and midstream to total N delivery for the whole YRB were about equal in 1900 (49% for upstream, 46% for midstream) with a small share of the downstream subbasin (5%), whereas the midstream subbasin became the main source of N delivery to surface waters from 1955. In 2010, 55% of the total N delivery to the Yangtze was from the midstream, and 39% from the upstream, and 6% from the downstream subbasin. The upstream subbasin was the main source of P delivery to the Yangtze with a stable share of around 57% during the period 1900-2010. The midstream and downstream subbasins saw a share change of P delivery from 35% to 39% and from 11% to 6%, respectively.

Within the upstream subbasin, agricultural N sources (groundwater and surface runoff) became dominant from the 1970s, and N from sewage water became the third dominant source since around the year 2000 (Figure 4.3e). P from surface runoff in agricultural areas remained the dominant source throughout the entire simulation period and increased rapidly since 1980 due to the increasing use of fertilizer and manure from livestock (Bouwman et al. 2013c) due to the increase of animal production. P from sewage (mid 1990s) started to exceed weathering and became the second dominant source, while other primarily natural sources remained stable, a direct consequence of increasing urbanization even in the upper portions of the YRB.

In the midstream subbasin, N from groundwater and surface runoff in agricultural areas started to increase rapidly in the 1970s. P delivery in the midstream subbasin follows the same trend as in the upstream subbasin, with sewage and aquaculture becoming the second and third dominant sources in the 1990s.

Results for the downstream subbasin are quite different from the upstream and midstream subbasins. N from groundwater in agricultural areas had been the dominant source in the downstream subbasin since the 1950s. N from sewage and groundwater in agricultural areas formed the dominant sources since the 1970s. P from surface runoff in agricultural areas was the dominant source, but its share in total P delivery decreased during the period 1900-1970 due to the shrinking agricultural areas. P from sewage and surface runoff in agriculture were the first and second dominant P sources since the

1980s. Aquaculture in the downstream subbasin has significantly increased nutrient delivery since 1990, becoming the third dominant source for P since 1992.

Groundwater receives nutrient inputs from leaching, especially in unconfined shallow aquifers under croplands (Puckett et al. 2011, Zhang et al. 2017). The residence times vary from years to decades or longer, and this means that large N and P amounts are temporarily stored in aquifers. This legacy implies that the surface water concentrations will persist for decades even after the fertilizer inputs have ceased (Sharpley et al. 2013, Van Meter et al. 2016). IMAGE-GNM accounts for the legacy of past agricultural N and P management. For N, legacies are related to the travel time of water and nitrate in aquifers, which typically exceeds the yearly timescale. In 1900, we calculated a temporary storage of 71 Gg N yr<sup>-1</sup>, which rose to 3026 Gg N yr<sup>-1</sup> in 2010, with a cumulative amount of 17797 Gg N over the whole 1900-2010 period. For P, IMAGE-GNM tracks all inputs and outputs in the soil P budget, which includes the effects of P accumulation and retention (from negative in 1900 to 1497 Gg P yr<sup>-1</sup> in 2010) in soils. These nutrients may thus be released into the fluvial system in the coming decades, even if policies to reduce N and P overuse in agriculture are implemented now. GNM does not include direct manure discharge into the river, since we concluded that its influence on the N and P cycling in the YRB has been only minor in the 1970-2010 period and it is most probably declining due to government policies (see SI4.3).

### 4.3.3 Nutrient retention and export

#### 4.3.3.1 Nutrient retention in waterbodies

The whole-basin retention in the Yangtze for 1900-2010 increased 9 fold from 239 Gg N yr<sup>-1</sup> to 2252 Gg N yr<sup>-1</sup> and 7 fold from 49 Gg P yr<sup>-1</sup> to 348 Gg P yr<sup>-1</sup> (Figure 4.4a,c). In contrast, due to increasing N concentrations and the removal of electron donors, denitrification rates dampened (equation5) and thus, the fraction of N retained decreased from 41% in 1900 to 28% in 2010. For P, it remained constant at 48% during the whole period (Figure 4.4a, c).

During this same period, total retention in streams and rivers of the YRB increased from 155 Gg N yr<sup>-1</sup> to 747 Gg N yr<sup>-1</sup> and from 38 Gg P yr<sup>-1</sup> to 154 Gg P yr<sup>-1</sup>. However, the share of this retention decreased from 65% to 33% for N and from 76% to 44% for P (Figure 4.4b, d). Total retention in lakes increased from 85 Gg N yr<sup>-1</sup> to 863 Gg N yr<sup>-1</sup> and from 12 Gg P yr<sup>-1</sup> to 87 Gg P yr<sup>-1</sup>, with the share of retention in lakes increasing from 35% in 1900 to 42% in 1996 and then decreasing to 38% in 2010 for N, while it remained steady at 24% during the entire 1900-2010 period for P (Figure 4.4b, d). The retention in reservoirs increased rapidly from 0 to 642 Gg N yr<sup>-1</sup> and from 0 to 107 Gg

$\text{P yr}^{-1}$ . The retention share in reservoirs to the total retention increased from 0% to 28% for N and from 0% to 31% for P (Figure 4.4b, d).

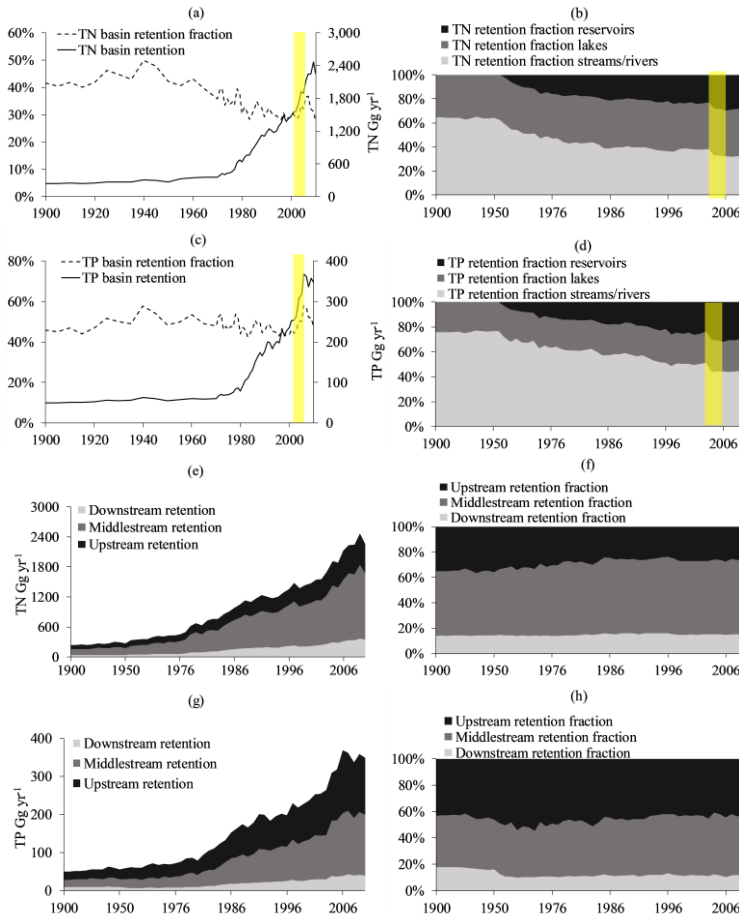


Fig 4.4. (a) Total retention of N and the river basin N retention fraction, and (b) fraction of retention in streams/ivers, lakes and reservoirs in total basin; (c) total retention of P and the river basin P retention fraction, and (d) fraction of retention in streams/ivers, lakes and reservoirs in the total basin. Yellow bar indicates the filling stage of the TGR; (e) Retention of N and (f) N retention fraction of midstream and downstream subbasins; (g) Retention of P and (h) P retention fraction of midstream and downstream subbasins for the period 1900-2010.

Total retention in the three subbasins increased both for N and P, but the fraction of nutrients removed in each subbasin has fluctuated (Figure 4.4f, h). The upstream N retention fraction decreased from 35% in 1900 to 26% in 2010, increased from 51% to

58% in the midstream subbasin, and was constant at 15% in the downstream subbasin. For P, the contribution of upstream retention was constant at 46% throughout the period 1900 to 2010, increased from 39% to 46% for the midstream subbasin, and decreased from 18% to 11% for the downstream subbasin.

Total N retention in the TGR increased from 1 Gg N yr<sup>-1</sup> in 2003 to 90 Gg N yr<sup>-1</sup> in 2004 and from 0.2 Gg P yr<sup>-1</sup> in 2003 to 20 Gg P yr<sup>-1</sup> in 2004 (Figure 4.5a,b). This increase in nutrient retention was mainly due to the infilling of the TGR, and contributed 5% for N and 10% for P of the nutrients load into the TGR (Figure 4.3a, b). Our estimate of N retention is fairly close to the observation (6%) of TDN (the dominant form of N) in the TGR (Ran et al. 2017). The P retention is lower (circa 44%) than a measurement performed in April 2004 (Ran et al. 2016) but higher than a measurement (circa 4.91%) in 2003 when the TGR impoundment occurred (Sun et al. 2013). Due to the increase of N and P retention in the TGR, the N concentration increased by 39% from an average 4.3 mg L<sup>-1</sup> in 1900s to 6.0 mg L<sup>-1</sup> after 2003 and the P concentration by 34% from 0.5 mg L<sup>-1</sup> in 1900s to 0.7 mg L<sup>-1</sup> after 2003 (Figure 4.5c, d). The contribution of TGR to the whole-basin retention increased from 0% before impounding to approximately 5% for N and 6% for P after the impounding. The TGR reduced the nutrient load to the downstream part of YRB, but its differential nutrient retention may lead to a high risk of eutrophication within the reservoir itself.

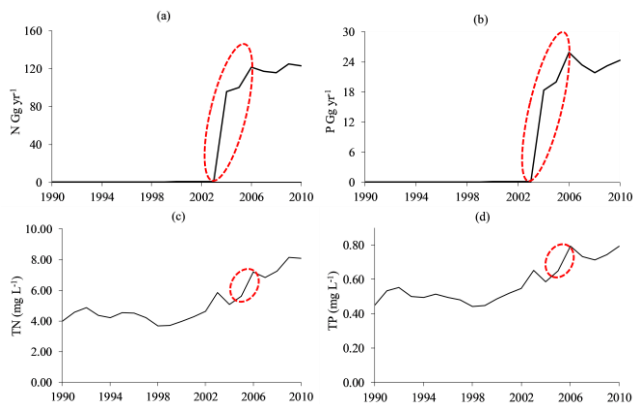


Figure 4.5. N (a) and P (b) retention and TN (c) and TP (d) concentrations in the TGR for the period 1900-2010. The retention is calculated as the total for all grid cells covered by the TGR, and the concentration is the average of all TGR grid cells.

### 3.3.2 Nutrient export to lower subbasin and the ECSYS

For the 1900-2010 period, the river N export at Yichang increased 13 fold from 196 Gg

N yr<sup>-1</sup> to 2562 Gg N yr<sup>-1</sup> (17 fold 339-5714 Gg N yr<sup>-1</sup> at Hukou, 17 fold 337-5896 Gg N yr<sup>-1</sup> at the mouth) (Figure 4.3k). The difference between Yichang and Hukou can be attributed to the increasing N contribution from the midstream subbasin. The N export to the ECSYS stems mainly from the midstream subbasin.

The P export at Yichang increased 7 fold from 37 Gg P yr<sup>-1</sup> to 249 Gg P yr<sup>-1</sup> (56-377 Gg P yr<sup>-1</sup> at Hukou, 58-381 Gg P yr<sup>-1</sup> at the river mouth) for the period 1900-2010 (Figure 4.3l). The difference between Yichang and Hukou stations was smaller than for N export. This is largely due to the P export to the ECSYS, which stemmed mainly from the upstream subbasin.

The downstream subbasin contributes a small fraction of nutrient export to the ECSYS. This small share results from the small area of the downstream subbasin (only 5% of the whole YRB) while the water area of the downstream subbasin covers 19% of the whole water area. This leads to higher retention efficiency downstream, with our results indicating that 71% of local N (99% for P) delivery to surface water was removed in the downstream subbasin in the 2000s.

Nutrient export estimates from the Yangtze River to the ECSYS are available from various literature sources (SI4.6, Table SI4.5) for the year 2000. For N, they vary from 1807 Gg N yr<sup>-1</sup> (Lumped regression (Ti et al. 2012)) to 1132 Gg N yr<sup>-1</sup> (Global NEWS-2 (Li et al. 2011, Mayorga et al. 2010, Seitzinger et al. 2005)) and 1142 Gg N yr<sup>-1</sup> (MARINA model (Strokal et al. 2016a, Strokal et al. 2016b)). For P, they range from 95 Gg P yr<sup>-1</sup> (Global NEWS-2 (Mayorga et al. 2010, Seitzinger et al. 2005)) to 172 Gg P yr<sup>-1</sup> (MARINA model (Strokal et al. 2016a, Strokal et al. 2016b)). In contrast, our estimate of 3497 Gg N yr<sup>-1</sup> and 296 Gg P yr<sup>-1</sup> overshadow these values. If we use an observational reference of TN and TP concentration measurements combined with observed discharge in the Datong station, we obtain export values of 3698 Gg N yr<sup>-1</sup> and 289 Gg P yr<sup>-1</sup> (SI4.6) in 2002 (no observation available in 2000), which closely resemble our simulation estimates. There are several reasons for the discrepancy between the export calculations based on concentration and discharge to those of the statistical regression models. For one, the statistical analysis that served as the basis for Global NEWS was based on discharge data from multiple rivers, and the Yangtze River may fall outside this global correlation. Furthermore, these lumped and statistical correlation models were calibrated with data from the Datong station (Li et al. 2011, Strokal et al. 2016a, Strokal et al. 2016b, Ti et al. 2012, Yan et al. 2010), and ignore the contribution of the 600 km (Yang et al. 2002) river reach downstream of this station. The largest city group of China, the Yangtze River Delta Agglomeration, drains into this reach, and according to IMAGE-GNM, wastewater discharged into this reach is currently the dominant N and P source for the whole downstream subbasin. Our results show that the



reach downstream of Datong contributes 78% of the total N export and 84% of total P export to the downstream subbasin. However, most of the N and P inflow is retained in the large areas of local water bodies such as Lake Tai. Consequently, this contribution represents a small fraction of the total N and P export to ECSYS (Figure 4.3k, l).

Results from IMAGE-GNM closely match the monitoring data at Datong station despite not implementing direct animal manure discharge of N and P to surface waters, which we argue has been significantly overestimated in previous models of the YRB (see SI4.3.3). IMAGE-GNM can furthermore provide the direct nutrient export from Shanghai, the largest city of China, to the ECSYS. This value increased from 2.3 Gg N yr<sup>-1</sup> to 99 Gg N yr<sup>-1</sup> and from 0.3 Gg P yr<sup>-1</sup> to 10 Gg P yr<sup>-1</sup> for the period 1900-2010, primarily due to the rapid urbanization and development since the 1960s.

The sensitivity analysis shows that there is a shift of natural processes being the most important factors to agriculture becoming dominant in the course of the twentieth century (see SI4.3.2).

#### 4.3.4. Implications for the ECSYS

Our results show that various human activities have become dominant drivers of the nutrient cycling in the YRB, especially since the 1970s. Agricultural practices dominate the nutrient delivery to the upper and middle subbasins, whereas point sources stemming from the Yangtze River Delta Agglomeration control those to the downstream subbasin (Figure 4.3, SI4.7). Therefore, policies to reduce YRB nutrient concentrations should focus on improving fertilizer and manure agricultural use efficiencies in the midstream and upstream subbasins and on improving urban wastewater management in the lower subbasin. The 17-fold increase in N export and a 7-fold increase in P export imply a dramatic increase in the availability of nutrients and could lead to declining oxygen concentrations in coastal waters (Breitburg et al. 2018). Furthermore, due to increasing nutrient loadings and unbalanced nutrient retention in dams, the Yangtze River discharge to the ECSYS has seen a marked variation in its nutrient stoichiometry. Nutrient stoichiometry is an important indicator for the risk of HAB proliferation. The molar N:P ratio calculated for the mouth of the Yangtze in 1900 was 13, a value that is very close to the Redfield ratio (Redfield 1934) (molar N:P = 16:1), indicating a healthy environment. However, in the year 2010, the water had a much higher N:P ratio of 35, indicating that exported water switched to P limitation. This change coupled to the decreasing silica (Si) export from the Yangtze River (Dai et al. 2011, Li and Chen 2001) has caused a coastal imbalance in the loading of N, P and Si. When N and P are discharged in excess of Si with respect to the requirements of siliceous algae (diatoms), non-diatoms, often undesirable algal species, will develop (Billen and Garnier 2007).

HABs in both freshwaters and marginal seas in China are strongly related to these overall changing nutrient loads and ratios (Glibert et al. 2014). With a cumulative amount of 17797 Gg N stored in groundwater, and because policy efforts to reduce P loading to surface water are often more successful than strategies to reduce N flows (Bouwman et al. 2017b), it will be challenging to restore the nutrient stoichiometry to a “healthy” level (molar N:P = 16:1).

#### 4.4 Conclusion

The model results from the dynamic, spatially explicit, mechanism non-calibrated IMAGE-GNM are in fair agreement with the measurements in the Cuntan, Yichang, Wuhan and Datong stations. To our knowledge, we have included the most comprehensive nutrients validation dataset covering from the upstream Cuntan station to the downstream Datong station for the period 1964-2010. The spatiotemporal simulations go beyond the finding from time-specific measurements and regression models calibrated to the Datong station nutrient data. This model thus elucidates the following findings:

Our results reproduced the observed enormous increase of N and P export by the YRB to the ECSYS, particularly since the 1970s. The increase of nutrient retention in the YRB could not balance the increase of the nutrient delivery to the river. The contribution of TGR to the whole-basin retention increased from 0% before impounding to approximately 5% for N and 6% for P after the impounding. This additional retention after 2004 is insufficient to change the trend in the export due to the rapidly increasing N and P delivery to the streams. The TGR reduced the nutrient load to the downstream parts of the YRB, but this retention also implies an increased risk of eutrophication within the reservoir itself.

The modeled results indicate that the N export to the ECSYS stems mainly from the midstream subbasin, while P export is primarily from the upstream subbasin. The dominant source in the downstream subbasin is from sewage wastewater. Most of the nutrients are sustained within the subbasin due to a high fraction of water area. Dramatically increasing nutrient loads with a high N:P ratio (molar N:P increase from 13 in 1900 to 35 in 2010) may be one of the reasons for the recent rapid increase in frequency and area coverage of harmful algal blooms in ECSYS.

Policies to reduce the N and P export from the Yangtze River basin should focus on the midstream and upstream subbasins to improve fertilizer and manure use efficiencies. More concrete scenarios analysis should focus on the effectiveness of current and future policies and regulations to reduce nutrient sources in different parts of the YRB (i.e. where and how to reduce the anthropogenic nutrient inputs).

## Supporting Information

### SI4.1. Model description

The IMAGE-GNM model couples the IMAGE Integrated Assessment Model (Stehfest et al. 2014) with the global hydrological model PCR-GLOBWB (Van Beek et al. 2011). For each grid cell, the nutrient and water flow pathway is given (Figure SI4.1). Figure SI4.2 indicates the data flows between PCR-GLOBWB and IMAGE.

IMAGE-GNM calculates the delivery of N and P to the surface water from point (local ones, i.e. wastewater discharge from humans, animals and industries in urban areas) and diffuse (spread-out ones, i.e. agriculture, aquaculture, natural ecosystems, atmospheric deposition and weathering) sources. For the diffuse sources, the model uses the N and P soil budget, which is the difference between inputs and outputs for each grid cell according to the land type (croplands, grassland and natural vegetation).

N inputs for the soil budget model include fertilizer ( $Nfert$ ), animal manure ( $Nman$ ), atmospheric deposition ( $Ndep$ ) and biological N fixation ( $Nfix$ ). Outputs consist of ammonia volatilization ( $Nvol$ ) and N withdrawal ( $Nwithdrawal$ ). In croplands,  $Nwithdrawal$  represents the N in harvested crop products. In grasslands,  $Nwithdrawal$  represents the grass consumed by animals or harvested grass (by cutting or mowing). The soil N budget ( $Nbudget$ ) is computed as follows:

$$Nbudget = Nfix + Ndep + Nfert + Nman - Nwithdrawal - Nvol \quad (S1)$$

P inputs include fertilizers ( $Pfert$ ) and manure ( $Pman$ ). Like N, P outputs ( $Pwithdrawal$ ) are crop uptake for croplands and grass harvest or grazing for grasslands. We assume no P inputs for natural ecosystems, and N inputs are only from atmospheric deposition and biological fixation. N and P outputs are ignored, assuming that natural vegetation is mature and not growing. Hence, the N and P budgets ( $Pbudget$ ) represent the amount of N or P that can potentially enter the soil-hydrological system.

$$Pbudget = Pfert + Pman - Pwithdrawal \quad (S2)$$

Leaching of N is the transport of N below the subsoil, simulated as a fraction of the soil N budget which enters the shallow groundwater system, and if present, a deep groundwater system. IMAGE-GNM thus accounts for the N residence time in these systems, so that nutrient legacies are actually simulated. Direct nutrient delivery occurs through runoff, calculated from land use, terrain slope and soil texture. Runoff from soils accounts for the changes of nutrient contents in soils due to accumulation or depletion by agricultural management and the erosion itself. Other direct nutrient delivery types include wastewater discharge, aquaculture, allochthonous organic

material inputs, atmospheric deposition, and weathering of the parent material. Due to the scarcity of industrial pollution data, we estimated industrial nutrient flows as a fraction of human urban nutrient flows. The calculation of nutrient discharge from wastewater (from humans, animals and industries in urban areas) is described by Morée et al. (Morée et al. 2013). Nutrient release from freshwater aquaculture is calculated using the country-scale model estimates of Bouwman et al. (2013), Bouwman et al. (2011), for finfish and for shellfish using FAO (2013) data for the period 1950-2010. Before 1950 aquaculture production was negligible.

Spatial allocation of aquaculture nutrient release occurs on the basis of three weighting factors: population density, presence of surface water bodies, and mean annual air temperature (Beusen et al. 2015). Atmospheric N deposition is included in the soil budgets, and direct deposition on water bodies is calculated in each grid cell. Nutrient inputs from allochthonous organic material are calculated as a fraction of the net primary production using N and P contents of the material depending on vegetation type. P release from weathering is based on runoff, lithological class, a soil-shielding factor, and finally, an Arrhenius equation that accounts for the impact of temperature on the weathering process.

For N, the main contributors to in-stream retention are denitrification, sedimentation, and uptake by aquatic plants. For P, the main contributors are sorption by sediment and sedimentation. Nutrient retention is calculated using the spiraling approach (Newbold et al. 1981, Wollheim et al. 2008).

$$R = 1 - \exp\left(\frac{-v_f}{H_L}\right) \quad (S3)$$

$H_L$  is the hydraulic load ( $\text{m yr}^{-1}$ , eq. S4), and  $v_f$  is net uptake velocity ( $\text{m yr}^{-1}$ ), which is calculated separately for N and for P.

The hydraulic load is calculated as follows:

$$H_L = \frac{D}{t} \quad (S4)$$

where  $D$  is the waterbody depth (m),  $t$  is the residence time (yr) which is calculated by volume  $V$  ( $\text{m}^3$ ) divided by discharge  $Q$  ( $\text{m}^3 \text{ yr}^{-1}$ ).

The net uptake velocity for P (eq. S5), and N (eq. S6) are calculated as follows:

$$v_{f,P} = 45f(t) \quad (S5)$$

$$v_{f,N} = 35f(t)f(c_N) \quad (S6)$$

$c_N$  is total N (TN) concentration in the waterbody considered,  $f(c_N)$  describes the effect of concentration on denitrification as a result of electron donor limitation in the case of high N loads and  $f(t)$  describes the effect of temperature:

$$f(t) = \alpha^{(t-20)} \quad (S7)$$

where  $\alpha$  is 1.0717 for N (Wollheim et al. 2008) and 1.06 for P (Marcé and Armengol 2009).

## SI4.2 Validation data

Observed discharge data for the Cuntan, Yichang, Wuhan and Datong monitoring stations were obtained from the Yangtze River Yearbook (Committee 2014). Nutrient concentration and discharge data (daily, monthly, annual) were collected from published articles and Changjiang Water Resources Commission (CWRC) (see Table SI4.1).

## SI4.3. Data analysis

### SI4.3.1. Root Mean Square Error

The Root Mean Squared Error (RMSE) is used to compare observations and modeled results at individual stations in the Yangtze River. RMSE has been widely used as a statistical metric to evaluate model performance (Chai and Draxler 2014).

$$RMSE = \frac{100}{\underline{o}} \sqrt{\frac{\sum_i^n (o_i - M_i)^2}{n}} \quad (S8)$$

Where  $M_i$  is the modeled result,  $o_i$  is mean observed value,  $\underline{o}$  is mean of the observations and  $n$  is the number of data pairs.

### SI4.3.2. Sensitivity analysis

A detailed discussion of all parameters for the sensitivity on the global nutrient delivery to the rivers (N\_load\_river and P\_load\_river), the instream retention (N\_retention and P\_retention) and the river mouth export to the coastal areas (N\_export\_mouth and P\_export\_mouth) for the year 2000 has been presented in Beusen et al. (2015). Here we performed a sensitivity analysis where we varied 48 parameters for N and 34 parameters for P around their default values (Table SI4.2). We executed 500 runs for P and 750 runs for N. We calculated the standardized regression coefficient (SRC) for the N and P delivery to the river, the instream retention and the nutrient export to the coastal seas for the years 1900, 1950, and 2000 for the whole Yangtze River basin. The input parameters are all described in the supplementary information of the previous study (Beusen et al.

2015). Here we only present those important input parameters with a SRC value within the range  $SRC > 0.2$  and  $SRC < -0.2$ , i.e. with an influence exceeding  $0.2 * 0.2 = 0.04$  or  $> 4\%$ . A short description of these important input parameters is given in Table SI4.2 and the result of the sensitivity is given in Table SI4.3 (N) and SI4.4 (P).

The nutrient delivery clearly shows a shift from a natural-dominated system to an agricultural-dominated system. For N in 1900 and 1950, input parameters for the natural system such as  $N_{\text{budget,nat}}$  and  $F_{\text{leach,nat}}$  are important factors, but in 2000 they have been supplanted by  $N_{\text{budget,crops}}$  and  $F_{\text{leach,crop}}$ . Also, the  $N_{\text{con,low}}$  is an important factor ( $SRC > 4\%$ ) in streams with a low N concentration in 1900 and 1950, but has no effect in 2000. The flooding process was also important in 1900 and 1950 (see parameters  $CN_{\text{aomi}}$ ,  $A_{\text{flooding}}$  and  $F_{\text{aomi}}$  and AOMI). In 2000 the flooding reduced by half, but the N delivery has increased by a factor of 10. Therefore, the flooding process has become relatively unimportant for the N delivery. Total runoff ( $q_{\text{tot}}$ ) has more effect on arable land compared to natural or grassland, illustrating the shift from natural land to agricultural land. For P, the factors  $B_{\text{soil}}$  and  $P_{\text{soil}}$  are important factors for the surface runoff process.

The SRC values of in-stream retention and nutrient export are strongly coupled. In general, parameters that have a positive SRC for instream retention have a negative influence (SRC) on nutrient export. This implies that the nutrient export is less when there is more retention and vice versa. This coupling is not shown for parameters that influence the amount of nutrients, like for example  $N_{\text{budget,crops}}$  and  $N_{\text{budget,crops}}$ ,  $B_{\text{soil}}$  and  $P_{\text{soil}}$ .

The instream N and P retention depend on the amount of water ( $q_{\text{tot}}$ ), temperature (Temp) and the net uptake velocity for lakes and rivers ( $v_{\text{f,lake}}$  and  $v_{\text{f,lake}}$ ) and the hydrological factors in the streams of in the lower Strahler order ( $R_L$ , A,  $R_a$  and  $L_1$ ).

### SI4.3.3. Estimating direct manure discharge to surface water

The direct discharge of animal manure to surface water in China has been included in some recent models. The MARINA model (Strokal et al. 2016a) is an update of Global NEWS by linking to the NUFER (Ma et al. 2010) food system model to obtain model input data. According to that model, around 50% (30-70% range for different Chinese provinces) of the animal manure is directly discharged to surface waters. We assessed whether this source has an important contribution to the nutrient export of the river to the coastal sea.

To estimate the amount of manure that could be available for direct discharge to surface water, we made several assumptions: 1) Only manure in the form of slurry can easily be drained to the surface water via e.g. canals. Therefore, we only consider liquid manure

from pigs (in animal houses with a washdown system where water is added to a manure handling system) and no direct discharge from poultry and cattle systems, which generally produce dry manure. 2) We consider only the intensive systems, with farms more than 500 heads. 3) No volatilization loss is considered because we assume the manure discharge to surface water directly without house storage.

$$M_{\text{dir\_sur}} = \text{Fra}_{\text{dir\_sur}} \times \text{Fra}_{\text{population}} \times \text{Pro}_{\text{intensive\_system}} \quad (\text{S9})$$

Where  $M_{\text{dir\_sur}}$  is the pig manure which is directly discharged to surface water.  $\text{Fra}_{\text{population}}$  is the fraction of the total Chinese population which lives in the Yangtze River basin.  $\text{Pro}_{\text{intensive\_system}}$  is the production of pig manure from the intensive system in China, totaling 1341 Gg N yr<sup>-1</sup> and 469 Gg P yr<sup>-1</sup> in 2005. The fraction of the Chinese pig population living in the Yangtze River basin is 35% (Xing and Zhu 2002).  $\text{Fra}_{\text{dir\_sur}}$  is the fraction of pig manure from intensive systems that drain directly to surface water. This parameter is highly uncertain and variable in time and space. Assuming that all pig manure is directly going to the surface water (the worst-case scenario,  $\text{Fra}_{\text{dir\_sur}} = 1.0$ ), results in a direct manure discharge for the year 2005 for the Yangtze River basin of 469 Gg N yr<sup>-1</sup> and 84 Gg P yr<sup>-1</sup> (Eq. 9).

According to our model, in 2005, the total nutrient load to surface water was 5858 Gg N yr<sup>-1</sup> and 630 P yr<sup>-1</sup>. 55% of diffuse N input reached (43% for P) the surface water.

Adjusting our current model result, the N load to the surface water corrected for direct manure discharge is  $5858 - 0.55 \times 469 + 469 = 6069$  Gg N yr<sup>-1</sup> and the corrected P load is  $630 - 0.43 \times 84 + 84 = 678$  Gg P yr<sup>-1</sup>. The difference between both methods amounts to 211 Gg N yr<sup>-1</sup> and 48 Gg P yr<sup>-1</sup>, which is only a small fraction of the total river nutrient load. IMAGE-GNM, therefore, ignores the direct discharge of manure, given the fact that prior to 1970 this practice did not exist (Hauck 1978) and the parameter ( $\text{Fra}_{\text{dir\_sur}}$ ) is highly uncertain and variable in time and space.

#### SI4.4. Modeled output data

Click the link for download

<https://www.sciencedirect.com/science/article/pii/S0043135418304500#appsec1>

The directory “Modeled output data” contains IMAGE-GNM output directories for the years 1900, 1950 and 2010. Each annual directory includes two directories “N” and “P”.

The directory “N” contains the following ascii grid files:

Discharge.asc: water flux for each grid cell (km<sup>3</sup> yr<sup>-1</sup>).

N\_budget.asc: Soil nitrogen budget for each grid cell ( $\text{kg yr}^{-1}$ ).

N\_surface\_runoff.asc: Nitrogen load from surface runoff system ( $\text{kg yr}^{-1}$ ).

N\_groundwater.asc: Nitrogen load from groundwater system ( $\text{kg yr}^{-1}$ ).

N\_gnpp.asc: Nitrogen load from vegetation in flooding system ( $\text{kg yr}^{-1}$ ).

N\_deposition.asc: Nitrogen load to surface water from deposition ( $\text{kg yr}^{-1}$ ).

N\_aquaculture.asc: Nitrogen load from aquaculture system ( $\text{kg yr}^{-1}$ ).

N\_point.asc: Nitrogen load from sewage wastewater system ( $\text{kg yr}^{-1}$ ).

N\_load\_to\_river.asc: Accumulated nitrogen load from all sources in the river for each grid cell, accounting for contribution of local cell and upstream cell ( $\text{kg yr}^{-1}$ ).

N\_retention.asc: Nitrogen retention fraction in waterbodies (-).

The directory “P” contains the following ascii grid files:

Discharge.asc: water flux for each grid cell ( $\text{km}^3 \text{ yr}^{-1}$ ).

Pbudget.asc: Soil phosphorus budget for each grid cell ( $\text{kg yr}^{-1}$ ).

P\_surface\_runoff.asc: Phosphorus load from surface runoff system ( $\text{kg yr}^{-1}$ ).

P\_gnpp.asc: Phosphorus load from vegetation in flooding system ( $\text{kg yr}^{-1}$ ).

P\_aquaculture.asc: Phosphorus load from aquaculture system ( $\text{kg yr}^{-1}$ ).

P\_point.asc: Phosphorus load from sewage wastewater system ( $\text{kg yr}^{-1}$ ).

P\_load\_to\_rivers.asc: Accumulated phosphorus load from all sources in the river for each grid cell, accounting for contribution of local cell and upstream cell ( $\text{kg yr}^{-1}$ ).

P\_retention.asc: Phosphorus retention fraction in waterbodies (-).

### SI4.5. Movies

Click the *Supporting information* link for download,

<https://www.sciencedirect.com/science/article/pii/S0043135418304500#appsec1>

The directory “Movies” contains modeled results showing the spatially explicit changes of discharge, soil N and P budgets, N and P loads to streams, and dominant sources of



N and P for the period 1900-2010

**Movie SI4.1.** Discharge in  $\text{km}^3 \text{ yr}^{-1}$  in the Yangtze River Basin for the period 1900-2010.

**Movie SI4.2.** Soil N budget in  $\text{kg yr}^{-1}$  in the Yangtze River Basin for the period 1900-2010.

**Movie SI4.3.** Soil P budget in  $\text{kg yr}^{-1}$  in the Yangtze River Basin for the period 1900-2010.

**Movie SI4.4.** N delivery in  $\text{kg yr}^{-1}$  to streams in the Yangtze River Basin for the period 1900-2010.

**Movie SI4.5.** P delivery in  $\text{kg yr}^{-1}$  to streams in the Yangtze River Basin for the period 1900-2010.

**Movie SI4.6.** Dominant source of N in  $\text{kg yr}^{-1}$  in the Yangtze River Basin for the period 1900-2010. Obtained by accounting for various diffuse and point source and in-stream retention of all upstream grid cells.

AQUA: Input from Freshwater aquaculture

POINT: Input from Urban wastewater

DEPO: Input from Deposition

VEGETATION: Input from Floodplains

SRO\_NAT: Input from Surface Runoff in Natural Area

SRO\_AGRI: Input from Surface Runoff in Agricultural Area

GRW\_NAT: Input from Groundwater Outflow in Natural Area

GRW\_AGRI: Input from Groundwater Outflow in Agricultural Area

**Movie SI4.7.** Dominant source of P in  $\text{kg yr}^{-1}$  in the Yangtze River Basin for the period 1900-2010. Obtained by accounting for various diffuse and point sources and in-stream retention of upstream grid cells.

AQUA: Input from Freshwater aquaculture

POINT: Input from Urban wastewater

VEGETATION: Input from Floodplains

WEATHERING: Input from Lithological Weathering

SRO\_NAT: Input from Surface Runoff in Natural Area

SRO\_AGRI: Input from Surface Runoff in Agricultural Area

#### **SI4.6. Comparing with other studies**

See table SI4.5

#### **SI4.7. Tables N and P sources to streams for the whole Yangtze river basin**

See the file N and P sources to streams for the whole Yangtze river basin.xlsx

Click the *Supporting information* link for download,

<https://www.sciencedirect.com/science/article/pii/S0043135418304500#appsec1>

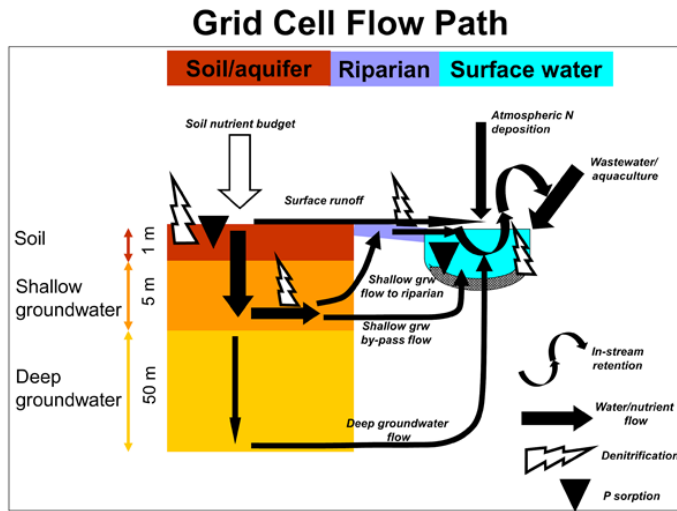


Figure SI4.1 Scheme of water and nutrients flows within one 0.5 by 0.5 degree grid cell, modified from the previous study (Beusen et al. 2015).

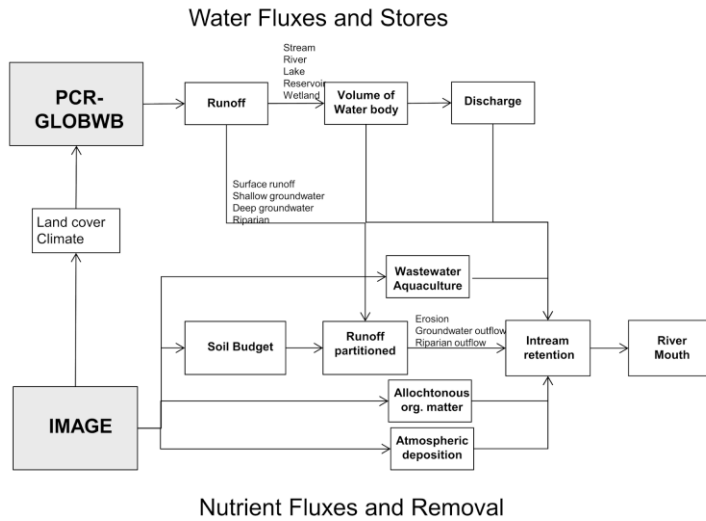


Figure S14.2 Scheme of Data flow between PCR-GLOBWB and IMAGE, modified from the previous study (Beusen et al. 2015).

Table SI4.1 Observations sources in different stations.

Stations	Year and sources	Observed nutrients forms*
Cuntan	1964-1985, 2004,2006 and from Changjiang Water Resources Commission(Committee 2014)	DIN, DIP
Yichang	1962-1970, 1975-1978, 1980-1985 and from Changjiang Water Resources Commission (Committee 2014)	DIN, DIP
	1986(Shen 1997), 1988(Shen 1997), 1990-2010(Sun et al. 2013)	DIN, NO <sub>3</sub> <sup>-</sup> -N, NO <sub>2</sub> <sup>-</sup> -N, NH <sub>4</sub> <sup>+</sup> -N, PO <sub>4</sub> <sup>3-</sup> -P, TP
	1997-1998(Liu et al. 2003, Shen et al. 2003)	TN, TDN, DIN, DON, TON, NO <sub>3</sub> <sup>-</sup> -N, NO <sub>2</sub> <sup>-</sup> -N, NH <sub>4</sub> <sup>+</sup> -N, TPN
Wuhan	1962-1986 (from Changjiang Water Resources Commission(Committee 2014))	DIN, DIP
Datong	1962-1986(Dai et al. 2010, Xu 2013) and from Changjiang Water Resources Commission(Committee 2014)	DIN, DIP
	1997-2010(Liu et al. 2003, Shen et al. 2003) <sup>(Dai et al. 2010)</sup>	TN, TDN, DIN, DON, TON, NO <sub>3</sub> <sup>-</sup> -N, NO <sub>2</sub> <sup>-</sup> -N, NH <sub>4</sub> <sup>+</sup> -N, TPN
Based on averaged measurements in stations located in the downstream subbasin	2012 ((Tong et al. 2017))	TN, TP

\*For computing TP load, a DIP/TP ratio of 13.75% (Yang et al. 2008) was used to transfer all the observed DIP data to TP for all stations. For computing TN load, a DIN/TN ratio of 50% (Yan et al. 2001, Zhang 1990) was used to transfer all the observed DIN data to TN for all stations. DIN is the sum of ammonia (NH<sub>4</sub><sup>+</sup>), nitrite (NO<sub>2</sub><sup>-</sup>) and nitrate (NO<sub>3</sub><sup>-</sup>). Annual TN and TP loads are calculated by multiplying concentrations with discharge.

Table SI4.2. Model parameters included in the sensitivity analysis that have an effect on the output parameters ( $SRC > 0.2$  and  $SRC < -0.2$ ), their symbol and description, the nutrient for which it is used, the default value of the parameter, and the min and maximum value of the range including the distribution for the sampling procedure.

Parameters	Description	Nutrient	Standard value in sampling	Min	Max	Distribution*
$CN_{aomi}$	CN weight ratio of gnpp (AOMI, see below) in flooding areas (-)	N	100	90	100	U3
$F_{leach,crop}$	Reduction fraction of N towards the shallow groundwater system from crop ecosystems (-)	N	1.0	0.9	1.0	U3
$F_{leach,nat}$	Reduction fraction of N towards the shallow groundwater system from natural ecosystems (-)	N	0.36	0.32	0.34	U3
$q^{tot}$	Runoff (total) (-)	N/P	1.0	0.9	1.1	U1
Temp	Mean annual air temperature (°C)	N/P	0.0	-1.0	1.0	U2
$N_{budget,crops}$	N budgets in croplands (-)	N	1.0	0.9	1.1	U1
$N_{budget,nat}$	N budgets in naturallands (-)	N	1.0	0.9	1.1	U1
$C_{sro,N}$	Correction coefficient for N in surface runoff (-)	N	0.3	0.27	0.33	U3
$C_{sro,P}$	Correction coefficient for P in surface runoff (-)	P	0.3	0.27	0.33	U3
Poros	Porosity of aquifer material (-)	N	1.0	0.9	1.1	U1
$v_{f,lake}$	Net uptake velocity for lakes ( $m\ yr^{-1}$ )	N	35	32	38	U3
$v_{f,lake}$	Net uptake velocity for lakes ( $m\ yr^{-1}$ )	P	44.5	40	49	U3
$v_{f,river}$	Net uptake velocity for rivers ( $m\ yr^{-1}$ )	N	35	32	38	U3
$v_{f,river}$	Net uptake velocity for rivers ( $m\ yr^{-1}$ )	P	44.5	40	49	U3
$A_{flooding}$	Area of flooding areas (-)	N/P	1.0	0.9	1.1	U1
$N_{con\_low}$	Retention multiplier for retention at low N concentrations (-)	N	7	6	9	U3
$F_{aomi}$	Reduction factor for litter load to surface water (-)	N/P	0.5	0.45	0.55	U1
$R_L$	Mean length ratio (-)	N/P	2.3	2.0	2.6	U3

R <sub>a</sub>	Drainage area ratio (-)	N/P	4.7	4.2	5.2	U3
AOMI	Litterfall in flooding areas (-)	N/P	1.0	0.9	1.1	U1
f <sub>qro</sub>	Overall runoff fraction (-)	N/P	1.0	0.9	1.1	U1
L <sub>1</sub>	Mean length first order stream (km)	N/P	1.6	1.4	1.8	U3
A	Width factor (m)	N/P	8.3	7.5	9.1	U3
P <sub>soil</sub>	P content of the soil (-)	P	1.0	0.9	1.1	U1
B <sub>soil</sub>	Bulk density of the soil (-)	N/P	1.0	0.9	1.1	U1

\* Samples values are applied to all grid cells. For sampling, either uniform or triangular distributions are used.

The distributions used are:

U1. Uniform: values are multipliers for standard values on a grid cell basis.

U2. Uniform: values are added to the standard values on a grid cell basis.

U3. Uniform: values are used as such.

Table SI4.3. Standardized regression coefficient (SRC)<sup>a</sup> representing the relative sensitivity of the N\_load\_river, N\_retention and N\_export\_mouth to the variations of 48 model parameters. Here we only present those important input parameters which have a SRC value within the range  $SRC > 0.2$  and  $SRC < -0.2$ , i.e. with an influence exceeding  $0.2 * 0.2 = 0.04$  or  $> 4\%$ .

Parameter	N_load_river			N_retention			N_export_mouth		
	1900	1950	2000	1900	1950	2000	1900	1950	2000
Year									
CN <sub>aomi</sub>	-0.23	-0.27	-0.04	0.05	0.06		-0.10	-0.11	-0.02
F <sub>leach,crop</sub>	0.05	0.04	0.24				0.01	0.01	0.14
F <sub>leach,nat</sub>	0.53	0.48	0.07	-0.16	-0.15		0.25	0.23	0.04
Q <sub>tot</sub>	0.17	0.14	0.31	-0.16	-0.10	-0.68	0.18	0.12	0.63
Temp	-0.06	-0.05	-0.09	0.37	0.38	0.53	-0.36	-0.36	-0.40
N <sub>budget,crops</sub>	0.11	0.07	0.66	-0.02	-0.02	-0.01	0.04	0.03	0.41
N <sub>budget,nat</sub>	0.53	0.49	0.08	-0.16	-0.15		0.25	0.24	0.05
C <sub>stro,N</sub>	0.09	0.12	0.28	-0.02	-0.04	-0.01	0.04	0.06	0.17
Poros	-0.11	-0.10	-0.24	0.03	0.04	0.01	-0.05	-0.05	-0.15
V <sub>lake</sub>				0.19	0.19	0.29	-0.17	-0.17	-0.19
V <sub>river</sub>				0.26	0.27	0.20	-0.24	-0.25	-0.13
A <sub>flooding</sub>	0.23	0.27	0.04	-0.05	-0.05		0.09	0.11	0.02
N <sub>con_low</sub>				0.75	0.74		-0.69	-0.68	
F <sub>aomi</sub>	0.23	0.27	0.03	-0.05	-0.06		0.09	0.11	0.02
R <sub>L</sub>				0.26	0.28	0.27	-0.24	-0.26	-0.18
AOMI	0.23	0.27	0.03	-0.05	-0.05		0.09	0.11	0.02

<sup>a</sup>Cells with no values represent insignificant SRC values; all cells with values show significant SRC; numbers without color indicate  $-0.2 < SRC < 0.2$ ; numbers with green and yellow colors indicate values  $< -0.2$  and  $> 0.2$  respectively; the value of SRC 0.2 indicates that the parameters have an influence of  $0.2^2 = 0.04$  (4%) on the model output variable. Positive values indicate that a higher parameter value generates a higher model output variable and vice versa.



Table SI4.4. Standardized regression coefficient (SRC)<sup>a</sup> representing the relative sensitivity of the P\_load\_river, P\_retention and P\_export\_mouth to the variations of 34 model parameters. Here we only present those important input parameters which have a SRC value within the range SRC>0.2 and SRC <-0.2, i.e. with an influence exceeding  $0.2 * 0.2 = 0.04$  or >4%.

Parameter	P_load_river			P_retention			P_export_mouth		
	1900	1950	2000	1900	1950	2000	1900	1950	2000
Year	1900	1950	2000	1900	1950	2000	1900	1950	2000
q <sup>tot</sup>	0.12	0.13	0.03	-0.52	-0.51	-0.63	0.45	0.45	0.45
Temp	0.09	0.09	0.02	0.35	0.35	0.41	-0.20	-0.18	-0.25
f <sub>qstro</sub>	0.02	0.02	0.27			0.01	0.01	0.02	0.21
C <sub>stro,P</sub>	0.02	0.02	0.28			0.01	0.01	0.02	0.20
V <sub>l,lake</sub>				0.23	0.22	0.25	-0.16	-0.15	-0.16
V <sub>l,river</sub>				0.41	0.41	0.31	-0.29	-0.28	-0.20
R <sub>a</sub>				-0.21	-0.22	-0.16	0.15	0.15	0.11
R <sub>L</sub>				0.43	0.44	0.34	-0.31	-0.31	-0.22
L <sub>l</sub>				0.25	0.26	0.19	-0.18	-0.18	-0.13
A			-0.01	0.19	0.20	0.15	-0.14	-0.14	-0.10
P <sub>soil</sub>	0.68	0.67	0.62			0.01	0.47	0.47	0.46
B <sub>soil</sub>	-0.68	-0.67	-0.62			-0.02	-0.46	-0.47	-0.46

<sup>a</sup> See annotation previous table

Table SI4.5 TN and TP exports by the Yangtze River at the Datong monitoring station from various approaches and models and for different years.

Method	Scale	Short description	Time period	N and P forms	Export to the East China Sea and Yellow Sea TN Unite (Gg yr <sup>-1</sup> )	Export to the East China Sea and Yellow Sea TP Unite (Gg yr <sup>-1</sup> )
Based on monitoring data at Datong	Basin	Calculated from observed N and P concentration and discharge at Datong station, includes seasonal change.	1964-2010	DIN, DON, PN, DIP, NO <sub>3</sub> <sup>-</sup> , DIP, NO <sub>2</sub> <sup>-</sup> , NH <sub>4</sub> <sup>+</sup>	1970*:TN: 489 1970*:TN: 492 1985*:TN: 1953 1990*:TN: 2468 1995*:TN: 2766 2002*:TN: 3698 2005*:TN: 3646 2007*:TN: 2595 2012*:TN:2460 whole period data see Figure 3 in main text	1970*:TP: 60 1970*:TP: 24 1985*:TP: 104 1990*:TP: 201 2002*:TP: 289 2005*:TP: 306 2007*:TP: 248 2012*TP:240 whole period data see Figure 3 in main text
Lumped regression model	Basin	Lumped regression model	1985-2010	TN	1985*:TN:1334 1990*:TN:1463 1995*:TN:1703 2000*:TN:1807 2005*:TN:1928 2007*:TN:1825	
Global News	Basin	Lumped regression model	1970 1985 and 2003	DIN, DON, DIP, DOP	1970 <sup>a</sup> :TN: 580 1970 <sup>b</sup> :TN: 936 2000 <sup>c</sup> :TN: 1132 2003 <sup>b</sup> :TN:3222	1970 <sup>a</sup> : TP: 58 1970 <sup>c</sup> :TP:33 1985 <sup>c</sup> :TP:60 2000 <sup>c</sup> :TP:95 2003 <sup>c</sup> :TP:185
Marina (Downscaled version Global NEWS-2)	Sub-basin	Lumped regression model for 10 subbasins	1970 and 2000	DIN, DON, DIP, DOP	1970 <sup>d</sup> :TN:530 2000 <sup>d</sup> :TN:1142  (20-60% from direct manure discharge)	1970 <sup>d</sup> :TP: 78 2000 <sup>d</sup> :TP: 172  (50-97% from direct manure discharge)

IMAGE-GNM model (This Study)	Grid cell	Dynamic, mechanistic spatially explicit model describing processes in all landscape components (soils, shallow groundwater, deep groundwater, riparian zones, floodplains, streams, rivers, lakes, and reservoirs).	1900-2010	TN, TP	1970:TN :635 1985:TN:1868 1995:TN:3131 2000:TN:3497 2003:TN:4008 2005:TN:3866 2007:TN:3767 2010:TN:5708  we chose Datong station here for comparison	1970:TP:65 1985:TP 149 2000:TP:296 2010:TP: 371  we chose Datong station here for comparison
------------------------------	-----------	---	-----------	--------	---	---

DON: Dissolved organic nitrogen; DOP: Dissolved organic phosphorus; PN: particulate nitrogen;  $\text{NO}_3^-$ : nitrate;  $\text{NO}_2^-$ : nitrite; and  $\text{NH}_4^-$ : ammonia;

\* Observed data listed see SI1, <sup>a</sup>Ti et al (Ti et al. 2012). <sup>b</sup>Yan et al.(Yan et al. 2010) calculated DIN, we used  $\text{DIN} \times 2$  as TN. <sup>c</sup>Li et al.(Li et al. 2011), calculated DIP, we used  $\text{DIP} \times 7.27$  as TP. <sup>d,e</sup>Strokal et al. (Strokal et al. 2016a, Strokal et al. 2016b) calculated DIN, DON, DIP and DOP, particulate N and P from Mayorga et al (2010). We used sum of DIN DON and PN as TN, the same for TP. <sup>f,g</sup>(Mayorga et al. 2010, Seitzinger et al. 2005) calculated DIN, DON, PN, DIP, DOP and PP, TN is the sum of DIN, DON and PN, and the same for TP.



## Chapter 5

# Nutrient legacies in the Rhine, Mississippi, Yangtze and Pearl River basins and consequences for future water quality

---

Xiaochen Liu, Arthur H.W. Beusen, Yu Deng, Junjie Wang, Wim Joost van Hoek, Xiangbin Ran, Bochao Xu, Qingzhen Yao, Zhigang Yu, Alexander F. Bouwman.

---

*A modified version of chapter 5 was submitted to Nature Communications, 2022.*

### Abstract

Here we present a detailed analysis of the historical accumulation of nitrogen (N) and phosphorus (P) in landscapes in the Rhine, Mississippi, Yangtze and Pearl's river basins and scenario analysis for the period up till 2050. Although all four rivers went through a phase of nutrient accumulation, there is a difference in the timing. The Rhine and Mississippi began this phase in the 1950s and the Yangtze and Pearl in the 1970s. The Mississippi and Yangtze are comparable in that they both have current large reservoir storage volumes of 191 km<sup>3</sup> (47 % of the annual discharge) for Mississippi and 140 km<sup>3</sup> (16 % of the annual discharge) for the Yangtze. Therefore, P accumulation in sediments in reservoirs and lakes has a large contribution to total P retention. Large amounts of N have been temporarily stored in groundwater in both rivers. Strategies to reduce N and P loading have been successful in the Rhine and less so in the Mississippi. However, N:P ratios have been changing, which may have significant ecological impacts. Both Rhine and Mississippi show rapidly increasing molar N:P ratios in the water exported to the North Sea and the Gulf of Mexico, respectively. We conclude that the Yangtze River has many similarities with the Mississippi in the 1970s. At the same time, the Yangtze scenarios indicate that the current policies to halt the increase of fertilizer use after 2020 will not be sufficient to stop the accumulation of nutrients in landscapes and waterscapes.

### 5.1 Introduction

Nitrogen (N) and phosphorous (P) are essential nutrients for plants. The same nutrients that make up the fertilizers that we credit for boosting global food production in the last century have also found their way into nearly every water body across the globe. In the 20<sup>th</sup> century, global nutrient loads to streams and rivers have increased rapidly from 24

to 64 Tg yr<sup>-1</sup> of N and from 5 to 9 Tg yr<sup>-1</sup> of P (Beusen et al. 2016). Excessive N and P discharge to surface water accelerate aquatic plant production (eutrophication). This may lead to oxygen-limited to hypoxic conditions, where the decay of the plant biomass consumes oxygen faster than its diffusion from the oxygen-rich surface.

Increasing N:P in inputs in food production, more efficient biogeochemical retention of P than of N in river basins, and groundwater N legacies may lead to increasing N:P ratios in rivers (Beusen et al. 2022) which may lead to harmful algal blooms (HABs) (Billen and Garnier 2007b), even in situations of declining river nutrient loads. Hypoxia (Diaz and Rosenberg 2008) and HABs (Glibert 2018) have developed into major global environmental problems.

Soils and groundwater are stores of P and N in landscapes (Böhlke 2002, Puckett et al. 2011, Sattari et al. 2012, Van Meter et al. 2016) which are filled during periods of accumulation (Haygarth et al. 2014), for example, due to excessive nutrient use in agriculture or absence of wastewater treatment (Powers et al. 2016). In the depletion phase, when agricultural nutrient use efficiency improves and sewage water is treated, the landscape buffer or memory acts differently compared to the accumulation phase. Due to the long residence and travel time, there may be a long delay in the delivery by groundwater to surface water (Morris et al. 2003). With declining nutrient inputs, soils may be releasing nutrients by organic matter decomposition (Van Meter et al. 2016).

River basins with substantial water volumes in lakes and reservoirs, such as the Mississippi, form a particular case. During periods of high P loading, sediments absorb P (Reddy et al. 1999). When concentrations in the water column decline due to wastewater treatment or reduced surface runoff, sediments may start to release P (Vilmin et al. 2020). These phenomena related to landscape stores are commonly referred to as nutrient legacy (Haygarth et al. 2014, Rowe et al. 2016, Sattari 2014, Sharpley et al. 2013, Van Meter et al. 2016).

Water quality of the Rhine River was already seriously deteriorated back to the 1850s due to increasing agricultural runoff and wastewater flows from households and industries (Frijters and Leentvaar 2003). Nutrient loading intensified, especially after 1950, and eutrophication problems were so severe that the nations bordering the Rhine developed the Rhine Action Plan. The European Union and a large group of countries participated in the OSPAR Convention to protect the marine environment of the North-East Atlantic. Several directives by the European Commission now regulate the nutrient loading, including the Nitrates Directive (EC 1991a) for reducing the diffuse nutrient emissions from agriculture, and the Urban Waste Water Treatment Directive (EC 1991b) for improved wastewater treatment; monitoring of water quality was instituted through

the Water Framework Directive (EC 2000) for reporting the ecological quality of surface water. There are no US national standards for  $\text{NH}_4^+$ , TN, or TP, although individual states use total maximum daily loads (EPA 2019) for these compounds according to the standards of the Clean Water Act section 303d (EPA 2019).

The experience obtained in the Rhine and Mississippi River basins can provide valuable lessons to other polluted river basins worldwide. This study aims to compare the long-term nutrient dynamics, accumulation and depletion in the Rhine and Mississippi with two major Chinese rivers, i.e. Yangtze and Pearl. With the massive deforestation, economic growth and urban development in the past four decades, massive river transport of nutrients to the South China Sea, East China Sea and the Yellow Sea led to excessively high N and P concentrations (Liu et al. 2018, Wang et al. 2020) and increasing frequency of HABs (Glibert et al. 2018).

Starting from the estimated long-term accumulation in these river basins, we will analyze scenarios for the future that account for changes in all nutrient sources based on the five Shared Socioeconomic Pathways (SSPs), the most recent family of community-consensus scenarios to study the future global environment. With these different outcomes, we will analyze the impact of legacies on the effectiveness of different strategies to control nutrient pollution.

Different models are available to study nutrients in rivers, for example, a model to estimate the N and P export by the Rhine (Loos et al. 2009, Wit 2001), the Soil and Water Assessment Tool (Bieger et al. 2017) applied to study nutrient processing in the East River and Pearl delta area. However, the demand for detailed input data hinders their implementation to the entire Rhine, Mississippi, Pearl or Yangtze River basins. Global NEWS is a lumped river-basin scale regression model which was applied globally (Seitzinger et al. 2010a) to analyze nutrient export for individual years. However, Global-NEWS does not allow to keep track of accumulated nutrients, which is a prerequisite for achieving the objective of this paper.

Here, we use the Integrated Model to Assess the Global Environment – Global Nutrient Model (IMAGE-GNM). The model has been used to analyze global nutrient delivery to surface water from natural and anthropogenic sources, in-stream processing and export to the coastal ocean for the 20<sup>th</sup> century (Beusen et al. 2022, Beusen et al. 2016), analyze the SSP scenarios for the period up till 2050 (Beusen et al. 2022), and to study the nutrient cycles in individual rivers such as the Yangtze for 1900-2010 (Liu et al. 2018). IMAGE-GNM is spatially explicit with 0.5 by 0.5 spatial degree resolution, typically used to study the long-term accumulation of nutrients in landscapes and waterscapes.

The four river basins that were considered in this study (section 5.1), IMAGE-GNM (5.2) and the scenarios used to explore changing nutrient dynamics in future decades up till 2050 (5.2) will be described. We will then present the results focusing on the historical changes in nutrient budget, delivery, retention and export, model validation against measured N and P concentrations and future nutrient accumulation and depletion (5.3). Section 5.4 discusses results, including a comparison with other studies and an exploration of current policy strategies to mitigate nutrient pollution in the context of the nutrient legacies according to the different SSP scenarios.

## 5.2 Methods and data used

The nutrient delivery data by source for the historical period 1900-2015 were obtained from the latest IMAGE-GNM model version (Beusen et al. 2022) with extended historical input data for 1900-2015, and with scenario data for the period 2016-2050. The data for the four river basins were extracted from the data in order to compute the nutrient accumulation (N and P) or depletion of landscape stores (N). Below we describe the characteristics of the four river basins, as well as the IMAGE-GNM model and the five SSP scenarios considered in this study.

### 5.2.1 Description of the river basins

The four rivers considered in this study (Figure 5.1) differ considerably in terms of hydrology, land use and population (Table 5.1). The Mississippi River drains the largest area, while the Yangtze is the longest river with the largest discharge. The Mississippi has the largest reservoir volume, both in absolute terms and as a fraction of the annual discharge. The fraction of agricultural land is smallest in the Rhine basin (43%) and largest in the Mississippi (73%) basin in the four basins in 2015.

Table 5.1. Basin area, river length, discharge, agricultural land and cropland, and the number of inhabitants and population density for the Rhine, Mississippi, Yangtze and Pearl rivers for 2015 unless indicated otherwise.

Property (unit)	Rhine	Mississippi	Yangtze	Pearl
Basin area ( $10^3 \text{ km}^2$ )	148	3149	1880	428
Length (km)	1550	6000	6300	2200
Discharge ( $\text{km}^3 \text{ yr}^{-1}$ )	66	409	892	336
Reservoir volume ( $\text{km}^3$ )	1	191	140	19
Agricultural land (%)	43	73	54	44
Inhabitants (million)	45 (2001)	70 (2002)	440	230
with year			(2002)	(2009)
Population density (inhabitants/ $\text{km}^2$ )	304	22	234	537

All data are from IMAGE-GNM.



The number of inhabitants in the Yangtze is the largest of the four river basins, but the population density is highest in the Pearl River (>500 inhabitants/km<sup>2</sup>) and Rhine (~300), while that in the Mississippi basin is lowest (~20).

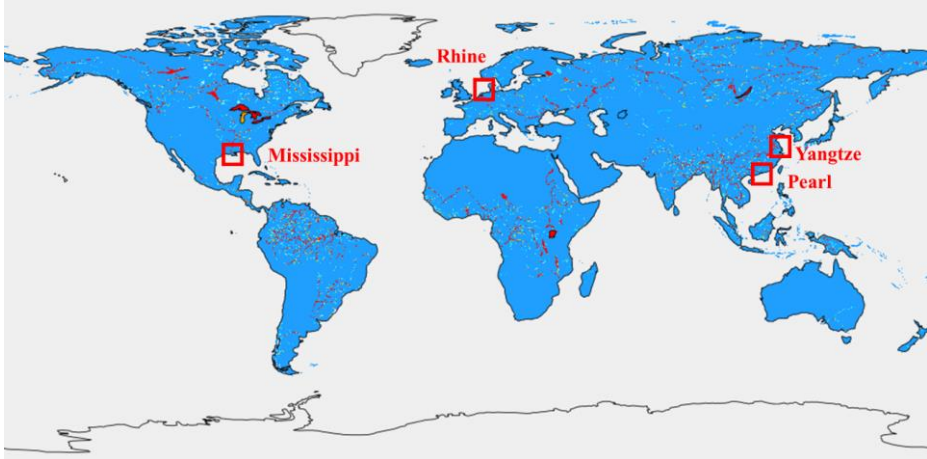


Figure 5.1. Mouth locations of the Mississippi, Rhine, Yangtze and Pearl Rivers.

## 5.2.2 Model description

IMAGE-GNM is described in detail elsewhere (Beusen et al. 2016, Beusen et al. 2015). Here, a brief summary is provided. IMAGE-GNM is a spatially explicit, distributed model with 0.5 by 0.5 degree resolution that couples IMAGE (Stehfest et al. 2014) with the global hydrological model PCR-GLOBWB (Sutanudjaja et al. 2018) as the basis for describing N and P flows and processing in landscapes (Figure 5.2). The model simulates the nutrient delivery to surface water, in-stream nutrient retention in streams, rivers, lakes and wetlands, and reservoirs, and subsequent export to the coastal ocean with an annual time step. Within landscapes, the soil-groundwater hydrological system is described based on global data to simulate surface runoff and erosion, leaching from soils to shallow and deep groundwater layers, groundwater transport and denitrification, processing in riparian zones, and discharge to surface waters.

IMAGE-GNM distinguishes point sources (wastewater from households and industries) and diffuse sources (Figure 5.2). Point sources are calculated starting from the number of inhabitants in a grid cell, the nutrient excretion based on human diets, the fraction of inhabitants with a sewage connection, the type of sewage treatment system present and its efficiency in nutrient removal and discharge to the surface water. The approach for point sources used here is documented by Van Puijenbroek et al. (2019).

## Reactions in Each Grid Cell

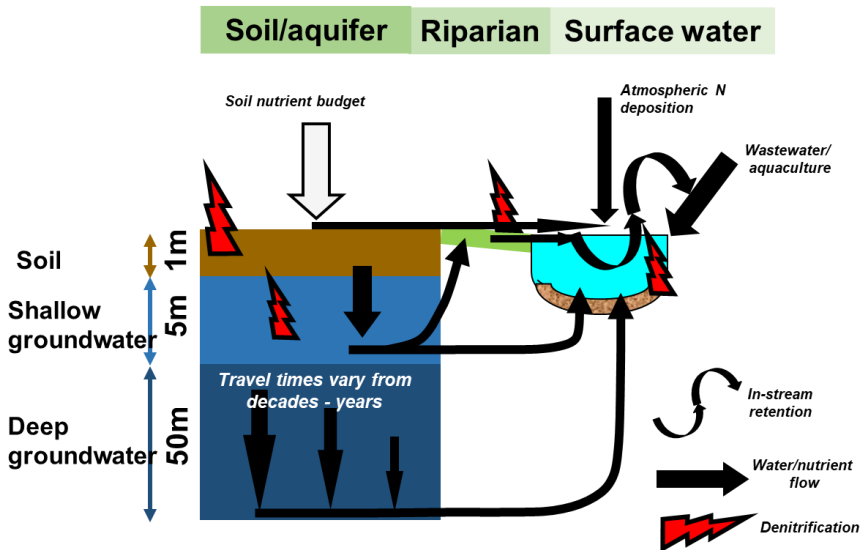


Figure 5.2. Scheme of the IMAGE-GNM model with all landscape components occurring in a grid cell, including soil, two groundwater layers, riparian areas and surface water, and the water/nutrient flows between the compartments. Modified from Liu et al. (2018).

Diffuse sources, which consist of nutrient flows from agricultural land and natural ecosystems, are based on the nutrient soil budget which is calculated for every grid cell in the world. Nutrient budgets have different inputs (where relevant, fertilizers, animal manure, biological N fixation, and atmospheric deposition) and outputs (uptake by crops and grass, and ammonia gaseous emissions). The difference between inputs and outputs can potentially be lost to the environment via multiple pathways, i.e. denitrification, leaching, surface runoff and erosion. Natural ecosystems are assumed to have constant biomass (i.e. net withdrawal is zero), except for vegetation in floodplains where part of the litter is transported by the water. Nutrient release by aquaculture is calculated using a budget approach with feed inputs and production and excretion outputs. Excreted nutrients may be released or recycled. Further diffuse sources to surface water include atmospheric deposition and weathering.

IMAGE-GNM uses long time series to compute the loading of N and P in landscapes. Three temporary stores are considered, i.e. soils, groundwater and sediments. Soil P can accumulate where the soil P budget is positive, which is accounted for when calculating

surface runoff and erosion. Further memories in the soil hydrological system are caused by retardation of water and nitrate flow in soils and groundwater, which may vary considerably due to the history of N inputs which in times of large surpluses may lead to high groundwater N loads which are discharged years to decades after. P retention in lakes and reservoirs is a third landscape memory considered by IMAGE-GNM.

### 5.2.3 Scenarios

Global riverine nutrient delivery to streams and rivers and export to the coastal zone in the coming century will strongly depend on global economic development. Here we use community consensus scenarios, i.e. the five SSPs (Kriegler et al. 2014, O'Neill et al. 2017, Riahi et al. 2017): A sustainability scenario (SSP1) in which there is good progress toward sustainability, with ongoing efforts to achieve development goals while reducing resource intensity and fossil fuel dependency. A middle of the road pathway (SSP2) or business-as-usual world, a fragmented world with regions differing widely in economic development (SSP3). A scenario with a highly unequal world in which a relatively small, wealthy global elite is responsible for most of the greenhouse gas emissions. At the same time, a larger, poor group that is vulnerable to the impact of climate change contributes little to the harmful emissions (SSP4) and SSP5 involving traditional development with a focus on economic growth with continued fossil fuel-based economy with high greenhouse gas emissions. The SSPs have been used and compared with various integrated assessment models. The implementation of the SSP1 storyline with the IMAGE model (Van Vuuren et al. 2017) is the marker scenario selected as a guide for the broader scenario comparisons (Riahi et al. 2017). Beusen et al. (2022) implemented the nutrient scenarios that were used in this chapter.

## 5.3 Results

### 5.3.1. Historical nutrient budget, delivery and export

Model results for the four rivers show that the magnitude and timing of the anthropogenic changes since 1900 are considerable. In the Mississippi and Rhine basins, the acceleration of the nutrient cycles as indicated by the N and P budgets started after the second world war, while nutrient use started to increase rapidly in the two Chinese rivers two decades later (Figure 5.3).

There is also a difference between the Mississippi and the Rhine basins. The N budget started to decline after 1980 in the Rhine (Figure 3a), while in the Mississippi, there is a stabilization since 1970 (Figure 5.3c). The P budget in the Mississippi and Rhine started to decline in the 1970s (Figure 5.3c, g); this decline continued in the Rhine basin to even negative values in recent years (Figure 5.3c), while in the Mississippi, there has

been a stabilization since the 1980s with a strong decline after 2000. The acceleration of nutrient cycles in the two Chinese rivers since the 1970s has been continuing up till 2015 (Figure 5.3i, k, m, o).

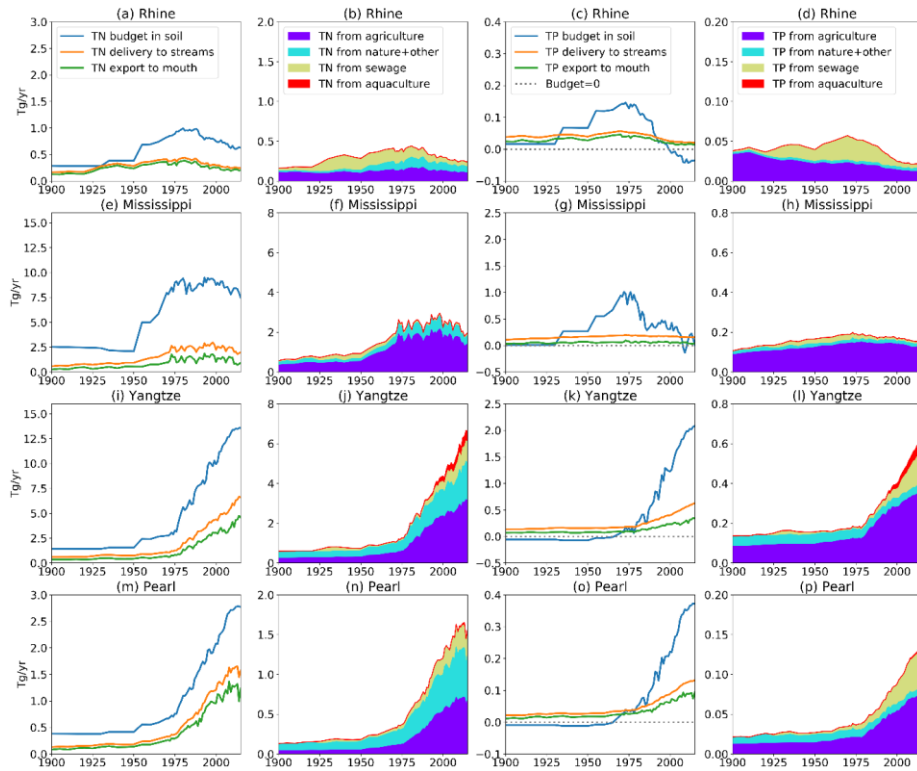


Figure 5.3. Soil budget, delivery, export (first two columns are for N in  $\text{Tg N yr}^{-1}$ , the last two columns are for P in  $\text{Tg P yr}^{-1}$ ), aggregated sources for N and P (second and fourth column) for the Rhine (top row), Mississippi (2nd row), Yangtze (3d row) and Pearl (4<sup>th</sup> row) for the period 1900-2015.

The simulated delivery of N and P to surface water (Figure 5.3) is a small fraction of the soil budget due to the landscape filter. Surface water acts as a further filter and sediments in lakes and reservoirs store significant amounts of nutrients, leading to a further reduction of the nutrient flow downstream towards coastal waters. Particularly in the rivers where lakes and artificial reservoirs are important stores for water (Table 1), retention of both N and P is high (30-80% in Yangtze, Mississippi and Pearl), and only 10-40% in the Rhine.

With regards to the sources, the Rhine has a larger sewage point source contribution than the other rivers for both N and P; sewage discharge was the dominant source for N and P prior to the second world war, with a strong reduction after 1970, particularly for P (Figure 3d). Agriculture dominates throughout the simulation period in the Mississippi River (Figure 5.3f, h). Natural ecosystems were dominant for N in the early period in the two Chinese rivers, where agriculture started to dominate in 1970 (Figure 5.3j, i, n, p). Since 1990, the sewage contribution in Pearl and Yangtze increased rapidly due to the development of megacities in the Pearl River Delta and Yangtze River Delta.

The global cumulative temporary N storage in soils and groundwater amounts to perhaps close to 400 Tg since 1900 (Bouwman et al. 2013a). For individual river basins, N storage amounts vary considerably, which is related to the geohydrological conditions, and historical agricultural production and nutrient management. Total N accumulation for the period 1900-2015 in soils and groundwater amounts to 1.8 Tg N in the Rhine, 74 Tg N in the Mississippi, 27 Tg in the Yangtze and 2.1 Tg in the Pearl (Figure 5.4).

P retention is strongest in basins where reservoirs play an important role (Table 5.1; Figure 5.6). The Mississippi has the most prominent in-stream retention from the four river basins, and the Rhine has the smallest in-stream retention. This explains the P accumulation in sediments, which also is largest in rivers where extensive lakes and reservoirs are present in the river basin (Table 1), i.e. 4.4 Tg P in the Mississippi and 5.2 Tg in the Yangtze versus 0.5 Tg in the Rhine and 0.2 Tg in the Pear River basin (Figure 5.4b, d, f, h).

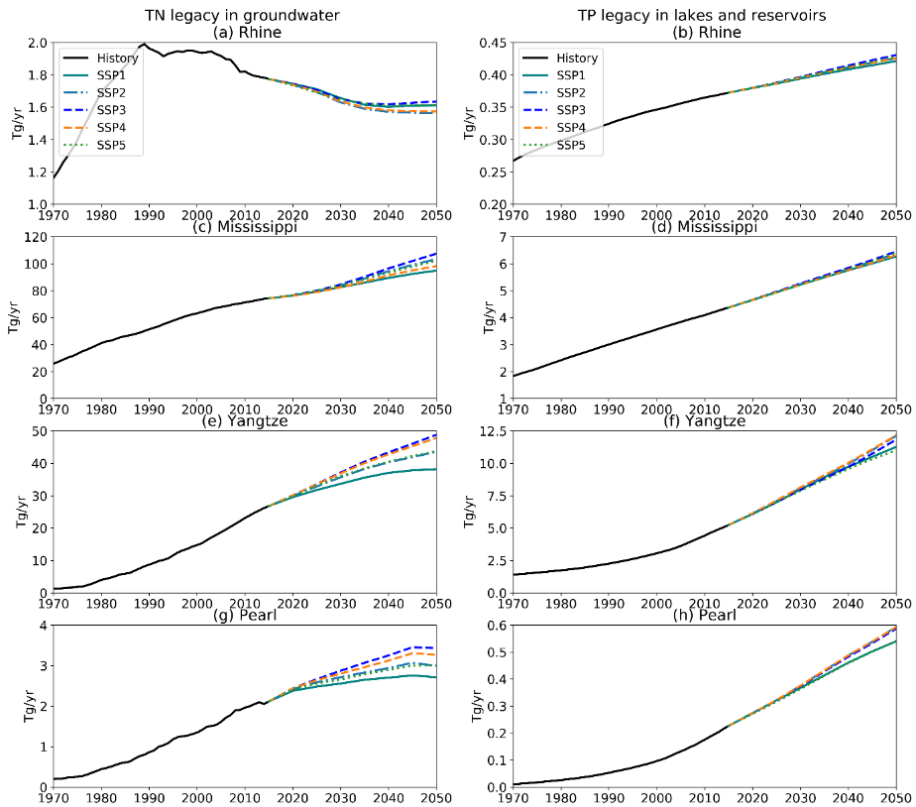


Figure 5.4. N accumulation in groundwater (left column) and P accumulation in sediments of lakes and reservoirs (right column) during the period 1970-2050 in the Rhine (top row), Mississippi (2<sup>nd</sup> row), Yangtze (3<sup>d</sup> row) and Pearl (4<sup>th</sup> row).

### 5.3.2 Validation

Validation of N and P concentrations simulated by IMAGE-GNM for a range of global rivers can be found in our previous studies (Beusen et al. 2016, Beusen et al. 2015) and validation for the Yangtze river in Liu et al. (2018). Here we repeated the validation for the four rivers, also because the IMAGE-GNM model runs used an update of the climate data. The modeled results show a good agreement with the observations (Figure 5.5). The Root Mean Square Error (RMSE) values for discharge and N and P concentrations are 21%, 27% and 33% respectively for the Lobith station in the Rhine, 52% 20% and 56% for St Francisville station in Mississippi; 7% 23% and 73% for Datong station in the Yangtze, and for discharge and N concentrations 7% and 30% for Gaoyao station in Pearl (no available P observation for Gaoyao station). The modeled trend and agreement for discharge and N and P concentrations are well-represented in the four river basins

with widely differing climates, geohydrology, economic activity levels, wastewater sources and agricultural coverage, considering that IMAGE-GNM is based on global databases.

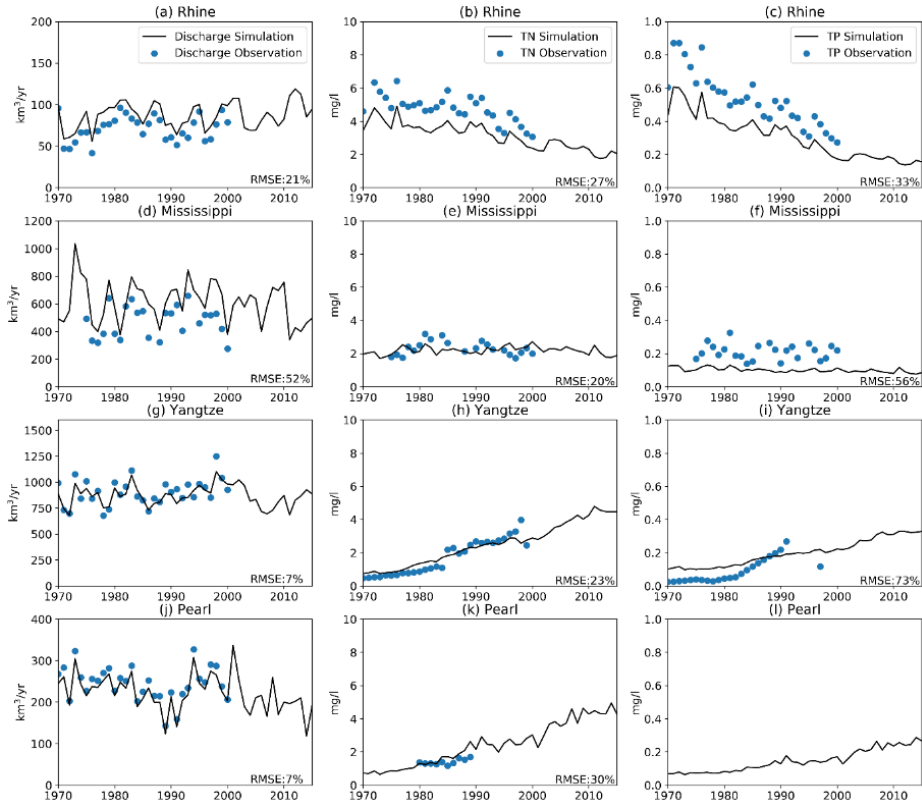


Figure 5.5. Comparison of simulated (black line) and observed (blue dots) discharge, TN and TP concentrations in the Lobith station in Rhine (a-c), St Francisville station in Mississippi (d-f), Datong station in the Yangtze (g-i), Gaoyao Station in Pearl (j-l) for the period 1970-2015.

### 5.3.3 Future Scenarios

The five SSP scenarios that represent contrasting futures in the Rhine, N delivery to surface water (sum of agriculture, sewage, aquaculture and others) is projected to decrease from  $0.24 \text{ Tg yr}^{-1}$  in 2015 to  $0.16 \text{ Tg yr}^{-1}$  in the SSP1 scenario and to  $0.2 \text{ Tg yr}^{-1}$  in 2050 in SSP5. The trend of N delivery in the Mississippi is similar to that in the Rhine (Figure 5.6).

The N delivery in the Yangtze also shows a continuous decrease from 6.6 Tg yr<sup>-1</sup> in 2015 to 5.2 Tg yr<sup>-1</sup> in 2050 in the SSP1 scenario and 6.3 Tg yr<sup>-1</sup> in the SSP5 scenario. The N delivery in the Pearl shows the same trend as simulated for the Yangtze, reflecting the projected future developments in China. The N delivery is primarily related to efficiency improvements in agriculture and improving treatment of sewage water (Figure 5.6). Therefore, all the SSPs in Yangtze and Pearl predict a decrease of N export along with the changes in agriculture and sewage discharge. The magnitude of the decrease strongly depends on the storyline, with largest reductions in SSP1, and smallest in SSP4 and SSP5.

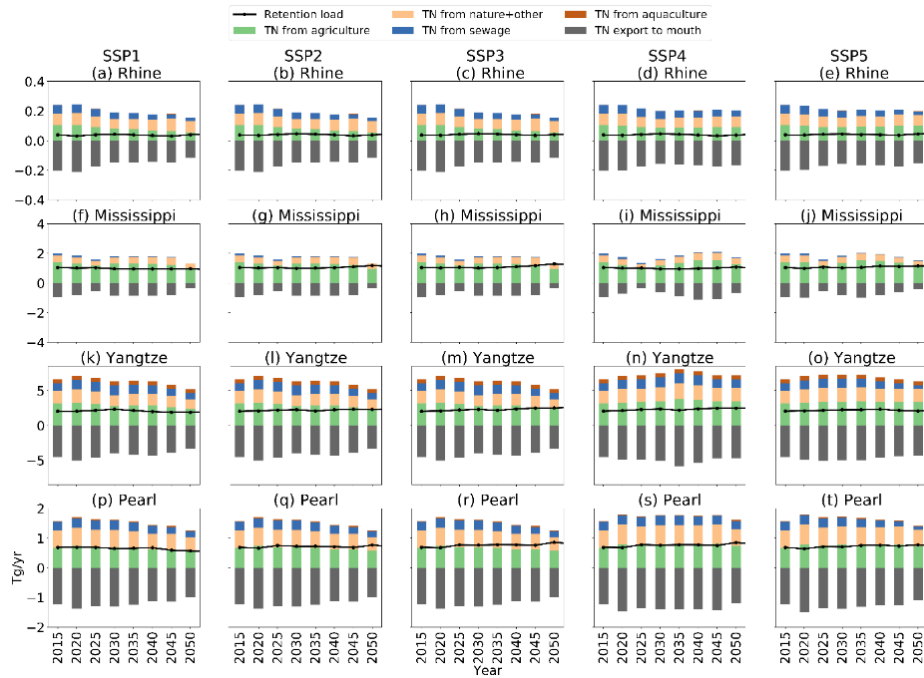


Figure 5.6. Projected TN sources, retention load and export for the Rhine, Mississippi, Yangtze and Pearl River basins for the five SSP scenarios for the period 2015-2050.



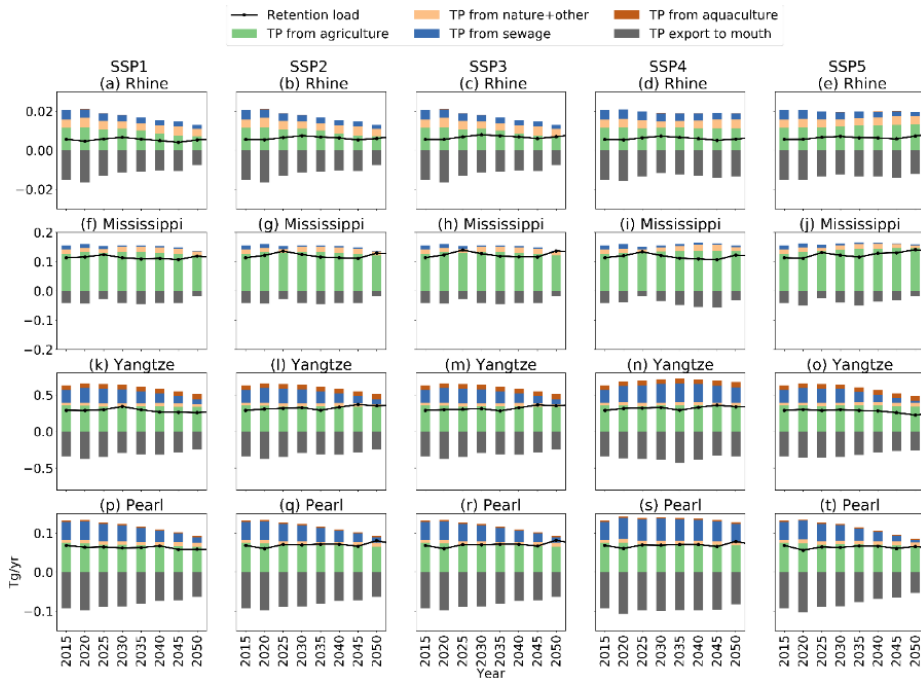


Figure 5.7. Projected TP sources, retention load and export for the Rhine, Mississippi, Yangtze and Pearl River basins for the five SSP scenarios for the period 2015-2050.

The trends for P show that in the SSP1, SSP2 and SSP3 scenarios, the P flux from sewage in Rhine and Mississippi is projected to decrease steadily during the period 2015-2050, while the P from sewage in Yangtze and Pearl will rapidly decrease by more than 60% over the same period (Figure 5.7). In SSP4, the sewage source P first increases until 2030 and gradually decreases beyond 2030. The P contribution from sewage will increase from 27% in 2015 to 31% in 2050 in the Yangtze in SSP4 (from 36% in 2015 to 37% in 2050 in Pearl). SSP5 in Yangtze and Pearl show a rapid decrease of sewage source P (Figure 5.7).

The N storage in groundwater is projected to increase in Mississippi and Yangtze in all the SSPs (Figure 5.4). For the Pearl, only in the SSP1 scenario, the groundwater N storage is projected to gradually decrease after 2040. The N storage in the Rhine basin is predicted to decline under all the SSPs (Figure 5.4a) which is a continuation of the decline during the past decades. In contrast, all SSPs project a continued increase of the P storage in lakes and reservoirs (Figure 5.4b, 5.4d, 5.4f, 5.4h).

## 5.4 Discussion

### 5.4.1 Rhine and Mississippi

After the nutrient accumulation phase, farmers in many industrialized countries have been able to increase their efficiency of nutrient use as a result of improved agricultural management, enhanced crop uptake, and the residual effect of accumulated soil reserves of N (Van Meter et al. 2016) and P (Sattari et al. 2012). Decades of efforts to reduce nutrient pollution in Europe have led to a reduction of nutrient losses from agriculture (Velthof et al. 2014) and nutrient discharge in wastewater (Van Puijenbroek et al. 2019) (Figure 5.3). Current P inputs in the Rhine basin are less than crop withdrawal (Figure 5.3c), and N budget surpluses are slowly declining (Figure 5.3). In the past decades, an increasing fraction of the population has been connected to sewage systems with wastewater treatment plants or other sanitary systems like septic tanks removing large fractions of N and P, leading to declining contributions from point sources (Figure 5.3).

As a result of these efforts, the water quality of the Rhine River improved significantly. Annual average total nitrogen (TN) concentration at the German-Dutch border declined from values  $>7$  mg/L in the 1970s to 2.3–2.6 mg/L during 2010–2013 (MIE 2019) (Figure 5.8), which is close to the EU standard of 2.5 mg/L (ICPR 2015). Total phosphorus (TP) concentrations declined from  $>0.9$  mg/L in the 1970s to values around 0.1 mg/L now (MIE 2019) (Figure 5.8), although the critical annual average TP concentration of 0.3 mg P/L is exceeded in many monitoring stations in the Rhine basin (ICPR 2015). The molar N:P ratio has thus increased from around 20 in the 1970s to  $>30$  at present.

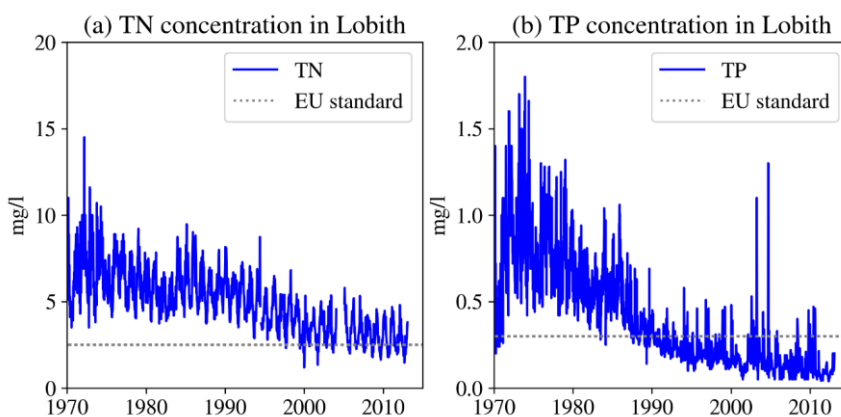


Figure 5.8. Observed TN and TP concentrations at the Lobith station at the German-Dutch border in the Rhine and the Europe Union water quality standard for TN and TP.

Although nutrient pollution overall has gone down in U.S. streams and rivers since 2004, it remains a severe problem in many waterways, and P pollution has gone up significantly (Manuel 2014). European and U.S. rivers currently feel the effects of excessive nutrient mobilization in the 1970s and 1980s, i.e. the legacy of historical nutrient use, as indicated by IMAGE-GNM results which show that as a result of declining N inflow in aquifers in the Rhine basin, there is now a net outflow of N, which is 4% of total N delivery to surface water in 2010s (Figure 5.4). In the Mississippi, the simulated N storage in the groundwater system seems to be increasing, which agrees with the observed increase of the flow-normalized N export since 1980, while observed increase of N concentrations at low stream flows is a strong indication that nitrate delivery by groundwater has a strong effect on river N concentrations (Sprague et al. 2011).

The P accumulated in sediments in lakes and reservoirs varies considerably between the Rhine and Mississippi (Figure 5.4). The reservoir volume in the Mississippi River has been increasing rapidly to more than 190 km<sup>3</sup> (a significant fraction of the discharge) in the past decades (Table 5.1), while volume in the Rhine has remained small at only 1 km<sup>3</sup>. P storage in the Mississippi (4.4 Tg between 1900 and 2015) is therefore much larger than in the Rhine basin (0.4 Tg between 1900 and 2015) (Figure 5.4). Recent work indicates that due to the reduced nutrient loading of the Mississippi and Yangtze Rivers, sediments are releasing dissolved inorganic nutrients so that the export of dissolved reactive nutrients is not declining (Vilmin et al. 2020).

There is a slow response of N concentrations to regulations in the European rivers due to the long travel time of groundwater and nitrate that entered aquifers years to decades ago. Our simulations suggest that the EU regulations have a stronger effect on P than on N (for example, the Rhine River, Figure 5.8). As a result, the molar N:P ratio of the Rhine water increased from below 20 in the 1970s to 30-35 in recent years (Figures 5.8 and 5.9a). This phenomenon of slow or no change in N and decreasing P is observed in the Rhine and in other European rivers draining into the English Channel, Atlantic, W. Mediterranean Sea and Northern Adriatic Sea (Romero et al. 2013). This may be related to the long travel time of groundwater and nitrate that entered aquifers years to decades ago, which may cause this slow response of N concentrations in the European rivers. The N:P ratio in the Mississippi discharge increased from 35 in 1970 to 56 in 1998, then slightly decreased to around 50 in the 2010s. This is mainly related to the slight decline of the P flux in the Mississippi (Beusen et al. 2022). This slow general decline in P suggests that improvements in agricultural land management, such as the enrollment of vulnerable areas into the USA Conservation Reserve Program and adoption of reduced and zero tillage, have reduced the surface runoff P losses in combination with improved wastewater treatment (Kreiling and Houser 2016).

The scenarios for the Mississippi and Rhine basins show that after efficiency improvements in the past decades, at most a stabilization of TN budgets will occur in future decades in SSP1 (Figure 5.10) resulting in a declining groundwater storage (Figure 5.4). For agricultural P budgets a similar picture is seen with stabilization in all scenarios for the Rhine basin, and stabilization in SSP1, and even increasing P budgets in the Mississippi according to the other SSP scenarios following production increases and limited efficiency improvements (Figure 5.11). The simulated N:P ratios in river export show a slight increase in all scenarios for the Mississippi, and a diverse result depending on the scenario for the Rhine basin, with even continued increase of N:P ratios in the sustainability scenario SSP1 and a decline in SSP3.

### 5.4.2 Yangtze and Pearl

There was no national legislation for controlling fertilizer and manure use in China until recently. As a result, TN and TP budgets and also TN and TP export to coastal waters have been steadily increasing in recent decades. The current average fertilizer applied per unit area of cropland area in China exceeds that in Europe by a factor of 2.6 (CMA 2015) due to double and triple cropping combined with low efficiency. Therefore, regulation was considered necessary and was implemented in 2015 with the strategy of ‘zero increase of fertilizer use’ (CMA 2015). Domestic wastewater in the large cities is mostly treated. However, the low nutrient removal rates associated with dominant secondary treatment systems still need to be improved by technology upgrading (Sun et al. 2016), and although China’s standards for wastewater emission have been developed from the “Integrated Wastewater Discharge Standard (GB8978-1996)” to the “Discharge Standard of Pollutants for Municipal Wastewater Treatment Plant (GB18918-2002)” (Zhang et al. 2016), treatment of industrial wastewater is still lagging. As a result, the N and P discharge from point sources is still increasing in both the Yangtze and Pearl.

Under the five future SSPs, N fertilizer use both in Yangtze and Pearl is declining considerably in the SSP1 scenario as reflected by the declining N budget (Figure 5.10) and will slightly decrease in the SSP2 scenario in the coming decades. The N budget will be stabilizing for all the other SSPs. However, in the Yangtze, we see that the temporary N storage in groundwater will increase in all the SSPs (Figure 5.4e), and groundwater outflow remains constant, while in the Pearl River, soils and groundwater are depleting and releasing N to surface water under SSP1 (Figure 5.4g) in the late 2040s.

P fertilizer will decrease from the 2020s in all the SSPs both in Yangtze and Pearl basins (Figure 5.11), while P will continuously accumulate in the sediment of lakes and reservoirs (Figure 5.4f, 5.4h). In response to future reduction of P losses from agriculture

and improved wastewater treatment, the accumulated P in sediment may be released to the water in the form of dissolved reactive P.

The molar N:P ratio increased from 17 in 1970 to 30 in 2015 in the Yangtze (from 24 in 1970 to 30 in 2015 in Pearl) (Figure 5.7c, 5.7d). The N:P ratio is mainly controlled by the fertilizer use and wastewater from the sewage system. The N:P ratio will continue its rising trend after 2015 in the fossil-fueled development scenario SSP5 in Yangtze and Pearl due to a rapid decline of the agricultural P budget in SSP5 (similar to SSP1) and a less rapid decline of the TN budget in SSP5 than in SSP1. This is because in SSP1 the mitigation strategies are much more stringent than in SSP5 for N, while P budgets follow the P needed to achieve the production targets in both scenarios. The Pearl River has experienced much less P accumulation and may have a much smaller P legacy and respond more directly to reduced nutrient loading.

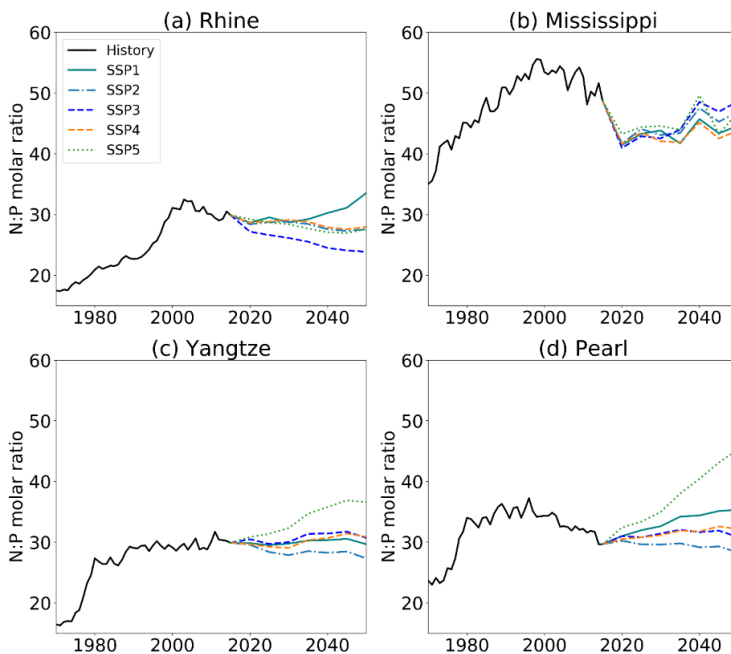


Figure 5.9. Molar N:P ratio in water exported to coastal waters during 1970-2015, and for 2016-2050 for the five SSPs for the rivers a) Rhine, (b) Mississippi, (c) Yangtze and (d) Pearl.

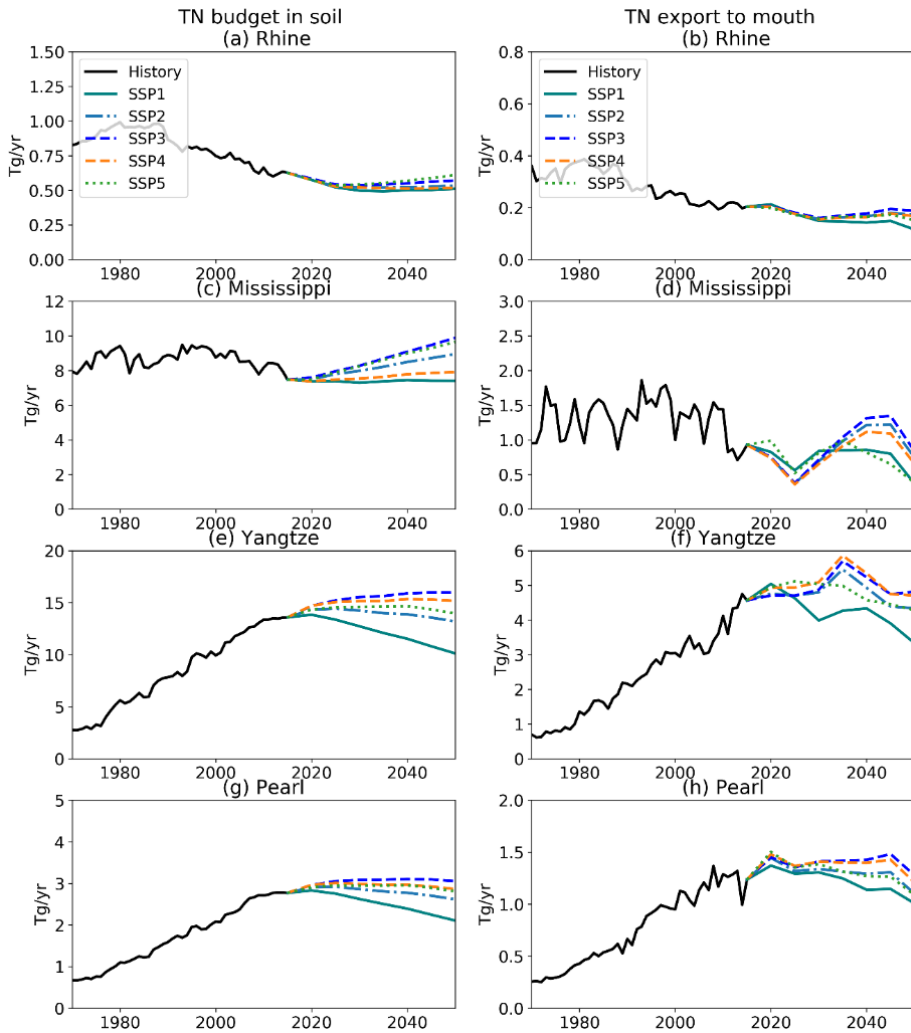


Figure 5.10. TN soil budget, export to the mouth in all waterbodies with the river basins of the Rhine (top row), Mississippi (2<sup>nd</sup> row), Yangtze (3<sup>d</sup> row) and Pearl (4<sup>th</sup> row) for 1970-2015 and for 2016-2050 according to the five SSP scenarios.

## 5.5 Concluding remarks

Our comparison reveals essential differences between the four rivers. Although all four rivers went through a phase of nutrient accumulation, there is a difference in the timing of these periods. The Rhine and Mississippi began this phase in the 1950s and the Yangtze and Pearl rivers in the 1970s.

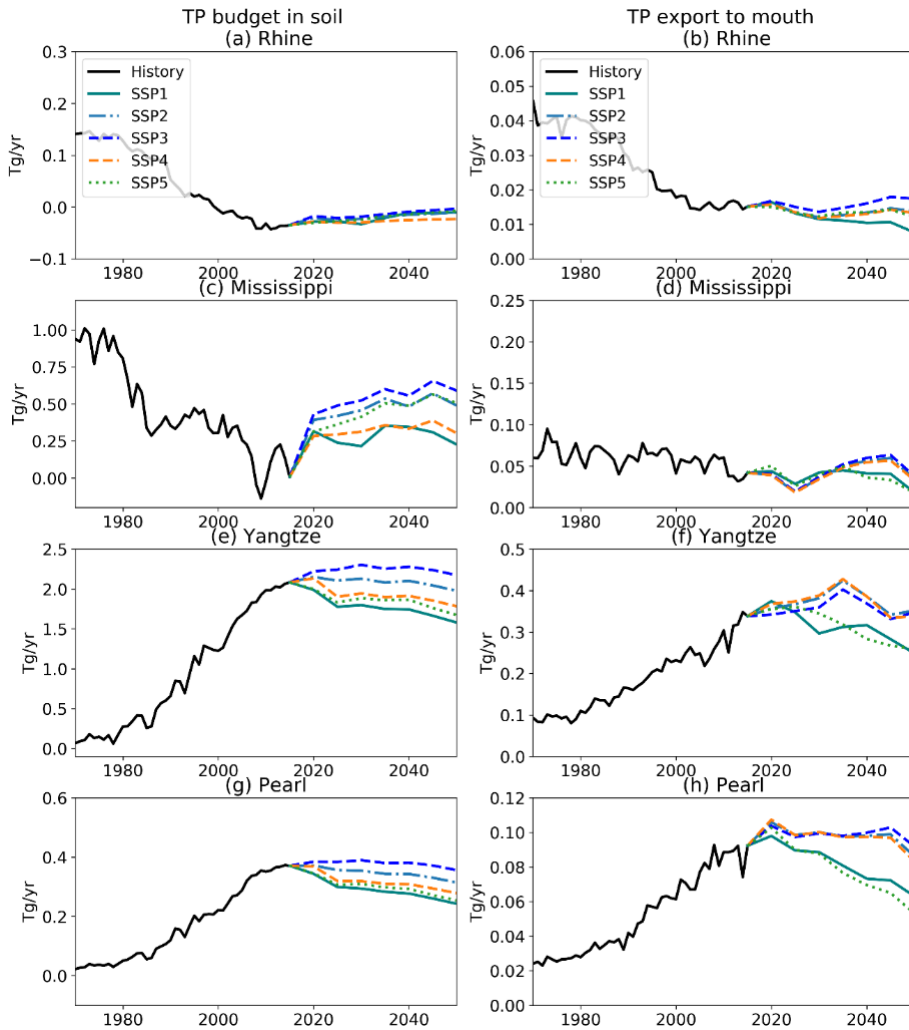


Figure 5.11. TP soil budget, export to the mouth in all waterbodies with the river basins of the Rhine (top row), Mississippi (2<sup>nd</sup> row), Yangtze (3<sup>d</sup> row) and Pearl (4<sup>th</sup> row) for 1970-2015 and for 2016-2050 according to the five SSP scenarios.

A second difference is the human interference in hydrology through dam construction. The Mississippi and Yangtze are comparable in that they both have current large reservoir storage volumes of 191 km<sup>3</sup> (47 % of the annual discharge) for Mississippi and 140 km<sup>3</sup> (16 % of the annual discharge) for the Yangtze. P accumulation in sediments in reservoirs and lakes therefore has a large contribution to total P retention. Large amounts of N have been temporarily stored in groundwater in both rivers.

The third difference in timing is the onset of the nutrient depletion phase. Rhine and Mississippi started this phase after the 1980s (Figure 5.11), while the two Chinese rivers are still in the accumulation phase, with increasing N and P discharge from both agriculture and point sources. The groundwater system in the Rhine is currently releasing N that has accumulated in ground water in previous decades. This release contributed 4% of the total N delivery to surface water in 2015. Due to the slowly declining soil N budget in recent years, the Mississippi shows a stabilizing groundwater release.

Strategies to reduce N and P loading have been successful in the Rhine and less so in the Mississippi basin. However, N:P ratios have changed, which may have substantial ecological impacts. Both Rhine and Mississippi show rapidly increasing molar N:P ratios in the water exported to the North Sea and the Gulf of Mexico, respectively. This is the result of many different simultaneous developments. First, P use in agricultural systems is declining in many industrialized countries. This is possibly due to the legacy of historical P surpluses that accumulated in soils and increased P availability to plants. Secondly, P removal from wastewater is more efficient than that of N. Thirdly, groundwater systems are now releasing N which has been accumulating in past decades. Fourthly, settling of particulate P in lakes and reservoirs leads to continued P accumulation. With changing P concentrations in the water column due to agricultural policies and wastewater treatment, accumulated sediment P may be released to the water column (Reddy et al. 1999).

Reducing the nutrient loading of rivers, especially by wastewater treatment plants and improving nutrient efficiency in agriculture are essential strategies to reduce the nutrient fluxes. Our comparison shows that the Yangtze River basin has many similarities with the situation of the Mississippi in the 1970s, while the Yangtze scenarios indicate that the current policies to halt the increase of fertilizer use after 2020, which lead to a stabilization of nutrient surpluses in agriculture, will not be sufficient to stop the accumulation of nutrients in landscapes and waterscapes. Hence, the large accumulated amounts of N that are temporarily stored in groundwater and P in sediments may in future release dissolved reactive N and P following reduction measures. These legacies may be difficult to control by environmental management and form unwanted and unexpected sources of nutrient pollution.



## References

- Admiraal, W., Breugem, P., Jacobs, D.M.L.H.A. and De Ruyter Van Steveninck, E.D. (1990) Fixation of dissolved silicate and sedimentation of biogenic silicate in the lower river Rhine during diatom blooms. *Biogeochemistry* 9(2), 175-185.
- Alvarez-Cobelas, M., Angeler, D. and Sánchez-Carrillo, S. (2008) Export of nitrogen from catchments: A worldwide analysis. *Environmental Pollution* 156(2), 261-269.
- Anderson, D.M., Glibert, P.M. and Burkholder, J.M. (2002) Harmful algal blooms and eutrophication: Nutrient sources, composition, and consequences. *Estuaries* 25(4), 704-726.
- Arrigo, K.R. (2005) Marine microorganisms and global nutrient cycles. *Nature* 437(7057), 349-355.
- Barat, R., Serralta, J., Ruano, M.V., Jiménez, E., Ribes, J., Seco, A. and Ferrer, J. (2013) Biological nutrient removal model no. 2 (BNRM2): A general model for wastewater treatment plants. *Water Science and Technology* 67(7), 1481-1489.
- Berner, E. and Berner, R. (1996) *Global environment: water, air, and geochemical cycles*.
- Beusen, A., Bouwman, A., Dürr, H., Dekkers, A. and Hartmann, J. (2009) Global patterns of dissolved silica export to the coastal zone: Results from a spatially explicit global model. *Global Biogeochemical Cycles* 23(4).
- Beusen, A., Doelman, J., Van Beek, L., Van Puijenbroek, P., Mogollón, J., Van Grinsven, H., Stehfest, E., Van Vuuren, D. and Bouwman, A. (2022) Exploring river nitrogen and phosphorus loading and export to global coastal waters in the Shared Socio-economic pathways. *Global Environmental Change* 72, 102426.
- Beusen, A.H., Bouwman, A.F., Van Beek, L.P., Mogollón, J.M. and Middelburg, J.J. (2016) Global riverine N and P transport to ocean increased during the 20th century despite increased retention along the aquatic continuum. *Biogeosciences* 13(8), 2441-2451.
- Beusen, A.H.W., Van Beek, L.P.H., Bouwman, A.F., Mogollón, J.M. and Middelburg, J.J. (2015) Coupling global models for hydrology and nutrient loading to simulate nitrogen and phosphorus retention in surface water – description of IMAGE–GNM and analysis of performance. *Geoscientific Model Development* 8(12), 4045-4067.
- Bieger, K., Arnold, J.G., Rathjens, H., White, M.J., Bosch, D.D., Allen, P.M., Volk, M. and Srinivasan, R. (2017) Introduction to SWAT+, a completely restructured version of the soil and water assessment tool. *JAWRA Journal of the American Water Resources Association* 53(1), 115-130.
- Billen, G. and Garnier, J. (2007a) River basin nutrient delivery to the coastal sea: Assessing its potential to sustain new production of non-siliceous algae. *Marine Chemistry* 106(1-2), 148-160.

- Billen, G., Garnier, J. and Barles, S. (2012) History of the urban environmental imprint: introduction to a multidisciplinary approach to the long-term relationships between Western cities and their hinterland, Springer.
- Billen, G., Garnier, J., Ficht, A. and Cun, C. (2001) Modeling the response of water quality in the Seine River estuary to human activity in its watershed over the last 50 years. *Estuaries* 24(6), 977-993.
- Billen, G., Garnier, J. and Hanset, P. (1994) Modelling phytoplankton development in whole drainage networks: the RIVERSTRAHLER Model applied to the Seine river system. *Hydrobiologia* 289(1-3), 119-137.
- Billen, G., Garnier, J., Némery, J., Sebilo, M., Sferratore, A., Barles, S., Benoit, P. and Benoît, M. (2007b) A long-term view of nutrient transfers through the Seine river continuum. *Science of the Total Environment* 375(1-3), 80-97.
- Billen, G., Garnier, J. and Rousseau, V. (2005) Nutrient fluxes and water quality in the drainage network of the Scheldt basin over the last 50 years. *Hydrobiologia* 540(1), 47-67.
- Billen, G., Garnier, J. and Silvestre, M. (2015) A simplified algorithm for calculating benthic nutrient fluxes in river systems. *Annales de Limnologie* 51(1), 37-47.
- Böhlke, J.-K. (2002) Groundwater recharge and agricultural contamination. *Hydrogeology Journal* 10(1), 153-179.
- Borah, D. and Bera, M. (2003) Watershed-scale hydrologic and nonpoint-source pollution models: Review of mathematical bases. *Transactions of the Asae* 46(6), 1553.
- Bouwman, A., Beusen, A., Lassaletta, L., Van Apeldoorn, D., Van Grinsven, H. and Zhang, J. (2017) Lessons from temporal and spatial patterns in global use of N and P fertilizer on cropland. *Scientific Reports* 7, 40366.
- Bouwman, A., Kram, T. and Klein Goldewijk, K. (2006) Intergrated modelling of global environmental change: An overview of IMAGE 2.4.
- Bouwman, A.F., Beusen, A.H.W., Overbeek, C.C., Bureau, D.P., Pawłowski, M. and Glibert, P.M. (2013a) Hindcasts and future projections of global inland and coastal nitrogen and phosphorus loads due to finfish aquaculture. *Reviews in Fisheries Science* 21(2), 112-156.
- Bouwman, A.F., Bierkens, M.F.P., Griffioen, J., Hefting, M.M., Middelburg, J.J., Middelkoop, H. and Slomp, C.P. (2013b) Nutrient dynamics, transfer and retention along the aquatic continuum from land to ocean: towards integration of ecological and biogeochemical models. *Biogeosciences* 10(1), 1-22.
- Bouwman, A.F., Pawłowski, M., Liu, C., Beusen, A.H.W., Shumway, S.E., Glibert, P.M. and Overbeek, C.C. (2011) Global Hindcasts and Future Projections of Coastal Nitrogen and Phosphorus Loads Due to Shellfish and Seaweed Aquaculture. *Reviews in Fisheries Science* 19(4), 331-357.
- Bouwman, A.F., Van Brecht, G. and Van Der Hoek, K.W. (2005a) Global and regional surface nitrogen balances in intensive agricultural production systems for the period 1970-2030. *Pedosphere* 15(2), 137-155.

- Bouwman, A.F., Van Drecht, G., Knoop, J.M., Beusen, A.H.W. and Meinardi, C.R. (2005b) Exploring changes in river nitrogen export to the world's oceans. *Global Biogeochemical Cycles* 19(1), 1-14.
- Bouwman, L., Goldewijk, K.K., Van Der Hoek, K.W., Beusen, A.H., Van Vuuren, D.P., Willems, J., Rufino, M.C. and Stehfest, E. (2013c) Exploring global changes in nitrogen and phosphorus cycles in agriculture induced by livestock production over the 1900-2050 period. *Proc Natl Acad Sci U S A* 110(52), 20882-20887.
- Bowes, M.J., Leach, D.V. and House, W.A. (2005) Seasonal nutrient dynamics in a chalk stream: The River Frome, Dorset, UK. *Science of the Total Environment* 336(1-3), 225-241.
- Breitburg, D., Levin, L.A., Oschlies, A., Grégoire, M., Chavez, F.P., Conley, D.J., Garçon, V., Gilbert, D., Gutiérrez, D. and Isensee, K. (2018) Declining oxygen in the global ocean and coastal waters. *Science* 359(6371), eaam7240.
- Brzezinski, M.A. (1985) The Si: C: N ratio of marine diatoms: interspecific variability and the effect of some environmental variables 1. *Journal of Phycology* 21(3), 347-357.
- Cerdan, O., Govers, G., Le Bissonnais, Y., Van Oost, K., Poesen, J., Saby, N., Gobin, A., Vacca, A., Quinton, J., Auerswald, K., Klik, A., Kwaad, F.J.P.M., Raclot, D., Ionita, I., Rejman, J., Rousseva, S., Muxart, T., Roxo, M.J. and Dostal, T. (2010) Rates and spatial variations of soil erosion in Europe: A study based on erosion plot data. *Geomorphology* 122(1-2), 167-177.
- Chai, T. and Draxler, R.R. (2014) Root mean square error (RMSE) or mean absolute error (MAE)?—Arguments against avoiding RMSE in the literature. *Geoscientific Model Development* 7(3), 1247-1250.
- Changjiang River Water Resource Committee (1955-1985) Changjiang River Water Resource Committee, 1955–1985. Hydrographic Data Collection in the Lower Reaches of the Yangtze River (Internal report), p. 585 (in Chinese). Changjiang Water Resources Commission.
- Changjiang Sediment Bulletin Committee (2015) Changjiang Sediment Bulletin. Data available at <http://www.cjh.com.cn/> (Retrieved 8 October 2014).
- Chen, X., Stokal, M., Van Vliet, M.T.H., Stuver, J., Wang, M., Bai, Z., Ma, L. and Kroeze, C. (2019) Multi-scale Modeling of Nutrient Pollution in the Rivers of China. *Environmental Science and Technology* 53(16), 9614-9625.
- Cheng, S., Li, Z., Uddin, S.M.N., Mang, H.-P., Zhou, X., Zhang, J., Zheng, L. and Zhang, L. (2018) Toilet revolution in China. *Journal of Environmental Management* 216, 347-356.
- Cheng, X. and Li, X. (2008) 20-year variations of nutrients (N and P) and their impacts on algal growth in Lake Dianshan. *China* 20(4), 409-419.
- China, M.o.A.o. (2014a) The Chinese agricultural statistical report (in Chinese). Data covering 1980-2011 retrieved 8 October 2014. China Agriculture Press, Beijing, China.

- China, N.B.o.S.o. (2014b) China statistical yearbook (in Chinese). Data covering 1981-2011 retrieved 8 October 2014. China Statistic Press, Beijing, China. .
- China, S.O.A.o. (2009) Bulletin of Marine Environmental Quality of China, data are available at: <http://www.soa.gov.cn/chichao/index.html> (Retrieved 10 December 2015).
- Clarke, F.W. (1920) The data of geochemistry, US Government Printing Office.
- Cloern, J.E. (1996) Phytoplankton bloom dynamics in coastal ecosystems: a review with some general lessons from sustained investigation of San Francisco Bay, California. *Reviews of Geophysics* 34(2), 127-168.
- CMA, C.M.o.A. (2015) Circular of the Chinese Ministry of Agriculture on printing and distributing the Action Plan for Zero Growth in the Application of Fertilizer by 2020 and the Action Plan for Zero Growth in the Application of Pesticide by 2020. Available at: [http://jiuban.moa.gov.cn/zwillm/tzgg/tz/201503/t20150318\\_4444765.htm](http://jiuban.moa.gov.cn/zwillm/tzgg/tz/201503/t20150318_4444765.htm) (in Chinese).
- Committee, C.L.Y.E. (2014a) China livestock yearbook (in Chinese). Data covering 1999-2011 retrieved 8 October 2014. China Agriculture Press, Beijing, China.
- Committee, C.P.S.Y.E. (2014b) China Population Statistics Yearbook (in chinese). Data covering 1949-2014 retrieved 8 November 2014. China Statistics Press, Beijing, China.
- Committee, C.S.B. (2015) Changjiang Sediment Bulletin. Data available at <http://www.cjh.com.cn/> (Retrieved 8 October 2014).
- Committee, C.W.R.C.E. (2014c) Yangtze River Yearbook (1992-2011), Changjiang Water Resources Commission.
- Conley, D.J. (1997) Riverine contribution of biogenic silica to the oceanic silica budget. *Limnology and Oceanography* 42(4), 774-777.
- Conley, D.J. (1999) Biogeochemical nutrient cycles and nutrient management strategies. *Hydrobiologia* 410, 87-96.
- Conley, D.J. (2002) Terrestrial ecosystems and the global biogeochemical silica cycle. *Global Biogeochemical Cycles* 16(4), 68-61.
- Conley, D.J., Kilham, S.S. and Theriot, E. (1989) Differences in silica content between marine and freshwater diatoms. *Limnology and Oceanography* 34(1), 205-212.
- Conley, D.J., Schelske, C.L. and Stoermer, E.F. (1993) Modification of the biogeochemical cycle of silica with eutrophication. *Marine Ecology Progress Series*, 179-192.
- Dai, Z., Du, J., Zhang, X., Su, N. and Li, J. (2011) Variation of riverine material loads and environmental consequences on the Changjiang (Yangtze) estuary in recent decades (1955-2008). *Environ Sci Technol* 45(1), 223-227.
- Dai, Z. and Liu, J.T. (2013) Impacts of large dams on downstream fluvial sedimentation: An example of the Three Gorges Dam (TGD) on the Changjiang (Yangtze River). *Journal of Hydrology* 480, 10-18.

- Derry, L.A., Kurtz, A.C., Ziegler, K. and Chadwick, O.A. (2005) Biological control of terrestrial silica cycling and export fluxes to watersheds. *Nature* 433(7027), 728.
- Diaz, R.J. and Rosenberg, R. (2008) Spreading dead zones and consequences for marine ecosystems. *Science* 321(5891), 926-929.
- Dodds, W. (2002) *Freshwater ecology: concepts and environmental applications*, Elsevier.
- Duan, S., Liang, T., Zhang, S., Wang, L., Zhang, X. and Chen, X. (2008) Seasonal changes in nitrogen and phosphorus transport in the lower Changjiang River before the construction of the Three Gorges Dam. *Estuarine, Coastal and Shelf Science* 79(2), 239-250.
- Dumont, E., Harrison, J., Kroeze, C., Bakker, E. and Seitzinger, S. (2005) Global distribution and sources of dissolved inorganic nitrogen export to the coastal zone: Results from a spatially explicit, global model. *Global Biogeochemical Cycles* 19(4).
- Dürr, H.H., Meybeck, M. and Dürr, S.H. (2005) Lithologic composition of the Earth's continental surfaces derived from a new digital map emphasizing riverine material transfer. *Global Biogeochemical Cycles* 19(4).
- Dürr, H.H., Meybeck, M., Hartmann, J., Laruelle, G.G. and Roubeix, V. (2011) Global spatial distribution of natural riverine silica inputs to the coastal zone. *Biogeosciences* 8(3), 597-620.
- EC, E.C. (1991a) Concerning the protection of waters against pollution caused by nitrates from agricultural sources, European Economic Community, Brussels.
- EC, E.C. (1991b) Council Directive of 21. May 1991 concerning urban waste water treatment (91/271/EEC). *J. Eur. Commun* 34, 40.
- EC, E.C. (2000) Water Framework Directive. Journal reference OJL 327, 1-73.
- Elser, J.J., Bracken, M.E., Cleland, E.E., Gruner, D.S., Harpole, W.S., Hillebrand, H., Ngai, J.T., Seabloom, E.W., Shurin, J.B. and Smith, J.E. (2007) Global analysis of nitrogen and phosphorus limitation of primary producers in freshwater, marine and terrestrial ecosystems. *Ecol Lett* 10(12), 1135-1142.
- Ensign, S.H. and Doyle, M.W. (2006) Nutrient spiraling in streams and river networks. *Journal of Geophysical Research: Biogeosciences* 111(G4).
- EPA, E.P.A. (2019) Clean Water Act Section 303(d): Impaired Waters and Total Maximum Daily Loads (TMDLs) <https://www.epa.gov/tmdl>, Changjiang Water Resources Commission.
- FAO (1977) China: recycling of organic wastes in agriculture, p. 107, Food and Agriculture Organization of the United Nations, Rome.
- FAOSTAT (2017) FAOSTAT Database Collections. Protein Supply Quantity, Food and Agriculture Organization of the United Nations Rome. <http://www.fao.org/faostat/en/#data/FBS>.
- Floyd, P., Zarogiannis, P. and Fox, K. (2006) Non-surfactant organic ingredients and zeolite-based detergents. Final Report.

- Fowler, D., Coyle, M., Skiba, U., Sutton, M.A., Cape, J.N., Reis, S., Sheppard, L.J., Jenkins, A., Grizzetti, B. and Galloway, J.N. (2013) The global nitrogen cycle in the twenty-first century. *Philosophical Transactions of the Royal Society B: Biological Sciences* 368(1621), 20130164.
- Frijters, I.D. and Leentvaar, J. (2003) Rhine case study, Unesco.
- Galloway, J.N. (1998) The global nitrogen cycle: changes and consequences. *Environmental Pollution* 102(1), 15-24.
- Galloway, J.N., Dentener, F.J., Capone, D.G., Boyer, E.W., Howarth, R.W., Seitzinger, S.P., Asner, G.P., Cleveland, C.C., Green, P.A. and Holland, E.A. (2004) Nitrogen cycles: past, present, and future. *Biogeochemistry* 70(2), 153-226.
- Galloway, J.N., Townsend, A.R., Erisman, J.W., Bekunda, M., Cai, Z., Freney, J.R., Martinelli, L.A., Seitzinger, S.P. and Sutton, M.A. (2008) Transformation of the nitrogen cycle: recent trends, questions, and potential solutions. *Science* 320(5878), 889-892.
- Gao, S. and Wang, Y.P. (2008) Changes in material fluxes from the Changjiang River and their implications on the adjoining continental shelf ecosystem. *Continental Shelf Research* 28(12), 1490-1500.
- Garnier, J., Beusen, A., Thieu, V., Billen, G. and Bouwman, L. (2010) N: P: Si nutrient export ratios and ecological consequences in coastal seas evaluated by the ICEP approach. *Global Biogeochemical Cycles* 24(4).
- Garnier, J., Billen, G. and Palfner, L. (2000) Understanding the oxygen budget and related ecological processes in the river Mosel: The RIVERSTRAHLER approach. *Hydrobiologia* 410, 151-166.
- Garnier, J., Bruno, L., Nathalie, S. and Philippon (1999) Biogeochemical mass-balances (C, N, P, Si) in three large reservoirs of the Seine Basin (France). *Biogeochemistry* 47(2), 119-146.
- Garnier, J., d'Ayguessives, A., Billen, G., Conley, D. and Sferratore, A. (2002) Silica dynamics in the hydrographic network of the Seine River. *Oceanis* 28(3-4), 487-508.
- Garnier, J., Sferratore, A., Meybeck, M., Billen, G. and Dürr, H. (2006) Modeling silicon transfer processes in river catchments. The silicon cycle. Human perturbations and impacts on aquatic systems 66, 139-162.
- Glibert, P.M., Berdalet, E., Burford, M.A., Pitcher, G.C. and Zhou, M. (2018) *Global ecology and oceanography of harmful algal blooms*, Springer.
- Gruber, N. and Galloway, J.N. (2008) An Earth-system perspective of the global nitrogen cycle. *Nature* 451(7176), 293-296.
- Harashima, A., Kimoto, T., Wakabayashi, T. and Toshiyasu, T. (2006) Verification of the silica deficiency hypothesis based on biogeochemical trends in the aquatic continuum of Lake Biwa–Yodo River–Seto Inland Sea, Japan. *AMBIO: A Journal of the Human Environment* 35(1), 36-43.

- Harrison, J.A., Frings, P.J., Beusen, A.H.W., Conley, D.J. and McCrackin, M.L. (2012) Global importance, patterns, and controls of dissolved silica retention in lakes and reservoirs. *Global Biogeochemical Cycles* 26(2).
- Harrison, J.A., Seitzinger, S.P., Bouwman, A.F., Caraco, N.F., Beusen, A.H.W. and Vörösmarty, C.J. (2005) Dissolved inorganic phosphorus export to the coastal zone: Results from a spatially explicit, global model. *Global Biogeochemical Cycles* 19(4).
- Hartmann, J. (2009) Bicarbonate-fluxes and CO<sub>2</sub> consumption by chemical weathering on the Japanese Archipelago - Application of a multi-lithological model framework. *Chemical Geology* 265(3-4), 237-271.
- Hartmann, J., Dürr, H.H., Moosdorf, N., Meybeck, M. and Kempe, S. (2012) The geochemical composition of the terrestrial surface (without soils) and comparison with the upper continental crust. *International Journal of Earth Sciences* 101(1), 365-376.
- Hartmann, J., Jansen, N., Kempe, S. and Dürr, H.H. (2007) Geochemistry of the river Rhine and the upper Danube: Recent trends and lithological influence on baselines. *Journal of Environmental Science for Sustainable Society* 1, 39-46.
- Hartmann, J., Lauerwald, R. and Moosdorf, N. (2014a) A brief overview of the GLObal River CHEmistry Database, GLORICH. *Procedia Earth and Planetary Science* 10, 23-27.
- Hartmann, J., Levy, J. and Kempe, S. (2011) Increasing dissolved silica trends in the Rhine River: an effect of recovery from high P loads? *Limnology* 12(1), 63-73.
- Hartmann, J., Moosdorf, N., Lauerwald, R., Hinderer, M. and West, A.J. (2014b) Global chemical weathering and associated p-release - the role of lithology, temperature and soil properties. *Chemical Geology* 363, 145-163.
- Hauck, F. (1978) China: recycling of organic wastes in agriculture. Food and Agricultural Organization of the United Nations, Rome.
- Haygarth, P.M., Jarvie, H.P., Powers, S.M., Sharpley, A.N., Elser, J.J., Shen, J., Peterson, H.M., Chan, N.I., Howden, N.J.K., Burt, T., Worrall, F., Zhang, F. and Liu, X. (2014) Sustainable phosphorus management and the need for a long-term perspective: The legacy hypothesis. *Environmental Science and Technology* 48(15), 8417-8419.
- Hendriks, A.T.W.M. and Langeveld, J.G. (2017) Rethinking Wastewater Treatment Plant Effluent Standards: Nutrient Reduction or Nutrient Control? *Environ Sci Technol* 51(9), 4735-4737.
- House, W.A., Leach, D.V. and Armitage, P.D. (2001) Study of dissolved silicon, and nitrate dynamics in a fresh water stream. *Water Research* 35(11), 2749-2757.
- Howarth, R.W., Billen, G., Swaney, D., Townsend, A., Jaworski, N., Lajtha, K., Downing, J., Elmgren, R., Caraco, N. and Jordan, T. (1996) Nitrogen cycling in the North Atlantic Ocean and its watersheds, pp. 75-139, Springer.

- Hu, C., Li, D., Chen, C., Ge, J., Muller-Karger, F.E., Liu, J., Yu, F. and He, M.X. (2010) On the recurrent *Ulva prolifera* blooms in the Yellow Sea and East China Sea. *Journal of Geophysical Research: Oceans* 115(C5).
- Hu, Z., Houweling, D. and Dold, P. (2012) Biological nutrient removal in municipal wastewater treatment: New directions in sustainability. *Journal of Environmental Engineering (United States)* 138(3), 307-317.
- Humborg, C., Blomqvist, S., Avsan, E., Bergensund, Y., Smedberg, E., Brink, J. and Mörtz, C.M. (2002a) Hydrological alterations with river damming in northern Sweden: Implications for weathering and river biogeochemistry. *Global Biogeochemical Cycles* 16(3), 12-11.
- Humborg, C., Blomqvist, S., Avsan, E., Bergensund, Y., Smedberg, E., Brink, J. and Mörtz, C.M. (2002b) Hydrological alterations with river damming in northern Sweden: Implications for weathering and river biogeochemistry. *Global Biogeochemical Cycles* 16(3), 12-11-12-13.
- Humborg, C., Conley, D.J., Rahm, L., Wulff, F., Cociasu, A. and Ittekkot, V. (2000) Silicon retention in river basins: Far-reaching effects on biogeochemistry and aquatic food webs in coastal marine environments. *Ambio* 29(1), 45-50.
- Humborg, C., Ittekkot, V., Cociasu, A. and Bodungen, B.V. (1997) Effect of Danube River dam on Black Sea biogeochemistry and ecosystem structure. *Nature* 386(6623), 385-388.
- Humborg, C., Pastuszak, M., Aigars, J., Siegmund, H., Mörtz, C.M. and Ittekkot, V. (2006) Decreased silica land-sea fluxes through damming in the Baltic Sea catchment - Significance of particle trapping and hydrological alterations. *Biogeochemistry* 77(2), 265-281.
- Humborg, C., Smedberg, E., Medina, M.R. and Mörtz, C.M. (2008) Changes in dissolved silicate loads to the Baltic Sea - The effects of lakes and reservoirs. *Journal of Marine Systems* 73(3-4), 223-235.
- Iler, R.K. (1979) *The chemistry of silica: solubility, polymerization, colloid and surface properties, and biochemistry*, Wiley, New York.
- Infrastructure, N.S.a.T. (2015) National Earth System Science Data Sharing Infrastructure. Available at <http://www.geodata.cn/> (last access: 20 December 2016).
- ICPR, I.C.f.t.P.o.t.R. (2015) Internationally Coordinated Management Plan 2015 for the International River Basin District of the Rhine. Available at: [https://www.iksr.org/fileadmin/user\\_upload/Dokumente\\_en/Brochures/CMP\\_2015\\_-\\_en.pdf](https://www.iksr.org/fileadmin/user_upload/Dokumente_en/Brochures/CMP_2015_-_en.pdf).
- Jiao, J., Lin, W. and Lu, S. (2005) Numerical simulation of transport and diffusion of Shanghai municipal sewage outfalls (in Chinese). *Environmental Pollution & Control* 27(6), 448456.
- Ju, L., Yu, D., Fang, H., Guo, Q., Xu, X., Li, S. and Zhao, L. (2018) Trends and food sources composition of energy, protein and fat in Chinese residents, 1992-2012. *Wei sheng yan jiu = Journal of hygiene research* 47(5), 689-704.



- Kelly, E.F., Chadwick, O.A. and Hilinski, T.E. (1998) The effect of plants on mineral weathering. *Biogeochemistry* 42(1-2), 21-53.
- Kemp, W., Testa, J.M., Conley, D.J., Gilbert, D. and Hagy, J.D. (2009) Temporal responses of coastal hypoxia to nutrient loading and physical controls. *Biogeosciences* 6(12), 2985-3008.
- Keung Wong, D.F., Li, C.Y. and Song, H.X. (2007) Rural migrant workers in urban China: Living a marginalised life. *International Journal of Social Welfare* 16(1), 32-40.
- Kobayashi, J. (1961) A chemical study on the average quality and characteristics of river waters of Japan. *Nogaku Kenkyu* 48(2), 63-106.
- Kreiling, R.M. and Houser, J.N. (2016) Long-term decreases in phosphorus and suspended solids, but not nitrogen, in six upper Mississippi River tributaries, 1991–2014. *Environmental Monitoring and Assessment* 188(8), 1-19.
- Laruelle, G.G., Roubex, V., Sferratore, A., Brodherr, B., Ciuffa, D., Conley, D.J., Dürr, H.H., Garnier, J., Lancelot, C., LeThiPhuong, Q., Meunier, J.D., Meybeck, M., Michalopoulos, P., Moriceau, B., Ni Longphuir, S., Loucaides, S., Papush, L., Presti, M., Ragueneau, O., Regnier, P., Saccone, L., Slomp, C.P., Spiteri, C. and Van Cappellen, P. (2009) Anthropogenic perturbations of the silicon cycle at the global scale: Key role of the land-ocean transition. *Global Biogeochemical Cycles* 23(4).
- LeBauer, D.S. and Treseder, K.K. (2008) Nitrogen Limitation of Net Primary Productivity in Terrestrial Ecosystems Is Globally Distributed. *Ecology* 89(2), 371-379.
- Lehner, B. and Döll, P. (2004) Development and validation of a global database of lakes, reservoirs and wetlands. *Journal of Hydrology* 296(1-4), 1-22.
- Lehner, B., Liermann, C.R., Revenga, C., Vörösmarty, C., Fekete, B., Crouzet, P., Döll, P., Endejan, M., Frenken, K., Magome, J., Nilsson, C., Robertson, J.C., Rödel, R., Sindorf, N. and Wisser, D. (2011) High-resolution mapping of the world's reservoirs and dams for sustainable river-flow management. *Frontiers in Ecology and the Environment* 9(9), 494-502.
- Leira, M. and Sabater, S. (2005) Diatom assemblages distribution in catalan rivers, NE Spain, in relation to chemical and physiographical factors. *Water Research* 39(1), 73-82.
- Li, G.L., Bai, X., Yu, S., Zhang, H. and Zhu, Y.G. (2012) Urban phosphorus metabolism through food consumption: The case of China. *Journal of Industrial Ecology* 16(4), 588-599.
- Li, J., Jin, X., Xu, X., Shen, M., Ji, Z., Jiang, W., Gao, Q. and Chen, X. (2009) Effect evaluation of non-hazardous treatment for lavatory improvement in rural areas of Jiangsu Province in 2008. *Chinese Journal of Schistosomiasis Control* 21(4), 293-296.
- Li, M., Xu, K., Watanabe, M. and Chen, Z. (2007) Long-term variations in dissolved silicate, nitrogen, and phosphorus flux from the Yangtze River into the East China

- Sea and impacts on estuarine ecosystem. *Estuarine, Coastal and Shelf Science* 71(1-2), 3-12.
- Li, X., Yang, L. and Yan, W. (2011) Model analysis of dissolved inorganic phosphorus exports from the Yangtze river to the estuary. *Nutrient Cycling in Agroecosystems* 90(1), 157-170.
- Liu, J., Tian, H., Liu, M., Zhuang, D., Melillo, J.M. and Zhang, Z. (2005) China's changing landscape during the 1990s: Large-scale land transformations estimated with satellite data. *Geophysical Research Letters* 32(2), 1-5.
- Liu, S., Hong, G.-H., Zhang, J., Ye, X. and Jiang, X.L. (2009) Nutrient budgets for large Chinese estuaries. *Biogeosciences* 6(10), 2245-2263.
- Liu, S.M., Zhang, J., Chen, H., Wu, Y., Xiong, H. and Zhang, Z. (2003) Nutrients in the Changjiang and its tributaries. *Biogeochemistry* 62(1), 1-18.
- Liu, X., Beusen, A.H., Van Beek, L.P., Mogollón, J.M., Ran, X. and Bouwman, A.F. (2018) Exploring spatiotemporal changes of the Yangtze River (Changjiang) nitrogen and phosphorus sources, retention and export to the East China Sea and Yellow Sea. *Water Research* 142, 246-255.
- Liu, X., Joost van Hoek, W., Vilmin, L., Beusen, A., Mogollón, J.M., Middelburg, J.J. and Bouwman, A.F. (2020a) Exploring Long-Term Changes in Silicon Biogeochemistry Along the River Continuum of the Rhine and Yangtze (Changjiang). *Environ Sci Technol* 54(19), 11940-11950.
- Liu, X., Shen, H. and Huang, Q. (2002) Concentration variation and flux estimation of dissolved inorganic nutrient from the Changjiang River into its estuary. *Oceanol. et Limnol. Sin.* 33 (5): 332-340. Chinses with English abstract.
- Longhurst, A., Sathyendranath, S., Platt, T. and Caverhill, C. (1995) An estimate of global primary production in the ocean from satellite radiometer data. *Journal of Plankton Research* 17(6), 1245-1271.
- Longo, S., Mauricio-Iglesias, M., Soares, A., Campo, P., Fatone, F., Eusebi, A.L., Akkersdijk, E., Stefani, L. and Hospido, A. (2019) ENERWATER—A standard method for assessing and improving the energy efficiency of wastewater treatment plants. *Applied Energy* 242, 897-910.
- Loos, S., Middelkoop, H., van der Perk, M. and van Beek, R. (2009) Large scale nutrient modelling using globally available datasets: A test for the Rhine basin. *Journal of Hydrology* 369(3-4), 403-415.
- Ma, L., Ma, W., Velthof, G., Wang, F., Qin, W., Zhang, F. and Oenema, O. (2010) Modeling nutrient flows in the food chain of China. *Journal of Environmental Quality* 39(4), 1279-1289.
- Maavara, T., Dürr, H.H. and Van Cappellen, P. (2014) Worldwide retention of nutrient silicon by river damming: From sparse data set to global estimate. *Global Biogeochemical Cycles* 28(8), 842-855.
- Mackenzie, F., Andersson, A., Lerman, A. and Ver, L. (2005) Boundary exchanges in the global coastal margin: implications for the organic and inorganic carbon cycles. *The sea* 13, 193-225.

- Manuel, J. (2014) Nutrient pollution: A persistent threat to waterways, NLM-Export.
- MIE, M.o.I.a.E. (2019) The Hague:Ministry of Infrastructure and Environment.
- Marcé, R. and Armengol, J. (2009) Modeling nutrient in-stream processes at the watershed scale using Nutrient Spiralling metrics. *Hydrology and Earth System Sciences* 13(7), 953-967.
- Maurer, M., Pronk, W. and Larsen, T. (2006) Treatment processes for source-separated urine. *Water Research* 40(17), 3151-3166.
- Mayorga, E., Seitzinger, S.P., Harrison, J.A., Dumont, E., Beusen, A.H., Bouwman, A., Fekete, B.M., Kroeze, C. and Van Drecht, G. (2010) Global nutrient export from WaterSheds 2 (NEWS 2): model development and implementation. *Environmental Modelling & Software* 25(7), 837-853.
- Meybeck, M. (1979) Concentrations des eaux fluviales en elements majeurs et apports en solution aux oceans. *Rev. Geol. Dyn. Geogr. Phys.* 21, 215-246.
- Meybeck, M., Dürr, H.H. and Vörösmarty, C.J. (2006) Global coastal segmentation and its river catchment contributors: A new look at land-ocean linkage. *Global Biogeochemical Cycles* 20(1).
- Middelburg, J.J. (2020) Are nutrients retained by river damming? *National Science Review*.
- MIE, M.o.I.a.E. (2019) The Hague:Ministry of Infrastructure and Environment.
- Ministry of Ecology and Environment of the People's Republic of China (2014) National list of operating centralized wastewater treatment plants.
- Ministry of Housing and Urban-Rural Development of the People's Republic of China (2016) China Urban-Rural Construction Statistical Yearbook 1981-2016.
- Moon, S., Chamberlain, C.P. and Hilley, G.E. (2014) New estimates of silicate weathering rates and their uncertainties in global rivers. *Geochimica et Cosmochimica Acta* 134, 257-274.
- Morée, A.L., Beusen, A.H.W., Bouwman, A.F. and Willems, W.J. (2013) Exploring global nitrogen and phosphorus flows in urban wastes during the twentieth century. *Global Biogeochemical Cycles* 27(3), 836-846.
- Moriasi, D.N., Gitau, M.W., Pai, N. and Daggupati, P. (2015) Hydrologic and water quality models: Performance measures and evaluation criteria. *Transactions of the ASABE* 58(6), 1763-1785.
- Morris, B.L., Lawrence, A.R., Chilton, P., Adams, B., Calow, R.C. and Klinck, B.A. (2003) Groundwater and its susceptibility to degradation: a global assessment of the problem and options for management.
- National Bureau of Statistics of China (2015) China Statistical Yearbook 1990-2015.
- Nelson, D.M., Tréguer, P., Brzezinski, M.A., Leynaert, A. and Quéguiner, B. (1995) Production and dissolution of biogenic silica in the ocean: revised global estimates, comparison with regional data and relationship to biogenic sedimentation. *Global Biogeochemical Cycles* 9(3), 359-372.

- Neset, T.S.S., Bader, H.P. and Scheidegger, R. (2006) Food consumption and nutrient flows: Nitrogen in Sweden since the 1870s. *Journal of Industrial Ecology* 10(4), 61-75.
- New, M., Hulme, M. and Jones, P. (2000) Representing twentieth-century space-time climate variability. Part II: Development of 1901-96 monthly grids of terrestrial surface climate. *Journal of Climate* 13(13), 2217-2238.
- Nyenje, P., Foppen, J., Uhlenbrook, S., Kulabako, R. and Muwanga, A. (2010) Eutrophication and nutrient release in urban areas of sub-Saharan Africa—a review. *Science of the Total Environment* 408(3), 447-455.
- Oddoye, E.A. and Margen, S. (1979) Nitrogen balance studies in humans: Long-term effect of high nitrogen intake on nitrogen accretion. *Journal of Nutrition* 109(3), 363-377.
- Oleszkiewicz, J.A. and Barnard, J.L. (2006) Nutrient removal technology in North America and the European Union: A review. *Water Quality Research Journal of Canada* 41(4), 449-462.
- Organization, F.a.A. (2013) FishStatJ - software for fishery statistical time series <http://www.fao.org/fishery/statistics/software/fishstatj/en> (release data March 2013), Fisheries and Aquaculture Information and Statistics Service, Food and Agriculture Organization of the United Nations, Rome.
- Organization, W.H. (2017) 2017 annual report WHO/UNICEF joint monitoring programme for water supply, sanitation and hygiene, pp. 20-20.
- Phillips, A.K. and Cowling, S.A. (2019) Biotic and abiotic controls on watershed Si cycling and river Si yield in western Canada. *Biogeochemistry* 143(2), 221-237.
- Potere, D. and Schneider, A. (2007) A critical look at representations of urban areas in global maps. *GeoJournal* 69(1-2), 55-80.
- Powers, S.M., Bruulsema, T.W., Burt, T.P., Chan, N.I., Elser, J.J., Haygarth, P.M., Howden, N.J., Jarvie, H.P., Lyu, Y. and Peterson, H.M. (2016) Long-term accumulation and transport of anthropogenic phosphorus in three river basins. *Nature Geoscience* 9(5), 353-356.
- Pronk, W. and Kone, D. (2009) Options for urine treatment in developing countries. *Desalination* 248(1-3), 360-368.
- Puckett, L.J., Tesoriero, A.J. and Dubrovsky, N.M. (2011) Nitrogen contamination of surficial aquifers-A growing legacy. *Environmental Science and Technology* 45(3), 839-844.
- Qi, M., Yang, Y., Zhang, X., Zhang, X., Wang, M., Zhang, W., Lu, X. and Tong, Y. (2020) Pollution reduction and operating cost analysis of municipal wastewater treatment in China and implication for future wastewater management. *Journal of Cleaner Production* 253.
- Qin, B., Zhang, Y., Zhu, G., Gong, Z., Deng, J., Hamilton, D.P., Gao, G., Shi, K., Zhou, J., Shao, K., Zhu, M., Zhou, Y., Tang, X. and Li, L. (2020) Are nitrogen-to-phosphorus ratios of Chinese lakes actually increasing? *Proceedings of the*

- National Academy of Sciences of the United States of America 117(35), 21000-21002.
- Qu, H.J. and Kroeze, C. (2010) Past and future trends in nutrients export by rivers to the coastal waters of China. *Science of the Total Environment* 408(9), 2075-2086.
- Quan, W., Shen, X., Han, J. and CHEN, Y.-q. (2005) Analysis and assessment on eutrophication status and developing trend in Changjiang Estuary and adjacent sea. *Marine Environmental Science* 24(3), 13-16.
- Quynh, L.T.P., Billen, G., Garnier, J., Théry, S., Fézard, C. and Minh, C.V. (2005) Nutrient (N, P) budgets for the Red River basin (Vietnam and China). *Global Biogeochemical Cycles* 19(2).
- Ran, X.-b., Chen, H.-t., Wei, J.-f., Yao, Q.-z., Mi, T.-z. and Yu, Z.-g. (2016) Phosphorus speciation, transformation and retention in the Three Gorges Reservoir, China. *Marine and Freshwater Research* 67(2), 173-186.
- Ran, X., Bouwman, A.F., Yu, Z. and Liu, J. (2019) Implications of eutrophication for biogeochemical processes in the Three Gorges Reservoir, China. *Regional Environmental Change* 19(1), 55-63.
- Ran, X., Bouwman, L., Yu, Z., Beusen, A., Chen, H. and Yao, Q. (2017) Nitrogen transport, transformation, and retention in the Three Gorges Reservoir: A mass balance approach. *Limnology and Oceanography* 62(5), 2323-2337.
- Ran, X., Yu, Z., Yao, Q., Chen, H. and Guo, H. (2013) Silica retention in the Three Gorges Reservoir. *Biogeochemistry* 112(1-3), 209-228.
- Reddy, K., Kadlec, R., Flaig, E. and Gale, P. (1999) Phosphorus retention in streams and wetlands: a review. *Critical reviews in environmental science and technology* 29(1), 83-146.
- Redfield, A. (1934) On the proportions of organic derivations in seawater and their relation to the composition of plankton (reprint). *Benchmark Papers in Ecology* 1.
- Redfield, A., Ketchum, B. and Richards, F. (1963) The influence of organisms on the composition of seawater. *The sea* 2, 26-77.
- Riegman, R. (1995) Nutrient-related selection mechanisms in marine phytoplankton communities and the impact of eutrophication on the planktonic food web. *Water Science and Technology* 32(4), 63-75.
- Robinson, T.P., Wint, G.W., Conchedda, G., Van Boeckel, T.P., Ercoli, V., Palamara, E., Cinardi, G., D'Aiotti, L., Hay, S.I. and Gilbert, M. (2014) Mapping the global distribution of livestock. *PloS one* 9(5), e96084.
- Romero, E., Garnier, J., Lassaletta, L., Billen, G., Le Gendre, R., Riou, P. and Cugier, P. (2013) Large-scale patterns of river inputs in southwestern Europe: seasonal and interannual variations and potential eutrophication effects at the coastal zone. *Biogeochemistry* 113(1), 481-505.
- Rousseau, V., Becquevort, S., Parent, J.Y., Gasparini, S., Daro, M.H., Tackx, M. and Lancelot, C. (2000) Trophic efficiency of the planktonic food web in a coastal

- ecosystem dominated by *Phaeocystis* colonies. *Journal of Sea Research* 43(3-4), 357-372.
- Rowe, H., Withers, P.J., Baas, P., Chan, N.I., Doody, D., Holiman, J., Jacobs, B., Li, H., MacDonald, G.K. and McDowell, R. (2016) Integrating legacy soil phosphorus into sustainable nutrient management strategies for future food, bioenergy and water security. *Nutrient Cycling in Agroecosystems* 104(3), 393-412.
- Saltelli, A., Tarantola, S. and Campolongo, F. (2000) Sensitivity analysis as an ingredient of modeling. *Statistical Science*, 377-395.
- Sattari, S.Z., Bouwman, A.F., Giller, K.E. and van Ittersum, M.K. (2012) Residual soil phosphorus as the missing piece in the global phosphorus crisis puzzle. *Proceedings of the National Academy of Sciences* 109(16), 6348-6353.
- Sattari, S.Z. (2014) *The legacy of phosphorus: Agriculture and future food security*, Wageningen University and Research.
- Scheffer, M. (2004) *Ecology of shallow lakes*, Springer Science & Business Media.
- Seitzinger, S., Harrison, J., Dumont, E., Beusen, A.H. and Bouwman, A. (2005) Sources and delivery of carbon, nitrogen, and phosphorus to the coastal zone: An overview of Global Nutrient Export from Watersheds (NEWS) models and their application. *Global Biogeochemical Cycles* 19(4).
- Seitzinger, S.P., Bouwman, A.F. and Kroeze, C. (2010a) Preface to special section on past and future trends in nutrient export from global watersheds and impacts on water quality and eutrophication. *Global Biogeochemical Cycles* 24(4).
- Seitzinger, S.P., Mayorga, E., Bouwman, A.F., Kroeze, C., Beusen, A.H.W., Billen, G., Van Drecht, G., Dumont, E., Fekete, B.M., Garnier, J. and Harrison, J.A. (2010b) Global river nutrient export: A scenario analysis of past and future trends. *Global Biogeochemical Cycles* 24(4).
- Sferratore, A. (2006) *Modelling the transfer, transformation and retention of silica along aquatic continuums: an upgraded deterministic approach*, Thesis. Université Paris VI.
- Sferratore, A., Garnier, J., Billen, G., Conley, D.J. and Pinault, S. (2006) Diffuse and point sources of silica in the Seine River Watershed. *Environmental Science and Technology* 40(21), 6630-6635.
- Shanghai, E.P.B.o. (2014) *Shanghai Environment Quality Reptot (in Chinese)*. Data covering 1991-2012 retrieved 8 October 2015. Shanghai Environmental Protection Bureau, Shanghai, China.
- Sharpley, A., Jarvie, H.P., Buda, A., May, L., Spears, B. and Kleinman, P. (2013) Phosphorus legacy: Overcoming the effects of past management practices to mitigate future water quality impairment. *Journal of Environmental Quality* 42(5), 1308-1326.
- Shen, Z.-L., Liu, Q. and Zhang, S.-M. (2003) Distribution, variation and removal patterns of inorganic nitrogen in the Changjiang River (in Chinese). *Oceanologia et Limnologia Sinica* 34(4), 355-363.

- Shen, Z. (1997) Preliminary study on the Changjiang river mainstream nutrients fluxes (in Chinese). *Oceanologia et Limnologia Sinica* 28(5), 522-528.
- Smil, V. (2000) Phosphorus in the environment: natural flows and human interferences. *Annual review of energy and the environment* 25(1), 53-88.
- Sprague, L.A., Hirsch, R.M. and Aulenbach, B.T. (2011) Nitrate in the Mississippi River and its tributaries, 1980 to 2008: Are we making progress? *Environ Sci Technol* 45(17), 7209-7216.
- Standardization Administration of China (2009) Laundry powders (Phosphorous) GB/T 13171.1-2009.
- Standardization Administration of China (2012) Hygienic specification for rural household latrine/National standard of the people's republic of China, GB 19379-2012.
- Stehfest, E., van Vuuren, D., Bouwman, L. and Kram, T. (2014) Integrated assessment of global environmental change with IMAGE 3.0: Model description and policy applications, Netherlands Environmental Assessment Agency (PBL).
- Stream Solute Workshop (1989) Concepts and methods for assessing solute dynamics in stream ecosystems.
- Strokal, M., Kroeze, C., Wang, M., Bai, Z. and Ma, L. (2016a) The MARINA model (Model to Assess River Inputs of Nutrients to seAs): Model description and results for China. *Science of the Total Environment* 562, 869-888.
- Strokal, M., Ma, L., Bai, Z., Luan, S., Kroeze, C., Oenema, O., Velthof, G. and Zhang, F. (2016b) Alarming nutrient pollution of Chinese rivers as a result of agricultural transitions. *Environmental Research Letters* 11(2), 024014.
- Struyf, E., Smis, A., Van Damme, S., Garnier, J., Govers, G., Van Wesemael, B., Conley, D.J., Batelaan, O., Frot, E., Clymans, W., Vandevenne, F., Lancelot, C., Goos, P. and Meire, P. (2010) Historical land use change has lowered terrestrial silica mobilization. *Nature Communications* 1(1), 129.
- Stumm, W. (1973) The acceleration of the hydrogeochemical cycling of phosphorus. *Water Res* 7, 131-144.
- Su, X., Yongyong, Z., Ming, D., Ruixiang, H. and Yujian, Z. (2017) Spatial distribution of land use change in the Yangtze River Basin and the impact on runoff. *PROGRESS IN GEOGRAPHY* 36(4), 426-436.
- Sun, C., Shen, Z., Liu, R., Xiong, M., Ma, F., Zhang, O., Li, Y. and Chen, L. (2013) Historical trend of nitrogen and phosphorus loads from the upper Yangtze River basin and their responses to the Three Gorges Dam. *Environmental Science and Pollution Research* 20(12), 8871-8880.
- Sutanudjaja, E.H., Van Beek, R., Wanders, N., Wada, Y., Bosmans, J.H.C., Drost, N., Van Der Ent, R.J., De Graaf, I.E.M., Hoch, J.M., De Jong, K., Karssenber, D., López López, P., Peßenteiner, S., Schmitz, O., Straatsma, M.W., Vannamete, E., Wisser, D. and Bierkens, M.F.P. (2018) PCR-GLOBWB 2: A 5 arcmin global hydrological and water resources model. *Geoscientific Model Development* 11(6), 2429-2453.

- Takahashi, T. (1985) Effect of Season and Exercise on Dermal Nitrogen Losses and Their Relation to Urinary Nitrogen Excretion. *Journal of Nutritional Science and Vitaminology* 31(3), 363-373.
- Tang, D., Di, B., Wei, G., Ni, I.H., Im, S.O. and Wang, S. (2006) Spatial, seasonal and species variations of harmful algal blooms in the South Yellow Sea and East China Sea. *Hydrobiologia* 568(1), 245-253.
- Tavernini, S., Pierobon, E. and Viaroli, P. (2011) Physical factors and dissolved reactive silica affect phytoplankton community structure and dynamics in a lowland eutrophic river (Po river, Italy). *Hydrobiologia* 669(1), 213-225.
- Ti, C., Pan, J., Xia, Y. and Yan, X. (2012) A nitrogen budget of mainland China with spatial and temporal variation. *Biogeochemistry* 108(1-3), 381-394.
- Tian, R.C., Hu, F.X. and Martin, J.M. (1993) Summer Nutrient Fronts in the Changjiang (Yantze River) Estuary. *Estuarine, Coastal and Shelf Science* 37(1), 27-41.
- Tockner, K., Uehlinger, U. and Robinson, C.T. (2009) *Rivers of Europe*, Academic Press.
- Tong, Y., Bu, X., Chen, J., Zhou, F., Chen, L., Liu, M., Tan, X., Yu, T., Zhang, W., Mi, Z., Ma, L., Wang, X. and Ni, J. (2017a) Estimation of nutrient discharge from the Yangtze River to the East China Sea and the identification of nutrient sources. *Journal of Hazardous Materials* 321, 728-736.
- Tong, Y., Wang, M., Peñuelas, J., Liu, X., Paerl, H.W., Elser, J.J., Sardans, J., Couture, R.-M., Larssen, T., Hu, H., Dong, X., He, W., Zhang, W., Wang, X., Zhang, Y., Liu, Y., Zeng, S., Kong, X., Janssen, A.B.G. and Lin, Y. (2020) Improvement in municipal wastewater treatment alters lake nitrogen to phosphorus ratios in populated regions. *Proceedings of the National Academy of Sciences* 117(21), 11566-11572.
- Tong, Y., Zhang, W., Wang, X., Couture, R.M., Larssen, T., Zhao, Y., Li, J., Liang, H., Liu, X., Bu, X., He, W., Zhang, Q. and Lin, Y. (2017b) Decline in Chinese lake phosphorus concentration accompanied by shift in sources since 2006. *Nature Geoscience* 10(7), 507-511.
- Tong, Y., Zhao, Y., Zhen, G., Chi, J., Liu, X., Lu, Y., Wang, X., Yao, R., Chen, J. and Zhang, W. (2015) Nutrient loads flowing into coastal waters from the main rivers of China (2006–2012). *Scientific Reports* 5.
- Treguer, P., Nelson, D.M., Van Bennekom, A.J., DeMaster, D.J., Leynaert, A. and Queguiner, B. (1995) The silica balance in the world ocean: a reestimate. *Science* 268(5209), 375-379.
- Tréguer, P.J. and De La Rocha, C.L. (2013) The world ocean silica cycle. *Annual review of marine science* 5, 477-501.
- Tuholske, C., Halpern, B.S., Blasco, G., Villasenor, J.C., Frazier, M. and Caylor, K. (2021) Mapping global inputs and impacts from of human sewage in coastal ecosystems. *PloS one* 16(11), e0258898.



- Turner, R.E., Qureshi, N., Rabalais, N.N., Dortch, Q., Justic, D., Shaw, R.F. and Cope, J. (1998) Fluctuating silicate:nitrate ratios and coastal plankton food webs. *Proc Natl Acad Sci U S A* 95(22), 13048-13051.
- Turner, R.E. and Rabalais, N.N. (1994) Coastal eutrophication near the Mississippi river delta. *Nature* 368(6472), 619-621.
- Uehlinger, U., Wantzen, K.M., Leuven, R.S.E.W. and Arndt, H. (2009) Rivers of Europe, pp. 199-245.
- United Nations (2018) Revision of world urbanization prospects, New York.
- Van Beek, L. and Bierkens, M. (2009) The Global Hydrological Model PCR-GLOBWB: Conceptualization, Parameterization and Verification, Report Department of Physical Geography, Utrecht University, Utrecht, The Netherlands. [vanbeek.geo.uu.nl/supinfo/vanbeekbierkens2009.pdf](http://vanbeek.geo.uu.nl/supinfo/vanbeekbierkens2009.pdf).
- Van Beek, L.P.H., Wada, Y. and Bierkens, M.F.P. (2011) Global monthly water stress: 1. Water balance and water availability. *Water Resources Research* 47(7).
- Van Bennekom, A. and Salomons, W. (1981) Pathways of nutrients and organic matter from land to ocean through rivers.
- Van der Weijden, C. and Middelburg, J. (1989) Hydrogeochemistry of the river Rhine: long term and seasonal variability, elemental budgets, base levels and pollution. *Water Research* 23(10), 1247-1266.
- Van Drecht, G., Bouwman, A.F., Harrison, J. and Knoop, J.M. (2009) Global nitrogen and phosphate in urban wastewater for the period 1970 to 2050. *Global Biogeochemical Cycles* 23(3).
- Van Drecht, G., Bouwman, A.F., Knoop, J.M., Beusen, A.H.W. and Meinardi, C.R. (2003) Global modeling of the fate of nitrogen from point and nonpoint sources in soils, groundwater, and surface water. *Global Biogeochemical Cycles* 17(4), 26-21 - 26-20.
- Van Meter, K.J., Basu, N.B., Veenstra, J.J. and Burras, C.L. (2016) The nitrogen legacy: Emerging evidence of nitrogen accumulation in anthropogenic landscapes. *Environmental Research Letters* 11(3).
- Van Puijenbroek, P.J.T.M., Beusen, A.H.W. and Bouwman, A.F. (2019) Global nitrogen and phosphorus in urban waste water based on the Shared Socio-economic pathways. *Journal of Environmental Management* 231, 446-456.
- Velthof, G.L., Lesschen, J., Webb, J., Pietrzak, S., Miatkowski, Z., Pinto, M., Kros, J. and Oenema, O. (2014) The impact of the Nitrates Directive on nitrogen emissions from agriculture in the EU-27 during 2000–2008. *Science of the Total Environment* 468, 1225-1233.
- Vilmin, L., Flipo, N., De Fouquet, C. and Poulin, M. (2015) Pluri-annual sediment budget in a navigated river system: the Seine River (France). *Science of the Total Environment* 502, 48-59.
- Vilmin, L., Mogollón, J.M., Beusen, A.H.W., van Hoek, W.J., Liu, X., Middelburg, J.J. and Bouwman, A.F. (2020) Modeling Process - Based Biogeochemical

- Dynamics in Surface Fresh Waters of Large Watersheds With the IMAGE - DGNM Framework. *Journal of Advances in Modeling Earth Systems* 12(11).
- Vitousek, P.M., Aber, J.D., Howarth, R.W., Likens, G.E., Matson, P.A., Schindler, D.W., Schlesinger, W.H. and Tilman, D.G. (1997) Human alteration of the global nitrogen cycle: sources and consequences. *Ecological Applications* 7(3), 737-750.
- van Hoek, W.J., Wang, J., Vilmin, L., Beusen, A.H., Mogollón, J.M., Müller, G., Pika, P.A., Liu, X., Langeveld, J.J. and Bouwman, A.F. (2021) Exploring Spatially Explicit Changes in Carbon Budgets of Global River Basins during the 20th Century. *Environ Sci Technol* 55(24), 16757-16769.
- Wang, H., Yang, Z., Wang, Y., Saito, Y. and Liu, J.P. (2008a) Reconstruction of sediment flux from the Changjiang (Yangtze River) to the sea since the 1860s. *Journal of Hydrology* 349(3), 318-332.
- Wang, J., Beusen, A.H., Liu, X. and Bouwman, A.F. (2019) Aquaculture production is a large, spatially concentrated source of nutrients in Chinese freshwater and coastal seas. *Environ Sci Technol* 54(3), 1464-1474.
- Wang, J., Beusen, A.H., Liu, X., Van Dingenen, R., Dentener, F., Yao, Q., Xu, B., Ran, X., Yu, Z. and Bouwman, A.F. (2020) Spatially explicit inventory of sources of nitrogen inputs to the Yellow Sea, East China Sea, and South China Sea for the period 1970–2010. *Earth's Future* 8(10), e2020EF001516.
- Wang, J., Yan, W., Chen, N., Li, X. and Liu, L. (2015) Modeled long-term changes of DIN: DIP ratio in the Changjiang River in relation to Chl- $\alpha$  and DO concentrations in adjacent estuary. *Estuarine, Coastal and Shelf Science* 166, 153-160.
- Wang, X., Yang, S., Ran, X., Liu, X.M., Bataille, C.P. and Su, N. (2018) Response of the Changjiang (Yangtze River) water chemistry to the impoundment of Three Gorges Dam during 2010–2011. *Chemical Geology* 487, 1-11.
- Wang, Y., Fang, Y. and Jiao, J. (2008b) Evaluation of night soil treatment efficiency of “three-grille-mode” septic tanks in the rural area of Jiangsu. *Journal of Ecology and Rural Environment* 24(2), 80-83.
- Willems, D. and Blom, E. (2018) *The Wetland Book II: Distribution, Description, and Conservation*, pp. 923-931.
- Wilsenach, J., Schuurbiers, C. and Van Loosdrecht, M. (2007) Phosphate and potassium recovery from source separated urine through struvite precipitation. *Water Research* 41(2), 458-466.
- Wit, M.d. (2001) Nutrient fluxes at the river basin scale. I: the PolFlow model. *Hydrological Processes* 15(5), 743-759.
- Wollheim, W.M., Vörösmarty, C.J., Bouwman, A., Green, P., Harrison, J., Linder, E., Peterson, B.J., Seitzinger, S.P. and Syvitski, J.P. (2008) Global N removal by freshwater aquatic systems using a spatially distributed, within-basin approach. *Global Biogeochemical Cycles* 22(2).
- World Bank (2015) PPP conversion factor. World Bank. <https://data.worldbank.org/indicator>.

- Wu, J., Huang, J., Han, X., Xie, Z. and Gao, X. (2003) Three-Gorges Dam - Experiment in habitat fragmentation? *Science* 300(5623), 1239-1240.
- Xiao, X., Agustí, S., Pan, Y., Yu, Y., Li, K., Wu, J. and Duarte, C.M. (2019) Warming Amplifies the Frequency of Harmful Algal Blooms with Eutrophication in Chinese Coastal Waters. *Environ Sci Technol* 53(22), 13031-13041.
- Xing, G. and Zhu, Z. (2002) Regional nitrogen budgets for China and its major watersheds. *Biogeochemistry* 57(1), 405-427.
- Xu, H. (2013) The Yangtze Estuary: Nutrients budget and transport response to human activities in the river basin (Doctoral dissertation), Retrieved from East China Normal University Library Database.
- Xu, H., Chen, Z., Finlayson, B., Webber, M., Wu, X., Li, M., Chen, J., Wei, T., Barnett, J. and Wang, M. (2013) Assessing dissolved inorganic nitrogen flux in the Yangtze River, China: Sources and scenarios. *Global and Planetary Change* 106, 84-89.
- Yan, W., Mayorga, E., Li, X., Seitzinger, S.P. and Bouwman, A. (2010) Increasing anthropogenic nitrogen inputs and riverine DIN exports from the Changjiang River basin under changing human pressures. *Global Biogeochemical Cycles* 24(4).
- Yan, W., Zang, S., Sun, P. and Seitzinger, S.P. (2003) How do nitrogen inputs to the Changjiang basin impact the Changjiang River nitrate: A temporal analysis for 1968-1997. *Global Biogeochemical Cycles* 17(4), 2-1.
- Yan, W., Zhang, S. and Wang, J. (2001) Nitrogen biogeochemical cycling in the Changjiang drainage basin and its effect on Changjiang river dissolved inorganic nitrogen: temporal trend for the period 1968-1997 (in Chinese). *Acta Geographica Sinica* 56(5), 505-514.
- Yang, S.-l., Zhao, Q.-y. and Belkin, I.M. (2002) Temporal variation in the sediment load of the Yangtze River and the influences of human activities. *Journal of Hydrology* 263(1), 56-71.
- Yang, X., Xiong, B. and Yang, M. (2008) Seasonal dynamics of phosphorus forms in water body and sediments of Nanhu Lake, Wuhan (in Chinese). *Chinese Journal of Applied Ecology* 19(09), 2029-2034.
- Yearbook, C.S. (2015) National Bureau of statistics of China. *China Statistical Yearbook*.
- Yu, C.Q., Huang, X., Chen, H., Godfray, H.C.J., Wright, J.S., Hall, J.W., Gong, P., Ni, S.Q., Qiao, S.C., Huang, G.R., Xiao, Y.C., Zhang, J., Feng, Z., Ju, X.T., Ciais, P., Stenseth, N.C., Hessen, D.O., Sun, Z.L., Yu, L., Cai, W.J., Fu, H.H., Huang, X.M., Zhang, C., Liu, H.B. and Taylor, J. (2019) Managing nitrogen to restore water quality in China. *Nature* 567(7749), 516-520.
- Yu, R.-C., Lü, S.-H. and Liang, Y.-B. (2018) *Global Ecology and Oceanography of Harmful Algal Blooms*, pp. 309-316, Springer.
- Zhang, J. (1996) Nutrient elements in large Chinese estuaries. *Continental Shelf Research* 16(8), 1023-1045.

- Zhang, J., Beusen, A.H.W., Van Apeldoorn, D.F., Mogollón, J.M., Yu, C. and Bouwman, A.F. (2017) Spatiotemporal dynamics of soil phosphorus and crop uptake in global cropland during the 20th century. *Biogeosciences* 14(8), 2055-2068.
- Zhang, J., Huang, W., Liu, M. and Cui, J. (1994) Eco-social impact and chemical regimes of large Chinese rivers—a short discussion. *Water Research* 28(3), 609-617.
- Zhang, J., She, Q., Chang, V.W.C., Tang, C.Y. and Webster, R.D. (2014) Mining Nutrients (N, K, P) from Urban Source-Separated Urine by Forward Osmosis Dewatering. *Environ Sci Technol* 48(6), 3386-3394.
- Zhang, S. (1990) A study of the mass transport rate of carbon, nitrogen, phosphorus and sulphur of the Changjiang River. *Study on the Background Values of Chemical Elements in Aquatic Environment* 1212131.
- Zhang, X., Qi, M., Chen, L., Wu, T., Zhang, W., Wang, X. and Tong, Y. (2020) Recent change in nutrient discharge from municipal wastewater in China's coastal cities and implication for nutrient balance in the nearshore waters. *Estuarine, Coastal and Shelf Science* 242.
- Zhao, J., Luo, Q., Deng, H. and Yan, Y. (2008) Opportunities and challenges of sustainable agricultural development in China. *Philosophical Transactions of the Royal Society of London B: Biological Sciences* 363(1492), 893-904.
- Zhiliang, S., Qun, L., Shumei, Z., Hui, M. and Ping, Z. (2003) A nitrogen budget of the Changjiang river catchment. *Ambio* 32(1), 65-69.
- Zhou, M., Shen, Z. and Yu, R. (2020) *Studies of the Biogeochemistry of Typical Estuaries and Bays in China*, pp. 159-173, Springer.
- Zhou, W., Huo, W., Yuan, X. and Yin, K. (2003) Distribution features of chlorophyll a and primary productivity in high frequency area of red tide in East China Sea during spring]. *Ying Yong Sheng Tai Xue Bao* 14(7), 1055-1059.

## Summary

Various types of models are being used to quantitatively assess the transfers of plant nutrients (nitrogen, N; phosphorus, P; silicon, Si) from land to streams and via rivers to coastal waters. Two model categories can be distinguished. One category is that of lumped river-basin scale models. The second category consists of distributed approaches. Lumped river-basin scale approaches are statistical models that relate lumped or aggregated river basin characteristics to river export to coastal waters. However, these lumped models do not help to improve our understanding of the changing biogeochemistry within river basins. The distributed approaches consider all components of landscapes (soil, vegetation, land types, riparian zones, wetlands, streams, lakes and reservoirs) to simulate nutrient transport and processing through various hydrological transport pathways (surface runoff transport, leaching, groundwater transport, direct discharge from sewage and atmospheric deposition). In contrast to the lumped approaches, the distributed models improve our understanding of the interaction of multiple processes within different landscapes and predict the biogeochemistry and temporary storage of nutrients along the river basin as a result of long travel times.

This thesis presents simulations of the N, P and Si transport from land to sea based on the distributed, spatially explicit, mechanistic Integrated Model to Assess the Global Environment-Dynamic Global Nutrient Model (IMAGE-DGNM).

Chapter 2 describes a new extended version of the DGNM wastewater model and its application to compute nitrogen (N) and phosphorus (P) emissions in wastewater and their fates in rural and urban areas in China, covering 1970-2015. The model uses long-term changes in the drivers of the N and P from point sources, and couples sanitation types, sewer connection rate, detergents use, wastewater treatment plants technologies (WWTPs) and their dynamic capacities, based on province-scale data on N and P in wastewater and detailed information on the location and functioning of WWTPs covering China. The following findings are essential for both scientists and policymakers:

- To bend the increase of N and P discharge to surface water, the stagnant treatment technologies in WWTPs need to be incrementally improved from secondary to tertiary treatment over time, especially in the 10 provinces of Eastern China.
- The rapid increase of P discharge to surface water during recent decades both in rural and urban areas is mainly due to the lack of a nation-wide ban of P-

based detergents and manifold increasing use of P-containing dishwasher and laundry detergents.

- The N and P emissions of rural populations have been neglected in quantitative studies until now. My model results suggest a considerable contribution of the rural population to N and P pollution of freshwater environments in China.
- The N:P molar ratio in wastewater discharge decreased from 20 to 15 during the period 1970-2015.

Chapter 3 presents a new model and applications to calculate silicon transport and biogeochemical processing in the Rhine and Yangtze River basins and the eventual export to the coastal seas for the period 1900-2010. The model is, by using long-term changes in the drivers of the Si cycle, and coupling climate, land use and hydrology with in-stream processing, a major step forward compared with regression models, basin-scale box models and reservoir box models that all produce snapshots for individual years and lack the capability to simulate legacies. Our approach, DISC-SILICON which forms part of the Integrated Model to Assess the Global Environment-Dynamic Global Nutrient Model (IMAGE-DGNM) is the first dynamic, spatially explicit, and distributed model that allows to describe the long-term spatial patterns of global Si supply from weathering, and transport and biogeochemical processing in the river continuum, from soil to streams via rivers up till the mouth including the role of lakes and reservoirs. Model results focus on the comparison of two major rivers with contrasting geohydrological conditions, history of land-use change and dam construction, i.e. the rivers Rhine and Yangtze. The major findings of chapter 3 are:

- The significant decrease in dissolved silicon export from the Yangtze River from 1900 to 2010 is due to the dramatic increase in the reservoir volume and the transformation of 40% of the natural vegetation to cropland. Land-use change has a large and long-term impact on the Si cycle in river basins
- The Three Gorges Reservoir has a large contribution to total primary production (11%) and burial (12%) in the whole Yangtze basin.
- Damming in the Yangtze River reduced the Si flux to coastal waters, implying an increased risk of harmful algal blooms within the reservoirs.
- Temporary storage of the elevated flooding-induced Si inputs cause legacies in the subsequent dry year both in the Rhine River and the Yangtze River.

Chapter 4 presents simulated changes in nutrient transport and biogeochemical processing and retention in the Yangtze River during a period of rapid population

growth and economic growth. The results demonstrate that the current nutrient load being exported from the Yangtze River basin toward the East China Sea and the Yellow Sea is much larger (almost twice) than previously estimated based on statistical models such as Global NEWS. Our revised nutrient export estimates are important, as the Yangtze River is one of the largest rivers in the world with a significant portion of the Chinese agricultural production and population. The following findings of chapter 4 are important for both scientists and policymakers:

- The anthropogenic nutrient export from the Yangtze River has increased rapidly between 1900 and 2010, particularly after 1970. This negatively affects coastal ecosystems, including those within the East China Sea and the Yellow Sea.
- The impact of the Three Gorges Reservoir on the total basin-wide nutrient retention is limited (5-6%).
- The changing N:P ratio in water exported to the coastal waters of the Yangtze River may have important ecological implications.
- There is a large accumulation of N in groundwater in the Yangtze River basin.
- Policies to reduce the N and P export from the Yangtze River basin should focus on the midstream and upstream subbasins to improve fertilizer and manure use efficiencies.

Chapter 5 explores nutrient dynamics in four river basins within four climate zones during the past century, the rivers Rhine, Mississippi, Yangtze and Pearl. The experience of nutrients reduction policies obtained in the Rhine and Mississippi river basins can provide valuable lessons to other polluted river basins worldwide, such as those in China. There are important differences between the four rivers. Although all four rivers went through a phase of nutrient accumulation, there is a difference in the timing of these periods. The Rhine and Mississippi began this phase in the 1950s and the Yangtze and Pearl in the 1970s. P accumulation in sediments in reservoirs and lakes, therefore, has a large contribution to total P retention. Large amounts of N have been temporarily stored in groundwater in the basins of Yangtze and Mississippi. Strategies to reduce N and P loading have been successful in the Rhine and less so in the Mississippi. However, N:P ratios have changed, which may have substantial ecological impacts. Both Rhine and Mississippi showed rapidly increasing molar N:P ratios in the water draining into the North Sea and the Gulf of Mexico, respectively. The scenarios indicate that the current policies to halt the increase of fertilizer use after 2020 will not be sufficient to stop the accumulation of nutrients in landscapes and waterscapes in the Yangtze River basin due

to long-term legacy impact from groundwater. Such policy strategies would lead to a stabilization of N surpluses in agriculture and not a decrease. However, with a large amount of N and P accumulated in groundwater and sediments, it will be especially difficult to improve water quality in the Yangtze River. The Pearl River has experienced much less accumulation and may respond more directly to reduced nutrient loading.



## Samenvatting in het Nederlands

Er worden verschillende soorten modellen gebruikt om het transport van plantenvoedingsstoffen (nutriënten; stikstof, N; fosfor, P; silicium, Si) van land naar beken en via rivieren naar kustwateren te kwantificeren. Deze modellen kunnen in twee categorieën worden ingedeeld. De eerste categorie is die van geaggregeerde modellen van stroomgebieden. De tweede categorie is die van gedistribueerde benaderingen. De geaggregeerde modellen voor stroomgebieden zijn statistische modellen die de kenmerken van een geheel stroomgebied relateren aan rivierexport. Echter, deze modellen helpen ons niet om de veranderende biogeochemie binnen stroomgebieden beter te begrijpen. De gedistribueerde benaderingen houden rekening met alle onderdelen van landschappen (bodem, vegetatie, landtypes, oeverzones, wetlands, beken, meren en reservoirs) om de biogeochemie van nutriënten tijdens het transport via verschillende hydrologische routes te simuleren (transport van oppervlaktewater, uitspoeling, grondwatertransport, directe lozing uit rioolwater en atmosferische depositie). In tegenstelling tot de geaggregeerde benaderingen, helpen de gedistribueerde modellen om de interactie van verschillende processen in landschappen beter te begrijpen en ook de tijdelijke opslag door lange reistijden van water en nutriënten in het stroomgebied te schatten.

Dit proefschrift presenteert simulaties van het transport van N, P en Si van land naar zee op basis van het gedistribueerde, ruimtelijk expliciete, mechanistische Integrated Model to Assess the Global Environment-Dynamic Global Nutrient Model (IMAGE-DGNM).

Hoofdstuk 2 beschrijft een nieuwe uitgebreide versie van het DGNM-afvalwatermodel en de toepassing ervan voor het berekenen van stikstof (N) en fosfor (P) emissies in afvalwater en hun lot in landelijke en stedelijke gebieden in China, voor 1970-2015. Het model gebruikt langjarige veranderingen in de sturende factoren van de N en P emissies naar oppervlaktewater via afvalwater, en koppelt sanitatietypes, rioolaansluitingspercentage, gebruik van wasmiddelen, technologieën voor afvalwaterzuiveringsinstallaties en de dynamische capaciteiten ervan, op basis van gegevens op provincieschaal over N en P in afvalwater en gedetailleerde informatie over de locatie en werking van zuiveringsinstallaties in China. De volgende bevindingen zijn van groot belang voor zowel wetenschappers als beleidsmakers:

- Om de toename van N- en P-afvoer naar oppervlaktewater te beperken, moeten de stagnerende zuiveringstechnologieën in afvalwaterzuiveringsinstallaties in de loop van de tijd stapsgewijs worden verbeterd van secundaire naar tertiaire zuivering, vooral in de 10 provincies in Oost-China.

- De snelle toename van de P-lozing in het oppervlaktewater, zowel in landelijke als stedelijke gebieden, is voornamelijk te wijten aan het ontbreken van een landelijk verbod op wasmiddelen op P-basis en een snel toenemend gebruik van P-houdende afwasmiddelen en wasmiddelen in de afgelopen tientallen jaren.
- N en P emissies door de plattelandsbevolking zijn tot nu toe in kwantitatieve onderzoeken verwaarloosd. Mijn modelresultaten suggereren een aanzienlijke bijdrage van de plattelandsbevolking aan N- en P-vervuiling van zoetwatermilieus in China.
- De molaire N:P verhouding in de afvalwaterlozing is in de periode 1970-2015 gedaald van 20 naar 15.

Hoofdstuk 3 presenteert een nieuw model en toepassingen voor het berekenen van siliciumtransport en biogeochemische omzettingen in de stroomgebieden van de Rijn en de Yangtze en de uiteindelijke export naar de kustzeeën voor de periode 1900-2010. Het model is, door gebruik te maken van langjarige veranderingen in de sturende factoren van de Si kringloop, het koppelen van klimaat, landgebruik, hydrologie, met biogeochemische omzettingen in het water, een grote stap voorwaarts in vergelijking met regressiemodellen en zwarte doos modellen voor stroomgebieden en reservoirs, die allemaal schattingen voor één enkel jaar produceren en niet de mogelijkheid hebben om de (uitstroom uit) tijdelijke opslag te simuleren. Onze benadering, DISC-SILICON, die deel uitmaakt van het Integrated Model to Assess the Global Environment-Dynamic Global Nutrient Model (IMAGE-DGNM), is het eerste dynamische, ruimtelijk expliciete en gedistribueerde model waarmee de ruimtelijke patronen op lange termijn van wereldwijde Si aanvoer door verwerking en transport en biogeochemische omzettingen in het riviercontinuüm, van bodem naar beken via bredere rivieren tot de monding, inclusief de rol van meren en reservoirs. Modelresultaten richten zich op de vergelijking van twee grote rivieren met contrasterende geohydrologische omstandigheden, geschiedenis van veranderingen in landgebruik en damconstructie, namelijk de Rijn en de Yangtze. De belangrijkste bevindingen van hoofdstuk 3 zijn:

- De aanzienlijke afname van de export van opgelost silicium door de Yangtze-rivier van 1900 tot 2010 komt door de dramatische toename van het reservoirvolume en de transformatie van 40% van de natuurlijke vegetatie naar akkerland. Veranderend landgebruik heeft een grote en langdurige invloed op de Si cyclus in stroomgebieden
- Het Drieklovenreservoir levert een grote bijdrage aan de totale primaire productie (11%) en sedimentatie (12%) in het hele Yangtze-bekken.

- De bouw van dammen in de Yangtze heeft geleid tot een vermindering van de Si-flux, wat een verhoogd risico op schadelijke algenbloei in de reservoirs veroorzaakt.
- Tijdelijke opslag van de Si aanvoer tijdens overstroming van uiterwaarden veroorzaakt een verhoogde flux (erfenis) in het daaropvolgende droge jaar, zowel in de Rijn als in de Yangtze.

Hoofdstuk 4 behandelt gesimuleerde veranderingen in nutriëntentransport en biogeochemische omzettingen en retentie in de Yangtze rivier tijdens een periode van snelle bevolkingsgroei en economische groei. De resultaten tonen dat de huidige nutriëntenbelasting die wordt geëxporteerd vanuit het Yangtze-stroomgebied naar de Oost-Chinese Zee en de Gele Zee veel groter is (bijna twee keer) dan eerder werd geschat met behulp van statistische modellen zoals Global NEWS. Onze herziene schattingen van de export van nutriënten vertegenwoordigen een zeer belangrijke bevinding, aangezien de Yangtze-rivier een van de grootste rivieren ter wereld met een aanzienlijk deel van de Chinese landbouwproductie en bevolking. De volgende bevindingen uit hoofdstuk 4 zijn belangrijk voor zowel wetenschappers als beleidsmakers:

- Het nutriëntenexport naar kustwateren veroorzaakt door menselijke activiteiten in de Yangtze-rivier is tussen 1900 en 2010 snel toegenomen, vooral na 1970. Dit heeft een negatief effect op kustecosystemen, waaronder die in de Oost-Chinese Zee en de Gele Zee.
- Het aandeel van het drieklovenreservoir in de totale retentie van nutriënten in het hele stroomgebied is beperkt (5-6%).
- De veranderende verhouding tussen stikstof en fosfor in de rivierexport naar kustwateren kan belangrijke ecologische gevolgen hebben.
- Er is een snelle stikstofaccumulatie in grondwater in het stroomgebied van de Yangtze rivier.
- Beleid om de N en P export uit het stroomgebied van de Yangtze-rivier te verminderen kan zich het beste richten op het verbeteren van de efficiëntie van het gebruik van kunstmest en mest in de centrale en stroomopwaartse delen van het stroomgebied.

Hoofdstuk 5 onderzoekt de nutriëntendynamiek in vier stroomgebieden in vier verschillende klimaatzones gedurende de afgelopen eeuw, namelijk de rivieren Rijn, Mississippi, Yangtze en Pearl. De ervaringen met het terugdringen van nutriënten in de

stroomgebieden van de Rijn en de Mississippi kunnen waardevolle lessen opleveren voor andere vervuilde stroomgebieden over de hele wereld, zoals die in China. Er zijn belangrijke verschillen tussen de vier rivieren. Hoewel alle vier de rivieren een fase van nutriëntenaccumulatie doormaakten, is er een verschil in de timing van deze perioden. De Rijn en de Mississippi begonnen deze fase in de jaren vijftig en de rivieren de Yangtze en de Pearl in de jaren zeventig. P-accumulatie in sedimenten in reservoirs en meren heeft daarom een grote bijdrage aan de totale P retentie. In de stroomgebieden van de Yangtze en Mississippi zijn grote hoeveelheden N tijdelijk opgeslagen in het grondwater. Strategieën om de N en P aanvoer te verminderen zijn succesvol geweest in de Rijn en in mindere mate in de Mississippi. De N:P-verhoudingen zijn echter veranderd, hetgeen aanzienlijke ecologische gevolgen kan hebben. Zowel de Rijn als de Mississippi vertoonden snel toenemende molaire N:P-verhoudingen in het water dat respectievelijk naar de Noordzee en de Golf van Mexico stroomt. De scenario's tonen dat het huidige beleid om de toename van het gebruik van kunstmest na 2020 een halt toe te roepen niet voldoende zal zijn om de ophoping van nutriënten in landschappen en waterlandschappen te stoppen als gevolg van de erfenis van geaccumuleerde N in het grondwater. Dergelijke beleidsstrategieën leiden tot een stabilisatie van de N-overschotten in de landbouw en niet tot een vermindering. Met een grote hoeveelheid N en P die zich echter ophoopt in grondwater en sedimenten, zal het bijzonder moeilijk zijn om de waterkwaliteit in de Yangtze te verbeteren. De Pearl heeft veel minder accumulatie ervaren en zal waarschijnlijk met minder vertraging reageren op verminderde nutriëntenbelasting.

## **Outlook**

Models are used by scientists to explore the complex chemical, physical and biological processes in the ecosystem. The big question is how to capture the most critical processes that drive the complex phenomena in the environment. In this study, we developed and applied different models for various purposes at the grid-cell level. The models very well reproduced historical fluxes of the nutrients and were found to be useful for analyzing scenarios of future global changes.

Data on nutrient concentrations in a limited number of stations are available for the validation of simulated results. Data for validation of sub-flows like surface runoff and erosion, groundwater outflow in the model are scant. This Ph.D. study shows that fundamental sensitivity analysis should be used next to the comparison of nutrient concentrations in water bodies to learn how and to what extent the various parameters and input data influence model results. This study focused on the annual time scale. Future developments of nutrient fluxes should aim at combining all the stream nutrients (C, N, P, Si) at different spatial and temporal scales. Mechanistic models are required

that distinguish different N, P and Si forms at time scales that are more appropriate than the annual scale when exploring dynamics and seasonality of algal bloom evolution.

The nutrient process descriptions in soil linked to land use and biological processes in surface water and groundwater should be further developed, particularly in river basins that experience intensive land-use changes. Such extended models will be able to simulate the nutrient observed retention in lakes, reservoirs, streams, flooding plains, and legacies of nutrients stored in landscapes under future global scenarios.



## Acknowledgement

There are many people I wish to thank for their support during my stay in the Netherlands. First and foremost, I would like to thank my promotors Lex Bouwman and Jack Middelburg. Jack, thank you so much for transferring my CV to Lex, that is how my UU journey started. Thanks for the brainstorm talks, I am deeply impressed by your erudition. Lex, I want to greatly thank you for offering me the chance to be part of the team. Thanks for all the valuable support, patience and encouragement during the past years. More importantly, I would like to acknowledge the insightful discussions about our model research, which guided me through my PhD experience and motivated me to think about being a pure scientist. Finally, of course, I want to thank all the beer time in downtown Utrecht, and wonderful trips in Amsterdam and Hoge Veluwe Park. Appreciate all the support to my family from you and Lies during my difficult time.

Many thanks to my supervisor Arthur Beusen, Haha, what a great honor to work with you, YOU are much more powerful than Google. Reading your code is like enjoying an art piece. Thanks for bringing me to the python world, Linux world, Cluster world and much much more. Of course, your fascinating humorous languages, I enjoy both the work and relax time with you. Thank you and Anneke for having me in your place, thanks the concern and kind support during my tough time. Rens van Beek, thank you for introducing me to the PCR-GLOBWB model and all the model output updating.

José was my first office mate and the first one who helped me to feel comfortable, Thank YOU. My fantastic buddy Wim Joost, and Lauriane, thanks for our friendship, our endless talk about our common model work and fun during our coffee breaks and Uitjes. Thanks so much for all that I have learned from you. Our happiness, struggles and sweat are valuable and too much to describe in detail. Wim Joost, thanks so much for everything, I am very honored what we have done together over the past years. We can easily communicate with the same wavelength both for our models and hobbies.

I met fantastic colleagues working in the group of Geochemistry of Utrecht University. I am super lucky to have had such lovely colleagues over the past years. I deeply enjoyed not only the discussion about research but also the coffee and tea breaks, and birthday cakes. The wonderful activities contributed a lot to me. Junjie, many thanks for your carefulness proofread. Thank you (random) Joep, Junjie and Zhu Zhang, Hao Wang and Lifang, Philip, Xiangbin, Nengwang, Jia, Anne, Mădălina, Salima, Jie, Nikki, Matthias, Anna, Marie-Louise, Alwina, Thilo, Caroline, Mariette, Lubos. I would like to thank everyone with whom I worked in CML of Leiden University for the good times. Ranran, Valerio, Paul and Jose, I have enjoyed our collaborating with you during the Greenpeace project.

Of course, I want to thank all my friends in the Chinese community in Netherlands, thank you (random order) Jiawang, Zhen Yang, Lin Xiao, Xueming, Tao Lv, Die Yang, Ran Shang, Jingyi Hu, Xuedong, Ming&Xin Li, Jinhu, Peng Wei, Cuijie Feng, Nan Jiang, Zheyi Zeng, Liangfu, RuiSheng, Jialong, Yichuan, Jiehuan, Xuezhou, Chaowen Wang, Liu Yang, Mengmeng, Jiao Chen, and everyone I had a good time with over the past years.

I am grateful to Annuska, Marjolein, Margot, Marco and Jan Willem for the great helps with all the administrative challenges.

Last but not least, THANKS my beloved BIG family for your BIG support, long distance kept us apart, but it feels great as I know you are concerned about me.

Xiaochen



## **Curriculum vitae**

Xiaochen Liu was born on 16 April 1986 in Gaomi, China. After his graduation, he first studied geography in Jinan University and obtained his bachelor's degree in 2009. He worked as a geography teacher in high school in Qingdao and then, he studied ecology (Ecological Restoration) at State Key Laboratory of Estuarine and Coastal Research of East China Normal University in Shanghai where he received a master degree in 2013.

He moved to Netherlands in 2013 and started working as a PhD candidate in Earth Science department at Utrecht University under the joint supervision of Prof. A.F. Bouwman and Prof. J.J. Middelburg.

2016-2019, Xiaochen worked as a business operation manager in Weifang CanghaiSangtian Co., Ltd.

Since 2021, Xiaochen worked as a postdoctoral researcher in institute of Environmental Sciences (CML) in Leiden University, where he simulated the water stress risk of coal power plants based on PCR-GLOBWB model.

Xiaochen is currently working at Utrecht University as a Postdoc, where he is developing the global Indicator for Coastal Eutrophication Potential (ICEP) financed by the World Resources Institute and UNESCO-International Oceanographic Committee (IOC).



# Publications

Dong, L., Li, X., **Liu, X.**, He, K. and Jiang, X. (2017) Determining the effects of major cations (K<sup>+</sup>, Na<sup>+</sup>, Ca<sup>2+</sup>, Mg<sup>2+</sup>) and pH on *Scirpus mariqueter* to Assess the Heavy Metal Biototoxicity of a Tidal Flat Ecosystem. *Journal of Coastal Research* 33(5), 1086-1094.

Li, X., Mao, Y. and **Liu, X.** (2015) Flue gas desulfurization gypsum application for enhancing the desalination of reclaimed tidal lands. *Ecological Engineering* 82, 566-570.

Liu, J., Bouwman, L., Zang, J., Zhao, C., **Liu, X.** and Ran, X. (2016) The silica-carbon biogeochemical cycle in the Bohai Sea and its responses to the changing terrestrial loadings. *Biogeosciences Discussions*, 1-36.

**Liu, X.**, Beusen, A.H., Van Beek, L.P., Mogollón, J.M., Ran, X. and Bouwman, A.F. (2018) Exploring spatiotemporal changes of the Yangtze River (Changjiang) nitrogen and phosphorus sources, retention and export to the East China Sea and Yellow Sea. *Water Research* 142, 246-255.

**Liu, X.**, Joost van Hoek, W., Vilmin, L., Beusen, A., Mogollón, J.M., Middelburg, J.J. and Bouwman, A.F. (2020) Exploring Long-Term Changes in Silicon Biogeochemistry Along the River Continuum of the Rhine and Yangtze (Changjiang). *Environ Sci Technol* 54(19), 11940-11950.

**Liu, X.**, Beusen, A., Puijenbroek, P.J.T.M., Zhang, X., Wang J., Joost van Hoek, W., and Bouwman, A.F. (2021) Wastewater nitrogen and phosphorus flows in urban and rural areas in China for the period 1970 to 2015. *Environ Sci Technol* (under revision).

**Liu, X.**, Beusen, A., Deng, Y., Wang, J., van Hoek, W.J., Ran, X., Xu, B., Yao, Q., Yu, Z., Bouwman, A.F. (2022) Nitrogen legacy in groundwater in the Rhine, Mississippi, Yangtze and Pearl river basins and consequences for future water quality. *Nature Communication* (Submitted)

**Liu, X.**, Wang, R., Barbarossa, V., Mogollón, J., Behrens, P. (2021) Coal generation and climate impacts on the freshwater resources and ecosystem health in the Maritsa River basin in Bulgaria.

Chen, N., Wang, J., **Liu, X.**, Zhang, C., Huang, B., Beusen, A., Middelburg, J.J., Bouwman, A.F. (2021) Exploring Seasonal and Annual Nitrogen Transfer and Ecological Response in River-coast Continuums based on Spatially Explicit Models. *JGR Biogeosciences*. (Accepted)

van Hoek, W.J., Wang, J., Vilmin, L., Beusen, A.H., Mogollón, J.M., Müller, G., Pika, P.A., **Liu, X.**, Langeveld, J.J. and Bouwman, A.F. (2021) Exploring Spatially Explicit Changes in Carbon Budgets of Global River Basins during the 20th Century. *Environ Sci Technol* 55(24), 16757-16769.

Vilmin, L., Mogollón, J., Beusen, A., Van Hoek, W., **Liu, X.**, Middelburg, J. and Bouwman, A. (2020) Modeling process-based biogeochemical dynamics in surface fresh waters of large watersheds with the IMAGE-DGNM framework. *Journal of Advances in Modeling Earth Systems* 12(11), e2019MS001796.

Wang, J., Beusen, A.H., **Liu, X.** and Bouwman, A.F. (2019a) Aquaculture production is a large, spatially concentrated source of nutrients in Chinese freshwater and coastal seas. *Environ Sci Technol* 54(3), 1464-1474.

Wang, J., Beusen, A.H., **Liu, X.**, Van Dingenen, R., Dentener, F., Yao, Q., Xu, B., Ran, X., Yu, Z. and Bouwman, A.F. (2020) Spatially explicit inventory of sources of nitrogen inputs to the Yellow Sea, East China Sea, and South China Sea for the period 1970–2010. *Earth's Future* 8(10), e2020EF001516.

Wang, J., Zhang, J., **Liu, X.**, Beusen, A., Yao, Q., Xu, B., Ran, X., Bouwman, L. and Yu, Z. (2019b) Inventory of Nitrogen Inputs to Chinese Seas for the Period 1970-2010, pp. GC51N-1164.